1998

Photochemical and computational study of sulfoxides, sulfenic esters, and sulfinyl radicals

Daniel D. Gregory
Iowa State University

INFORMATION TO USERS

This manuscript has been reproduced from the microfilm master. UMI films the text directly from the original or copy submitted. Thus, some thesis and dissertation copies are in typewriter face, while others may be from any type of computer printer.

The quality of this reproduction is dependent upon the quality of the copy submitted. Broken or indistinct print, colored or poor quality illustrations and photographs, print bleedthrough, substandard margins, and improper alignment can adversely affect reproduction.

In the unlikely event that the author did not send UMI a complete manuscript and there are missing pages, these will be noted. Also, if unauthorized copyright material had to be removed, a note will indicate the deletion.

Oversize materials (e.g., maps, drawings, charts) are reproduced by sectioning the original, beginning at the upper left-hand corner and continuing from left to right in equal sections with small overlaps. Each original is also photographed in one exposure and is included in reduced form at the back of the book.

Photographs included in the original manuscript have been reproduced xerographically in this copy. Higher quality 6" x 9" black and white photographic prints are available for any photographs or illustrations appearing in this copy for an additional charge. Contact UMI directly to order.

UMI

A Bell & Howell Information Company
300 North Zeeb Road, Ann Arbor MI 48106-1346 USA
313/761-4700 800/521-0600

Photochemical and computational study of sulfoxides, sulfenic esters, and sulfinyl radicals

by

Daniel D. Gregory

A dissertation submitted to the graduate faculty

in partial fulfillment of the requirements for the degree of

DOCTOR OF PHILOSOPHY

Major: Organic Chemistry

Major Professor: William S. Jenks

Iowa State University

Ames, Iowa

1998

Graduate College

Iowa State University

This is to certify that the Doctoral dissertation of

Daniel D. Gregory

has met the dissertation requirements of Iowa State University

Signature was redacted for privacy.

Major Professor

Signature was redacted for privacy.

For the Major Program

Signature was redacted for privacy.

For the Graduate College

To

Mary

My wife and best friend.

TABLE OF CONTENTS

ABSTRACT

Despite a fairly long history of research, sulfoxide photochemistry has not been extensively developed. This is particularly true in terms of structural effects on the observed sulfoxide photochemistry. Because of this, our group has embarked on an extensive study to gain a better understanding of sulfoxide photochemistry and the effects of structure on this photochemistry. The intention of this research is to obtain knowledge of sulfoxide photochemistry that can be used as a predictive tool in the photolysis of other sulfoxide systems. Sulfoxide photochemistry can be divided into four general reaction types. These include α-cleavage, hydrogen abstraction, stereomutation, and deoxygenation. All of these reactions will be discussed to varying extents in this dissertation with an emphasis on the deoxygenation reaction.

Photolysis of dibenzothiophene sulfoxide results in the formation of dibenzothiophene and oxidized solvent. Though quantum yields are low, chemical yields of the sulfide are quite high. Yields of the oxidized solvents can also be high. Typical products are phenol from benzene, cyclohexanol, and cyclohexene from cyclohexane and 2-cyclohexenol and epoxycyclohexane from cyclohexene. A number of experiments designed to elucidate the mechanism of the hydroxylation were carried out, including measurements of quantum yields as a function of concentration, solvent, quenchers, and excitation wavelength. These data are inconsistent with a mechanism involving a sulfoxide dimer, which also does not properly account for the solvent oxidations. It is suggested that the active oxidizing agent may be atomic oxygen $O(^3P)$ or a closely related noncovalent complex, based on the nature

of the oxidation chemistry, comparison to known rate constants for $O(^3P)$ reactivity, and the quantum yield data.

A computational study on the thermochemistry of several simple sulfenic acids (RSOH) and esters (RSOR') is reported. The enthalpies of R-S, S-O, and O-R' homolytic cleavage are calculated at the G2 level of theory and compared to related peroxides and disulfides. Less expensive B3LYP calculations were unsatisfactory. When R and R' are both alkyl, the O-C bond is expected to be the weakest in the molecule; for CH_3SOCH_3, C-S, S-O, and O-C bond dissociation enthalpies of 67, 64, and 49 kcal/mol are predicted by G2. Compared to peroxides, sulfenic esters are predicted to have weaker O-C bonds and S-O bonds that are stronger than the analogous O-O bonds. The C-S bonds of sulfenic esters are predicted to be somewhat stronger than those of disulfides. A rationalization is given for the observation that radical stabilization is greater for RSO• than ROO•, RSS•, or ROS•.

The sulfinyl radical has been proposed to be an important sulfur containing molecule in environmental, combustion, and certain biological processes. A computational investigation of sulfinyl radicals is reported. The ground and excited electronic states are developed using *ab initio* and density functional methods. The self coupling reaction of sulfinyl radicals is investigated using the G2 method. The meso isomer of the α-disulfoxide was found to be more stable than the eclipsed dl isomer by 4.2 kcal/mol at the G2(MP2) method. Of the three possible coupling pathways, the two paths which forms the OS-sulfenyl sulfinate and the α-disulfoxide are both calculated to be very close in energy. The rearrangement of the methyl OS-sulfenyl sulfinate to the thiosulfonate via S-S homolysis was calculated to be endothermic by 44 kcal/mol, which may suggest a concerted rearrangement.

The reaction of the methane sulfenyl radical with oxygen was also investigated using the G2 method. Despite earlier computational results, analysis with more advanced methods show the conformation of the methanesulfenylperoxyl radical where the CSO dihedral is ~90° is calculated to be the lowest energy conformation. The rearrangement of the methanesulfenylperoxyl radical to form the methyl sulfonyl radical has an energy barrier of 23 kcal/mol. The decomposition of radical to form a methyl sulfinyl radical and a triplet oxygen atom is endothermic by 23 kcal/mol.

CHAPTER I
PHOTOCHEMISTRY OF SULFOXIDES: A GENERAL REVIEW

1.1 Dissertation organization

This dissertation contains five chapters. Chapters 1 and 2 focus on the photochemical aspects of the sulfoxide functional group and chapters 3 and 4 pertain to computational work done on potential intermediates of sulfoxide photochemistry. Chapter 1 consists of a general overview of the sulfoxide functional group and a review of sulfoxide photochemistry. Included is this review is a short discussion of the α-cleavage, hydrogen abstraction, and stereomutation reactions. In Chapter 2, the photo-deoxygenation of the dibenzothiophene sulfoxide is discussed in detail. Chapter 3 is a computational study aimed at developing the energetics of the sulfenic acids and esters. In Chapter 4, both the structure and reactions of the sulfinyl radical is investigated computationally. In Chapter 5, the conclusions of each of the first four chapters are summarized. Appendix A is short review of the computational methods used to investigate the sulfenic esters and sulfinyl radicals. Appendix B contains the cartesian coordinates for all of the molecules investigated computationally.

1.2 The sulfoxide functional group

Even though the sulfoxide functional group is sometimes envisioned as structurally related to the carbonyl group, it exhibits several characteristics that are not found in carbonyls. The greatest similarity of the two functional groups is probably the polarization of the S-O and C-O bonds. Despite this similarity, fundamental differences emerge between the two. Probably the biggest difference comes in the hybridization of the sulfur. Unlike the sp^2 hybridized carbon atom in the carbonyl group, the sulfur atom in a ground state sulfoxide can be thought of as approximately sp^3 hybridized. Importantly, there is not a distinct π bond

between the S and O atoms unlike the carbonyl functional group. However, the bonding is more complex than a simple sigma bond. Due to the complex nature of bonding between the sulfur and oxygen atoms, several different pictorial representations are commonly used to represent sulfoxides. Structure **3**, a ylide where more electron density is centered on the oxygen atom, seems to be a reasonably accurate representation of a sulfoxide, and much of the observed ground state chemistry of sulfoxides is consistent with this representation. Acknowledging this, in the interest of clarity and consistency with the literature, structure **1**, with the lone pair electrons omitted, has been chosen to represent the sulfoxide group in this dissertation.

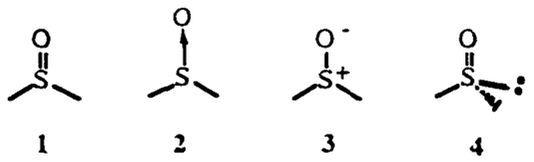

1 **2** **3** **4**

Furthermore, examination of the geometry of sulfoxides and of computational results makes it clear that the 3 ligands on the sulfur and its lone pair are not based on four equivalent sp^3 orbitals. For instance, the CSC bond angle in dimethyl sulfoxide (DMSO) is ~95°. Again, however, we will adopt the sp^3 notation as a convenient and useful shorthand. The sp^3 hybridization and resulting stable configurational stereochemistry of the sulfoxide has allowed it to play a very important role in organic transformations. Substitution of two different organic groups on the sulfoxide results in a stereogenic sulfur center due to a large energy barrier to inversion. The configurational stability coupled with the relative ease of producing optically pure samples of chiral sulfoxides have allowed them to be used extensively as chiral auxiliaries in organic transformations. Often, chiral sulfoxides are used to induce stereochemistry into an adjacent part of the molecule and then removed from the

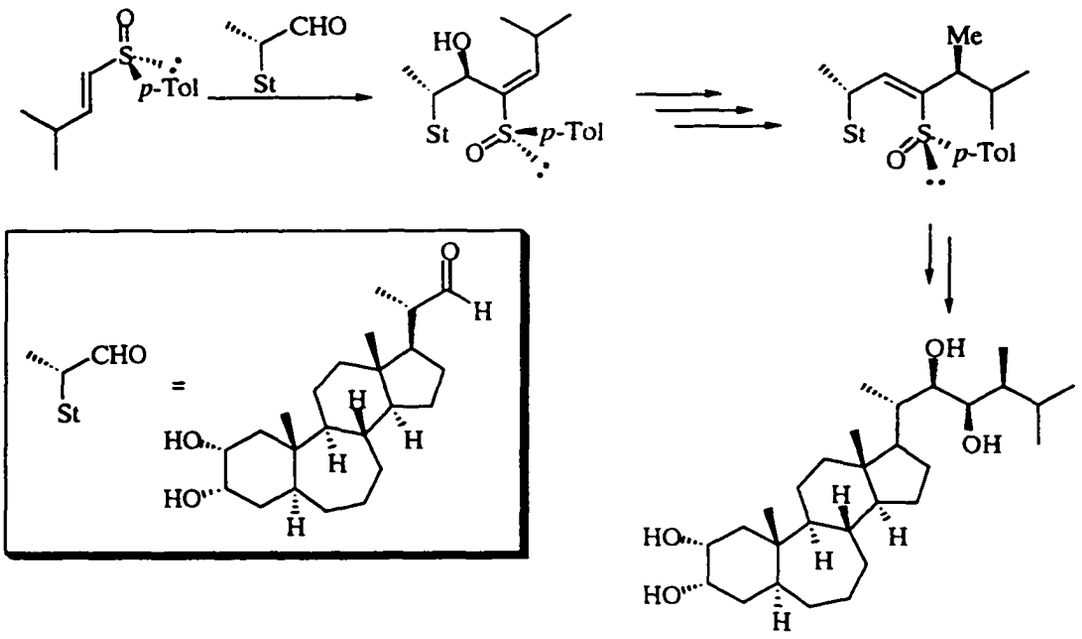

Brassinolide

molecule at a later time.[1,2] One recent example of this strategy is found in the synthesis of brassinolide.[3]

Another important aspect of the sulfoxide functional group is its intermediate oxidation state. Because of this, the sulfoxide can be either oxidized to the sulfone or reduced to the sulfide group rather easily. This changes both the thermodynamic and photolytic properties of the sulfur atom and the molecule. Due to the fact that the sulfur atom can exist in several oxidation states, there are many different organic functional groups associated with it. Figure 1 is meant to be a helpful reference for the names and structures of many different sulfur functional groups.

A reliable orbital description of the photochemistry of the sulfoxide group has not yet been established. However, low level computer calculations have shown that the HOMO of simple dialkyl sulfoxides is π antibonding between the S and O and sigma bonding between the C and S. The LUMO is localized mostly on the sulfur and is π antibonding along the S-O bond and sigma antibonding between the C-S bond.[4,5] The orbital descriptions of diaryl

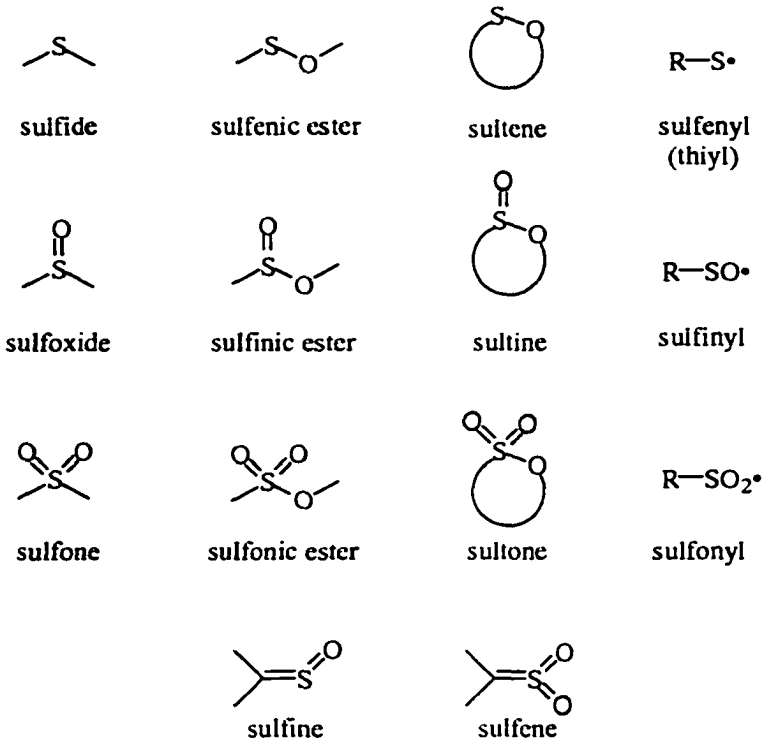

Figure 1. Different sulfur containing functional groups.

sulfoxides are very similar to that of the dialkyl sulfoxides except there is significant delocalization of electron density throughout the π system in both the HOMO and LUMO.

Estimates of the singlet and triplet energies for simple dialkyl sulfoxides are still rather undeveloped. Because they do not fluoresce, the best estimate for the singlet energy (105 kcal/mol) comes from the onset of absorption of dimethyl sulfoxide in the gas phase.[4] By introducing a heavy atom (Xe) to increase the $S_0 \rightarrow T_1$ absorption, a value of 83 kcal/mol was estimated for the triplet energy of dialkyl sulfoxides.[6]

The luminescence of aryl sulfoxides **5-7** have been investigated. Few of the molecules fluoresced, significantly either.[7] Singlet energies for the diaryl sulfoxides like 5 and 6 were 90-100 kcal/mol. Although the phosphorescence quantum yield was very low,

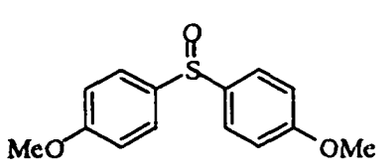

5

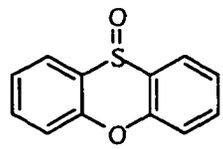

6

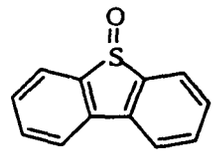

7

the triplet energies for alkyl aryl sulfoxides were estimated at 80 kcal/mol and diaryl sulfoxides were estimated to range from 75-78 kcal/mol.

Despite a fairly long history of research, sulfoxide photochemistry has not been extensively developed.[5,8-11] This is particularly true in terms of structural effects on the observed sulfoxide photochemistry. Because of this, our group has embarked on an extensive study to gain a better understanding of sulfoxide photochemistry and the effects of structure on this photochemistry. The intention of this research is to obtain knowledge of sulfoxide photochemistry that can be used as a predictive tool in the photolysis of other sulfoxide systems. Sulfoxide photochemistry can be divided into four general reaction types. These include α-cleavage, hydrogen abstraction, stereomutation, and deoxygenation. The second chapter of this dissertation will deal with a detailed investigation of the deoxygenation reaction. Some general conclusions about the remaining reactions will be discussed in the following sections of this chapter.

1.3 The α-cleavage reaction

The α-cleavage reaction is probably the most common photochemical reaction of sulfoxides. It consists of the homolytic cleavage of the C-S bond to form a sulfinyl radical **8** and a carbon containing radical. At this point in the reaction, several different things can happen. The two radicals can recouple to form starting material, or in the case of a chiral sulfoxide, undergo racemization. Recombination of the organic radical and the sulfinyl radical at the oxygen terminus will lead to the formation of the sulfenic ester **9**. Escape of

the two radicals from the solvent cage will lead to the observation of additional reactions such as coupling of the organic or sulfinyl radicals. The product distribution resulting from the photolysis of sulfoxides is further complicated by the secondary photolysis of intermediates like sulfenic esters. Because of this, every aspect of the reaction ranging from time of photolysis and temperature to the solvent polarity must be considered when using product studies to gain insight into the photochemical reactions of sulfoxides.

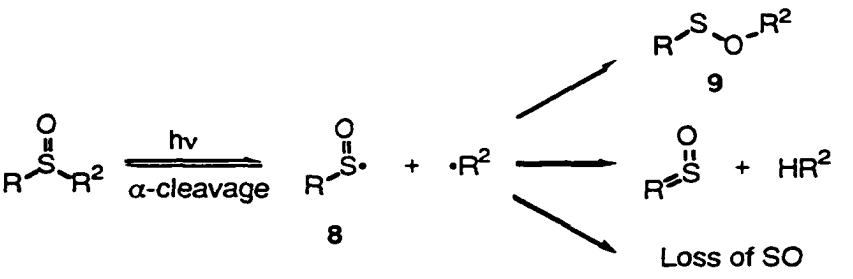

Evidence for the α-cleavage mechanism is illustrated by the direct detection of several sulfinyl radicals and their spin trapping products in steady state electron paramagnetic resonance experiments (epr) at low temperatures.[12-15] Lüdersdorf and coworkers have also used chemically induced nuclear polarization (CIDNP) to investigate the α-cleavage reaction (see sec 2.3.1).[16,17] Recently, the phenyl sulfinyl radical was directly observed at room temperature by flash photolysis and studied computationally.[18] A detailed discussion of the sulfenic esters and sulfinyl radicals can be found in the second half of this dissertation. Nonetheless, the α-cleavage reaction can be divided into several major categories dialkyl, benzylic, aryl alkyl, diaryl systems, and extrusion.

1.3.1 α-Cleavage of dialkyl systems

The prototype for dialkyl sulfoxide photochemical investigations is generally dimethyl sulfoxide (DMSO). In the early 1960's, several authors investigated the photolysis of DMSO both under direct and sensitized conditions. Irradiation of neat liquid DMSO led

to the formation of methane, ethane and carbon monoxide.[19] The methane and ethane were suggested to be α-cleavage products and the carbon monoxide was said to originate from over oxidation of the methyl radical and formaldehyde. Sensitized photolysis of DMSO led only to the formation of the corresponding sulfone and sulfide.[20,21] Gollnick *et al.* investigated the direct and sensitized photolysis of DMSO more extensively.[4] It was concluded that the excited state singlet could follow one of three pathways. Path A is an α-cleavage to form the methyl sulfinyl and methyl radicals. Path B is a bimolecular disproportionation to form sulfone and sulfide, and path C is the deactivation of the excited state sulfoxide to the ground state.

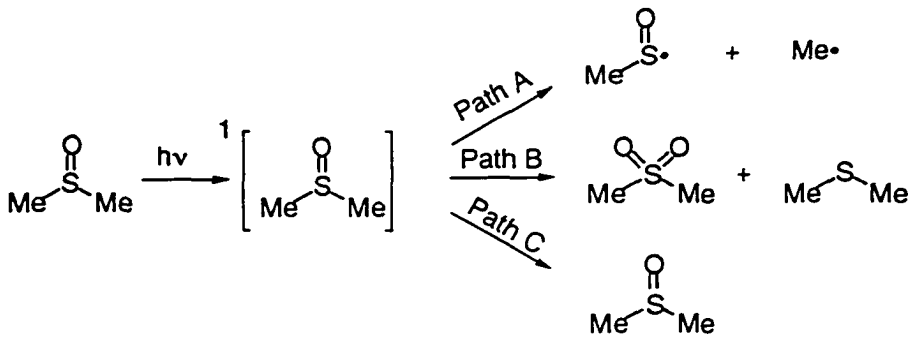

Other dialkyl sulfoxides investigated include di-*n*-butyl and di-isopropyl sulfoxides.[22] The products formed in the butyl sulfoxide case were *n*-butyraldehyde, *n*-butyl mercaptan, and di-*n*-butyl disulfide. The products obtained from the di-isopropyl sulfoxide were acetone and diisopropyl disulfide. These products led the authors to suggest that homolysis, presumably α-cleavage, was required for the formation of the aldehyde products.

Recently, the gas phase photolysis of DMSO at 193 nm was investigated using molecular beam time of flight mass spectrometry (TOF).[23] In this work several reaction channels were investigated for the $(CH_3)_2SO$. Analysis of the TOF data show that methyl, methyl sulfinyl and SO radicals were all detected as products. This was taken as support for

the $CH_3SO\bullet$ + $CH_3\bullet$ reaction is an important decomposition pathway for photolysis of DMSO at 193 nm. It was suggested the SO was formed secondary photolysis of DMSO and about 55% of the methyl sulfinyl radical underwent this decomposition.

1.3.2 α-Cleavage of benzylic sulfoxides

Although dibenzyl systems are technically dialkyl systems, the presence of the aryl groups makes their photochemistry very similar to diaryl systems, and their photochemistry may be due to the phenyl chromophore. Nonetheless, the α-cleavage reaction is expected to be more favored in this system due to the formation of two stabilized radicals, the benzylsulfinyl radical **10** and the benzyl radical **11**. In the mid 1960's, Sato and co-workers showed the photolysis of dibenzyl sulfoxide led to the formation of benzyl mercaptan (isolated as dibenzyl disulfide **16**), benzaldehyde **14**, dibenzyl **15**, and benzyl alcohol **17**.[24] Current understanding would account for these products in the following way.

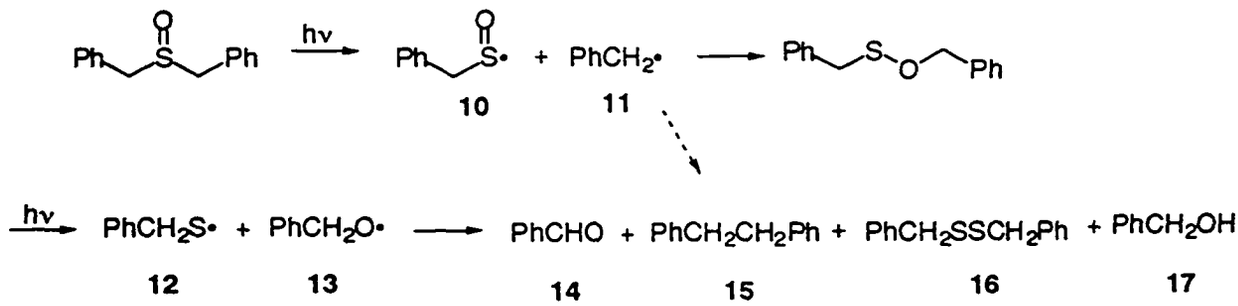

1.3.3 α-Cleavage of alkyl aryl and diaryl sulfoxides

There have been many different diaryl and alkyl aryl systems investigated which have been suggested to undergo α-cleavage upon photolysis.[5,11] Because of this, only a few of the more interesting cases will be commented on here. Probably the biggest advantage alkyl aryl and diaryl sulfoxides have over dialkyl sulfoxides is that their UV absorption is red shifted (lower in energy) when compared with those of the dialkyl sulfoxides. Kharasch and

coworkers isolated biphenyl, diphenyl disulfide, and phenol from the photolysis of diphenyl sulfoxide in benzene.[25] The formation of the diphenyl disulfide has since been shown to be formed by secondary photolysis of the sulfenic ester.[26]

In the late 1970's, several diaryl sulfoxides **18** were investigated using electron spin resonance esr spectroscopy.[13,15] Weak esr signals were detected at low temperatures that were assigned to the aromatic sulfinyl radicals.

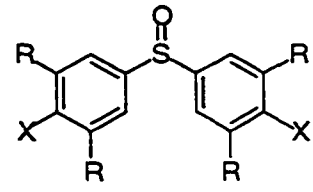

R = H, *t*-Bu
X = H, Me, Br, OH

18

Still and coworkers have investigated a series of substituted thiochromanone sulfoxides.[27-29] From these investigations it was suggested that three major types of reactions can be observed. The first type of reaction is observed when electron-donating substituents are located on the aryl ring (Figure 2). A surprising aryl-sulfur α-cleavage reaction was suggested to explain the resulting disulfide product **21** in 10% yield. Despite the low yield, no other products, save 40% starting material, were characterized. In support of the mechanism shown in Figure 1, labeling studies showed the phenolic oxygen originated from the sulfoxide oxygen.[27]

The second type of reaction was observed in systems that were substituted in the ß position to the sulfoxide (Figure 3).[29] The fundamental difference between the mechanism proposed in Figures 2 and 3 is the orientation of the α-cleavage. The yield of the observed products are higher in this system (2-benzoylisobutyraldehyde 31% and benzoic acid 12%).

Two mechanisms were proposed for this reaction both of which undergo an α-cleavage reaction. In the first mechanism α-cleavage leads to the formation of the sulfinyl

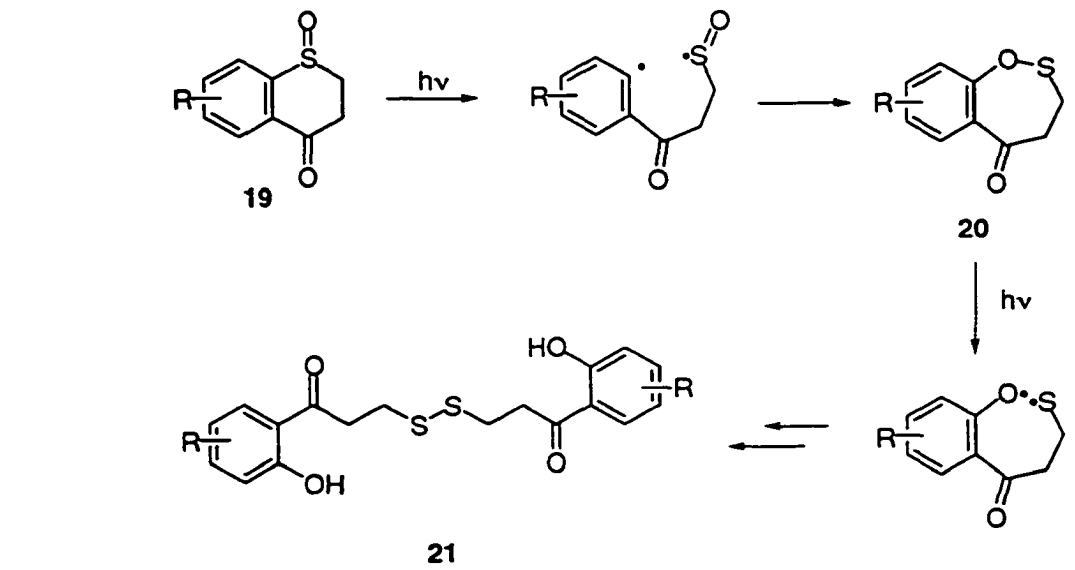

Figure 2. Photolysis of systems with electron donating groups on aryl ring.

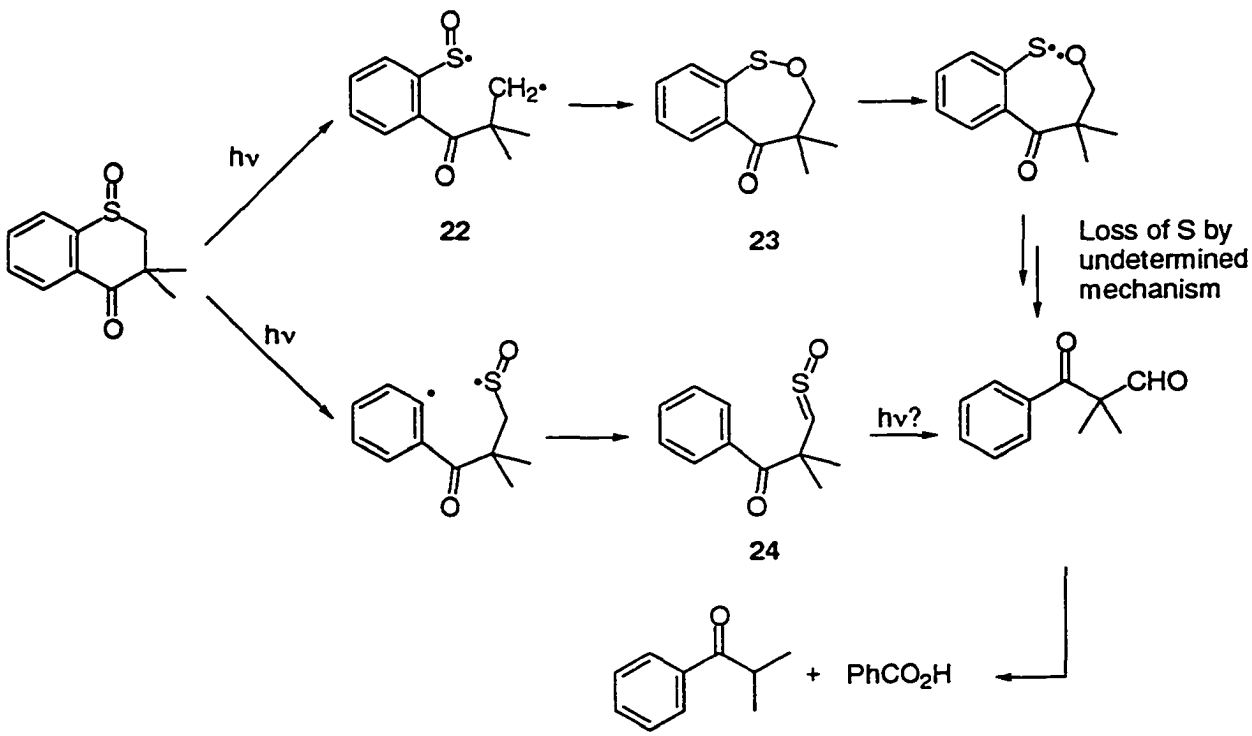

Figure 3. Proposed mechanism for substituted thiochromanone systems

radical **22** and primary alkyl radical. Subsequent recombination forms the sultene **23**. The second mechanism leads to the formation of the radicals centered on the phenyl ring and on the sulfur. An intramolecular hydrogen atom transfer leads to the formation of the sulfine **24**.

The third type of reaction observed with the thiochromanone system is observed when there is substitution at the α position to the sulfoxide.[29] Although this reaction was suggested to go via a hydrogen abstraction reaction, the results can also be explained by an α-cleavage reaction (see Section 1.3)

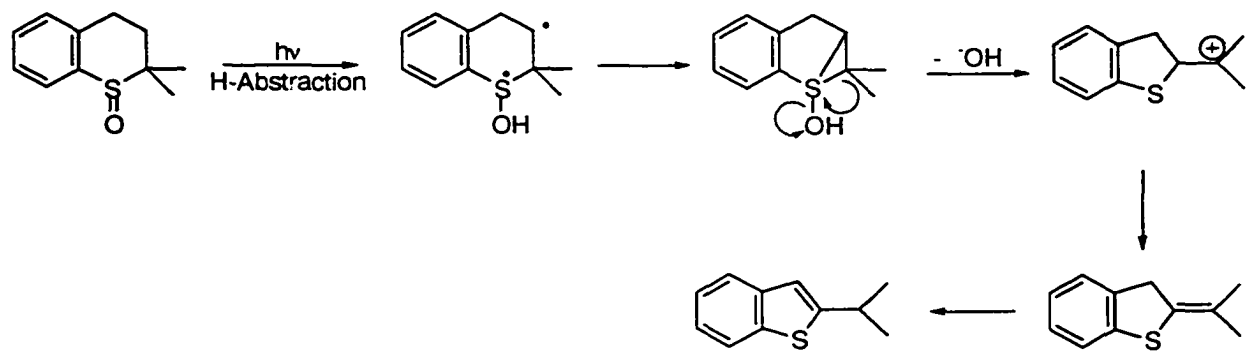

Another interesting example of sulfoxide α-cleavage is found in the photolysis of several aryl substituted 1,4-dithiin sulfoxide **25**, Figure 4.[30] The interest here is that thermolysis of these molecules lead to an extrusion of SO followed by a ring-contracting rearrangement. Under photolysis conditions, however, the extrusion reaction is not observed, but the ring contraction remains and forms **26** and **27**.[30,31] The initial process for the proposed mechanism for this reaction was again an α-cleavage.

Another system of interest in terms of the α-cleavage reaction is the aryl benzyl system investigated by Jenks and Guo.[26] This system is of particular importance to the computational work presented in the second half of this dissertation and, therefore, it is discussed in detail in Section 3.1.

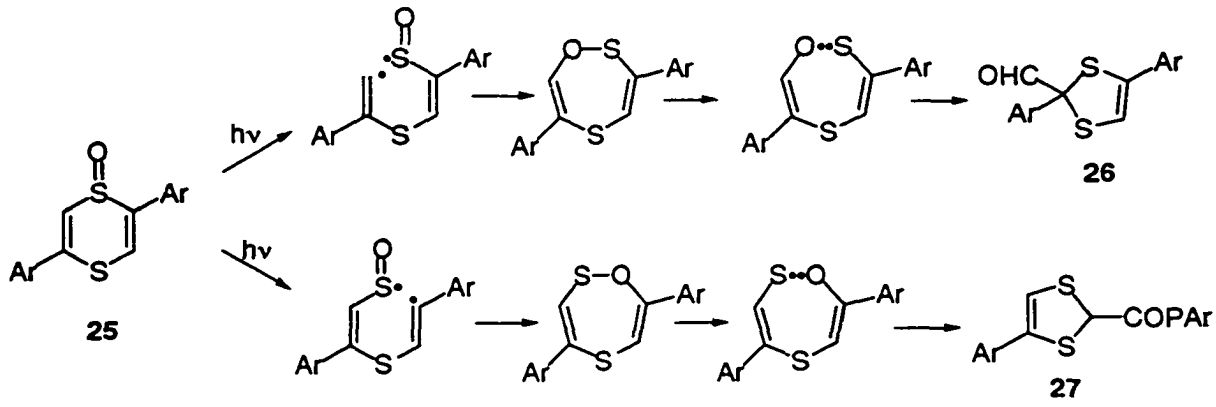

Ar = C_6H_6, *p*-ClC_6H_5, *p*-$CH_3C_6H_6$

Figure 4. Photolysis of substituted 1,4-dithiin sulfoxide.

1.4 SO extrusion reactions of sulfoxides

Although it is not as common as loss of SO_2 from sulfones, certain sulfoxides have been shown to undergo SO photoextrusions. It should be noted that loss of SO is not a general process and is generally limited to cases were there is a substantial driving force to drive the second step in a stepwise extrusion pathway.

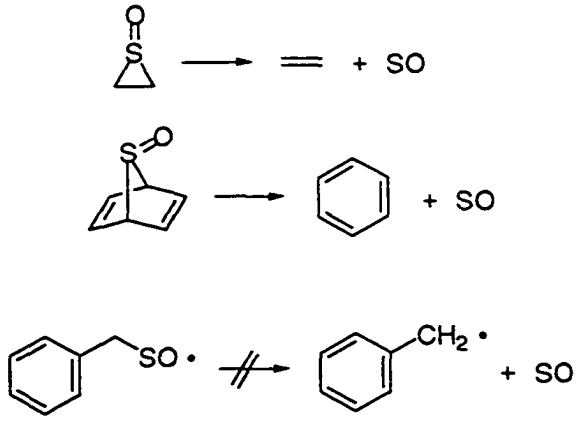

The reaction involves the cleavage of two C-S bonds and is generally observed in strained cyclic systems. In principle, the reaction can proceed either in a stepwise or concerted fashion. Although research in this area is lacking, the work done thus far seems to support a stepwise mechanism.[32]

Among the earliest work done on SO photoextrusions was done on a series of highly substituted thiophene sulfoxides **28** by Kellogg and Prins.[32] The major products formed in this reaction were substituted dienes with mixed stereochemistry. From these results, the authors suggest there is a biradical intermediate.

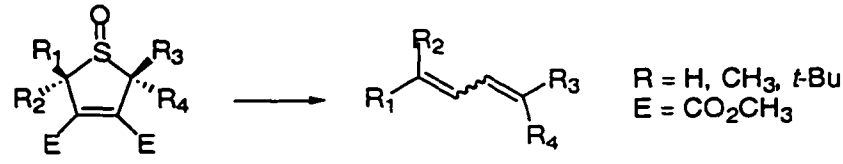

28

Several years later, Carpino showed photolysis of 2,3-diphenylthiirene 1-oxide **29** yielded diphenylacetylene **30** nearly quantitatively. However, thermolysis of **31** gave benzil as the only product. In this system, the authors also suggest a biradical type intermediate, however, a concerted mechanism could not be ruled out.

Recently, Kato and coworkers observed SO extrusion in the photolysis of **32**. The products were formed by extrusion of the SO and decomposition of the cyclopropane ring.

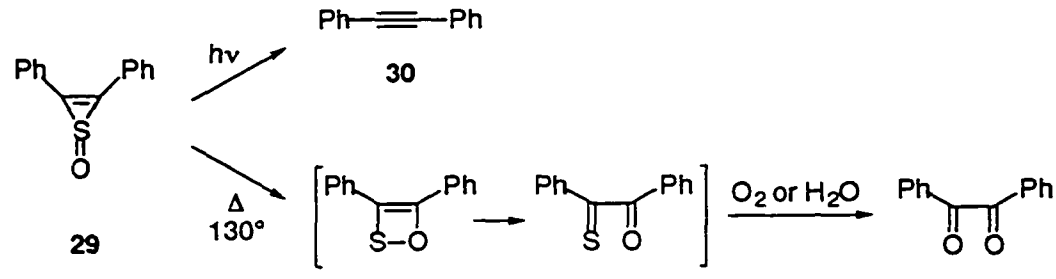

29

31

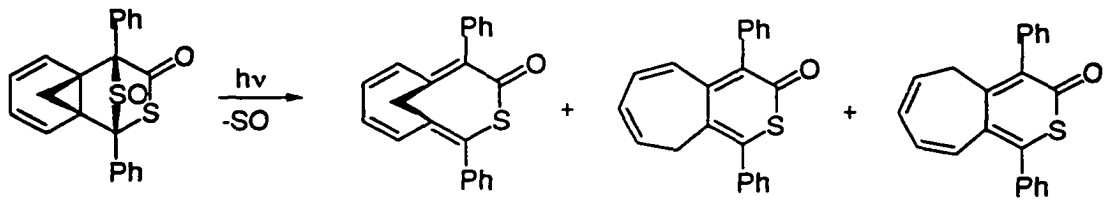

32

1.5 Hydrogen abstraction

Another reaction that has been invoked in sulfoxide photochemistry is the hydrogen abstraction reaction. This reaction draws an analogy from hydrogen abstraction observed in carbonyl photochemistry. However, it should be noted that although it is reasonable to suggest a hydrogen abstraction mechanism, there exists little actual evidence for it.[5] In fact, much of the observed chemistry that has been proposed to go through hydrogen abstraction can also be explained by the α-cleavage mechanism. Because of this, all of a examples given below will be written with both the hydrogen abstraction mechanism and an α-cleavage mechanism.

Most often hydrogen abstraction has been proposed to be the main mode of reaction in cyclic systems.[33,34] Archer and Kitchell were amongst the first to suggest the hydrogen abstraction mechanism to explain the products formed in the photolysis of 2,2-dimethylthiachroman-1-oxide **33**. The major product was 2-isopropylbenzothiophene **34**. The proposed mechanism is shown below in Figure 5.

Similarly, Schultz and Schlessinger invoked the hydrogen abstraction reaction to explain the photolysis of a disubstituted naphthalene system **35**.[33] Experiments with labeled hydrogens showed that only the hydrogen that was proposed to be abstracted was lost in the reaction. However, like the other examples presented thus far, the results of this reaction can be explained by invoking the α-cleavage mechanism (Figure 6).

Recently, Jenks and Guo investigated the hydrogen abstraction mechanism with system designed to favor both ß- and γ-hydrogen abstractions.[26] Two of the systems

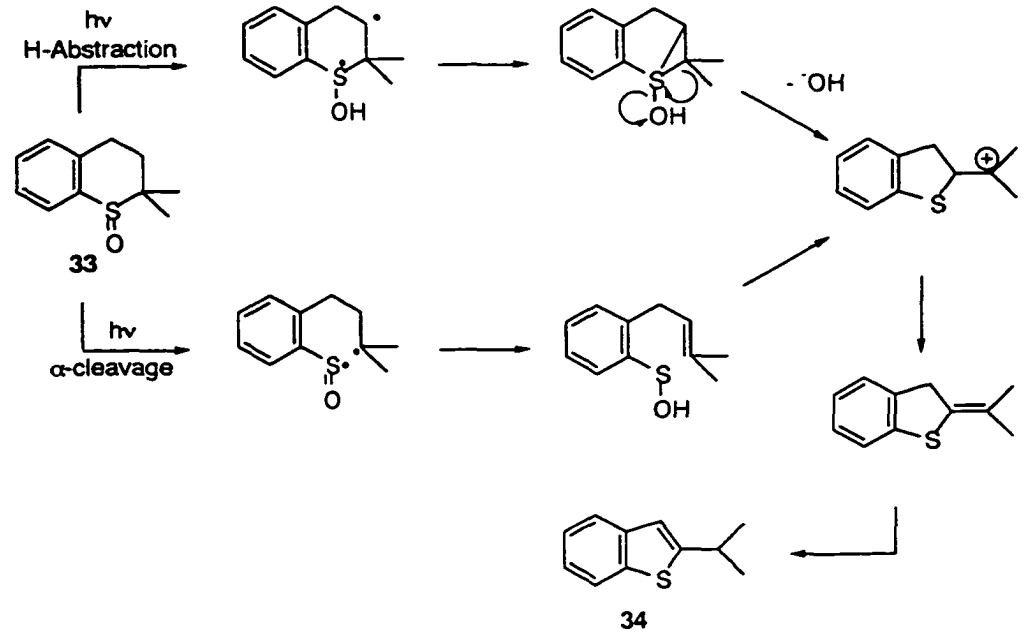

Figure 5 Photolysis of 2,2-dimethylthiachroman-1-oxide **33**

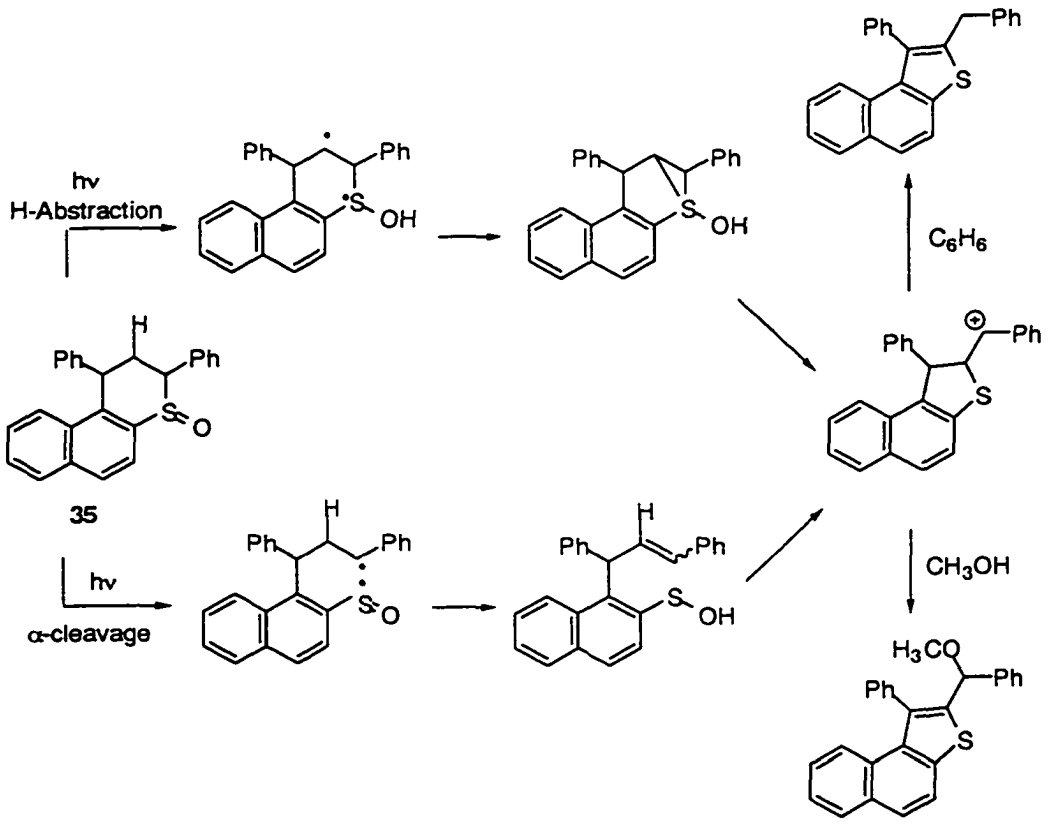

Figure 6 Photolysis of a disubstituted naphthalene system

investigated are shown below (Figure 7). All attempts to isolate products that could be formed only by the hydrogen abstraction mechanism failed. Thus, even though hydrogen abstraction can not be completely ruled out, there remains little evidence for it.

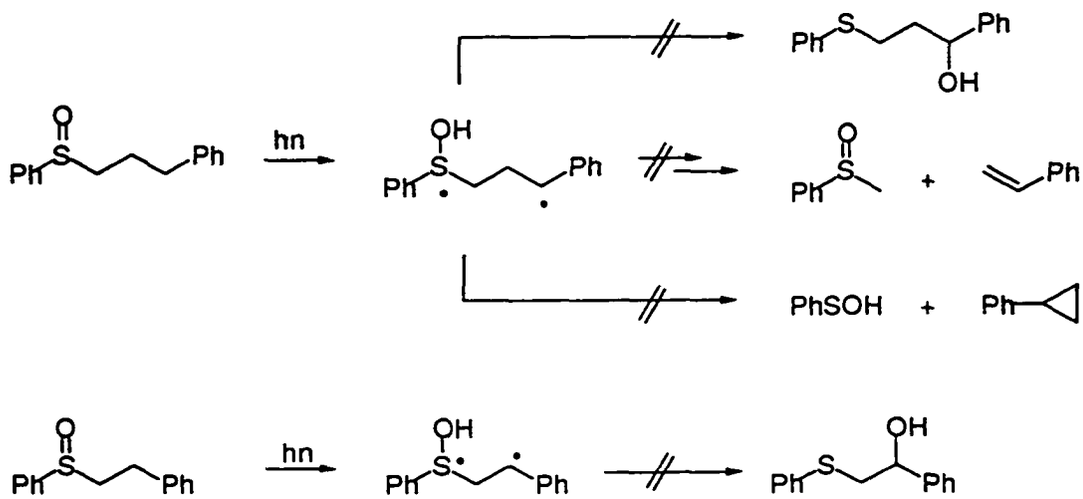

Figure 7 Photolysis of system designed to favor ß- and γ-hydrogen abstractions

1.6 Stereomutation

As mentioned above, the sulfoxide functional group is a stereogenic center when two different organic groups are attached, and thus their potential usefulness in organic chemistry is very high. In order to fully utilize the sulfoxides as chiral auxiliaries, a knowledge of both their thermodynamic and photolytic configurational stability is very important.

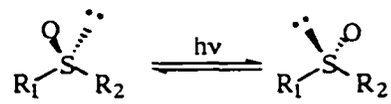

Despite this fundamental importance, little work has been done to investigate the photolytic stability of chiral sulfoxides.

There are at least two different mechanisms that can explain photochemical stereomutation that is observed. The first is an α-cleavage reaction followed by

recombination of the radical pair shown in Figure 6. Another plausible explanation for the stereomutation shown in Figure 5 is the direct inversion of the sulfoxide in the excited state where the inversional barrier could be small. Evidence is mounting that photochemical stereomutation of sulfoxides is a competition between both of these mechanism.[26,35]

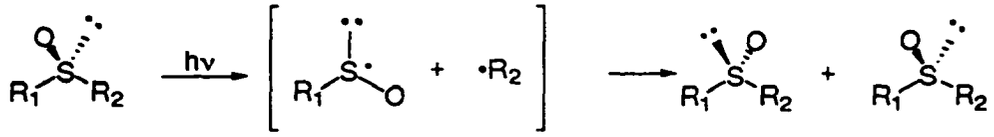

Figure 5. Photostereomutation via the α-cleavage mechanism.

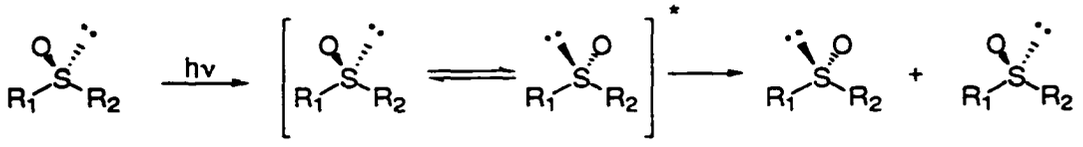

Figure 6. Photostereomutation via the direct inversion mechanism.

Mislow and coworkers conducted most of the characterization and mechanistic work done on thermal stereomutations of sulfoxides.[36-38] Mislow, along with Hammond, was also involved in much of the early photostereomutation work.[39-43] Several important trends were established from this work. First, there are substantial structural effects on sulfoxide racemization. Second, both direct and sensitized photostereomutation could be accomplished. However, direct photolysis generally led to increased decomposition compared to sensitized photolysis. Third, both intramolecular and intermolecular photosensitization could be accomplished. Fourth, dialkyl sulfoxides decomposed without any observable stereomutation in both direct and sensitized experiments. Because the arene group seemed to be required for stereomutation, the authors proposed the active intermediate was an exciplex.[43] Additional evidence in support of this was recently obtained by Charlesworth and coworkers.[44]

Further investigations into the photostereomutation mechanism were done by Kropp and coworkers.[45] Photolysis of phenyl norbornyl sulfoxides led to the formation of both products **36** and **37** along with other rearrangements. The important point here is the presence of a second stereogenic center on the norbornane ring. The isolation of both **36** and **37** supports the α-cleavage mechanism.

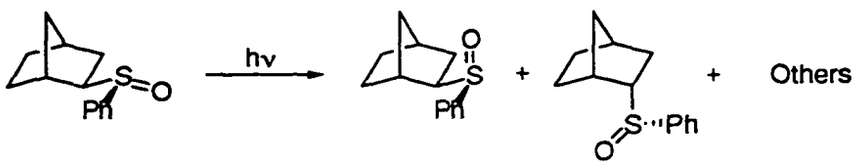

36 **37**

Evidence that there may be additional mechanisms competing with the α-cleavage reaction is given by Jenks and Guo.[26] In these experiments a comparison of the quantum yield for loss of optical rotation to the quantum yield for loss of starting material was made for several sulfoxide systems. It was found that the loss of optical rotation was much higher than the loss of starting material for compounds expected to be poor α-cleavage substrates, which suggests the α-cleavage reaction is not the only reaction taking place that leads to stereomutation.

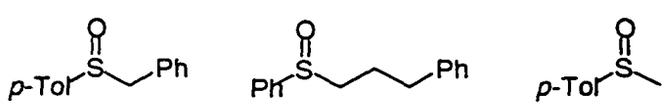

Φ (loss cf optical rotation)	0.42	0.81	0.83
Φ (loss of starting material)	0.21	0.04	0.04

References

(1) Dosugi, H.; Kanno, O.; Uda, H. *Tetrahedron: Asymmetry* **1994**, 1139-1142.

(2) Solladie, G.; Huser, N. *Tetrahedron: Asymmetry* **1994**, *5*, 255-260.

(3) Marino, J. P.; de Dios, A.; Anna, L. J.; de la Pradilla, F. *J. Org. Chem.* **1996**, *61*, 109-117.

(4) Gollnick, K.; Stracke, H. U. *Pure Appl. Chem.* **1973**, 217-245.

(5) Jenks, W. S.; Gregory, D. D.; Guo, Y.; Lee, W.; Tetzlaff, T. In *Organic Photochemistry*; V. Ramamurthy and K. S. Schanze, Ed.; Marcel Dekker, Inc.: New York, 1997; Vol. 1; pp 1-56.

(6) Chen, X.; Asmar, F.; Wang, H.; Weiner, B. R. *J. Phys. Chem.* **1991**, *95*, 6415-6417.

(7) Jenks, W. S.; Lee, W.; Shutters, D. *J. Phys. Chem.* **1994**, *98*, 2282-2289.

(8) Block, E. *Quarterly Reports on Sulfur Chem.* **1969**, *4*, 315-326.

(9) Still, I. W. J. In *Studies in Organic Chemistry 19*; F. Bernard; I. G. Csizmadia and A. Mangini, Ed.; Elsevier Science Publishers B. V.: Amsterdam, 1985; pp 596-659.

(10) Coyle, J. D. *Chem. Soc. Rev.* **1975**, *4*, 523-533.

(11) Still, I. W. J. In *The Chemistry of Sulfones and Sulfoxides*; S. Patai; Z. Rappaport and C. J. M. Stirling, Ed.; John Wiley & Sons Ltd.: New York, 1988; pp 873-887.

(12) Chatgilialoglu, C.; Gilbert, B. C.; Kirk, C. M.; Norman, R. O. C. *J. Chem. Soc. Perkin Trans 2* **1979**, 1084-1088.

(13) Chatgilialoglu, C.; Gilbert, B. C.; Gill, B.; Sexton, M. D. *J. Chem. Soc. Perkin Trans. 2* **1980**, 1141-1150.

(14) Gilbert, B. C.; Kirk, C. M.; Norman, O. C.; Laue, H. A. H. *J. Chem. Soc. Perkins 2* **1977**, 497-501.

(15) Gilbert, B. C.; Gill, B.; Sexton, M. D. *J. Chem. Soc. Chem. Commun.* **1978**, 78-79.

(16) Muszkat, K. A.; Praefcke, K.; Khait, I.; Lüdersdorf, R. *J. Chem. Soc. Chem. Commun.* **1979**, 898-899.

(17) Khait, I.; Lüdersdorf, R.; Muszkat, K. A.; Praefcke, K. *J. Chem. Soc., Perkins Trans 2* **1981**, 1417-1429.

(18) Darmanyan, A. P.; Gregory, D. D.; Guo, Y.; Jenks, W. S.; Burel, L.; Eloy, D.; Jardon, P. *J. Am. Chem. Soc.* **1998**, *120*, 396-403.

(19) Horner, L.; Dorges, J. *Tetrahedron Lett.* **1963**, 757-759.

(20) Schenk, G. O.; Drauch, C. H. *Chem. Ber* **1963**, *96*, 517-519.

(21) Sato, T.; Yamada, E.; Akiyama, T.; Inoue, H.; Hata, K. *Bull. Chem. Soc. Japan* **1965**, *38*, 1225-1225.

(22) Petrova, R. G.; Freidlina, R. K. *Bull. Akad. Sci. USSR Div. Chem. Soc. (Engl. Transl.)* **1966**, 1797-1798.

(23) Zhao, H. Q.; Cheung, Y. S.; Heck, D. P.; Ng, C. Y.; Tetzlaff, T.; Jenks, W. S. *J. Chem. Phys.* **1996**, *106*, 86-93.

(24) Sato, T.; Yamada, E.; Akiyama, T.; Inoue, H.; Hata, K. *Bull. Chem. Soc. Japan* **1965**, 1225-1225.

(25) Kharasch, N.; Khodair, A. I. A. *J. Chem. Soc., Chem. Commun.* **1967**, 98-100.

(26) Guo, Y.; Jenks, W. S. *J. Org. Chem.* **1995**, *60*, 5480-5486.

(27) Still, I. W. J.; Arora, P. C.; Chauhan, M. S.; Kwan, M. H.; Thomas, M. T. *Can. J. Chem.* **1976**, *54*, 455-470.

(28) Still, I. W. J.; Cauhan, M. S.; Thomas, M. T. *Tetrahedron Lett.* **1973**, 1311-1314.

(29) Still, I. W. J.; Thomas, M. T. *Tetrahedron Lett.* **1970**, 4225-4228.

(30) Kobayashi, K.; Mutai, K. *Tetrahedron Lett.* **1981**, *22*, 5201-5204.

(31) Kobayashi, K.; Mutai, K. *Phosph. and Sulf.* **1985**, *25*, 43-51.

(32) Kellogg, R. M.; Prins, W. L. *J. Org. Chem.* **1974**, *39*, 2366-2374.

(33) Schultz, A. G.; Schlessinger, R. H. *Tetrahedron Lett.* **1973**, 4787-4890.

(34) Kampmeier, J. A.; Jordan, R. B.; Liu, M. S.; Yamanaka, H. In *ACS Symposium Series 69. Organic Free Radicals*; Washington, D. C., 1978; pp 275-289.

(35) Schultz, A. G.; Schlessinger, R. H. *J. Chem. Soc. Chem. Commun.* **1970**, 1294-1295.

(36) Rayner, D. R.; Miller, E. G.; Bickert, P.; Gordon, A. J.; Mislow, K. *J. Am. Chem. Soc.* **1966**, *88*, 3138-3139.

(37) Miller, E. G.; Rayner, D. R.; Mislow, K. *J. Am. Chem. Soc.* **1966**, *88*, 3139-3140.

(38) Bickart, P.; Carson, F. W.; Jacobus, J.; Miller, E. G.; Mislow, K. *J. Am. Chem. Soc.* **1968**, *90*, 4869-4876.

(39) Ganter, C.; Moser, J.-F. *Helv. Chim. Acta.* **1971**, *54*, 2228-2251.

(40) Mislow, K.; Axelrod, M.; Rayner, D. R.; Gottardt, H.; Coyne, L. M.; Hammond, G. S. *J. Am. Chem. Soc.* **1965**, *87*, 4958-4959.

(41) Hammond, G. S.; Gottardt, H.; Coyne, L. M.; Axelrod, M.; Rayner, D. R.; Mislow, K. *J. Am. Chem. Soc.* **1965**, *87*, 4959-4960.

(42) Balavoine, G.; Jugé, S.; Kagan, H. B. *Tetrahedron Lett.* **1973**, 4159-4162.

(43) Cooke, R. S.; Hammond, G. S. *J. Am. Chem. Soc.* **1968**, *90*, 2958-2959.

(44) Charlesworth, P.; Lee, W.; Jenks, W. *J. Phys. Chem.* **1996**, *100*, 15152-15155.

(45) Kropp, P. J.; Adkins, R. L. *J. Am. Chem. Soc.* **1991**, *113*, 2709-2717.

CHAPTER II

PHOTO-DEOXYGENATION OF DIBENZOTHIOPHENE SULFOXIDE: EVIDENCE FOR A UNIMOLECULAR S-O CLEAVAGE MECHANISM

Partially based on a paper published in the *Journal of American Chemical Society*[1]

Daniel D. Gregory, Zehong Wan, and William S. Jenks

Abstract: Photolysis of dibenzothiophene sulfoxide results in the formation of dibenzothiophene and oxidized solvent. Though quantum yields are low, chemical yields of the sulfide are quite high. Yields of the oxidized solvents can also be high. Typical products are phenol from benzene, cyclohexanol, and cyclohexene from cyclohexane and 2-cyclohexenol and epoxycyclohexane from cyclohexene. A number of experiments designed to elucidate the mechanism of the hydroxylation were carried out, including measurements of quantum yields as a function of concentration, solvent, quenchers, and excitation wavelength. These data are inconsistent with a mechanism involving a sulfoxide dimer, which also does not properly account for the solvent oxidations. It is suggested that the active oxidizing agent may be atomic oxygen $O(^3P)$ or a closely related noncovalent complex, based on the nature of the oxidation chemistry, comparison to known rate constants for $O(^3P)$ reactivity, and quantum yield data.

2.1 Introduction

One of the most interesting photoreactions of sulfoxides is the photo-deoxygenation reaction. In this reaction, the sulfoxide, upon absorption of a photon of light, undergoes extrusion of the oxygen atom to form the sulfide and oxidized solvent. The interest in this reaction stems from the fact no analogy to this reaction is observed in ketone photochemistry.

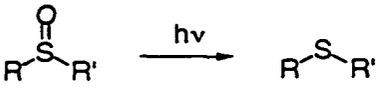

There have been several sulfoxide systems that have been reported to undergo photo-deoxygenation to varying extents. Among the earliest reported systems were those reported by Shelton and Posner. In the early 1970's, Shelton showed *t*-butyl phenyl sulfoxide **3** produced a small amount of the corresponding sulfide upon photolysis.[2] At about the same time Posner showed that methyl phenyl sulfoxide **1** and diphenyl sulfoxide **2** also deoxygenated upon photolysis.[3] In the mid 1980's, Still investigated a series of thiochromanones. Although the primary photochemistry for the thiochromanones was α-cleavage, compound **4** and **5** were shown to also undergo a significant amount of deoxygenation.[4-7] This led to the suggestion that deoxygenation will only occur if more common photoreactions such as α-cleavage are energetically disfavored.[8] This is consistent with the fact that, in most cases, deoxygenation seems to be only a minor pathway followed.

An exception to this is dibenzothiophene sulfoxide (DBTO) **6**. In the photolysis of DBTO, deoxygenation is essentially the only photoreaction observed. The photophysics and

photochemistry of **6** is discussed in Section 2.5. Other systems that undergo deoxygenation to a much lesser extent were reported by Lüdersdorf and Kobayashi (**7-9**).

Even though the photo-deoxygenation reaction has been observed to varying extents in several systems, [2-4,7,9,10] its mechanism is still unclear. One important mechanistic result, which should be mentioned at the onset of this discussion, is the reaction is not a simple disproportionation reaction where two sulfoxides form one sulfone molecule and one sulfide molecule (Figure 1). Even though disproportionation reactions are common in the photolysis of small dialkyl sulfoxides such as dimethyl sulfoxide (DMSO), the sulfone is not observed in any of these systems discussed in this manuscript.

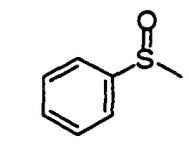

1

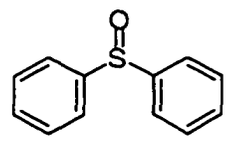

2

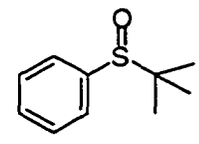

3

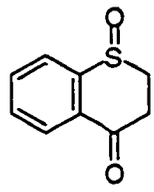

4

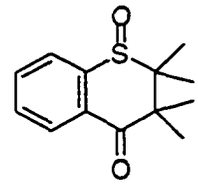

5

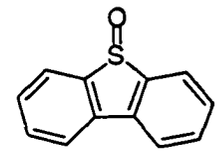

6

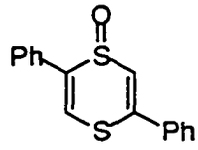

7

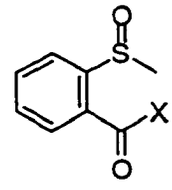

8

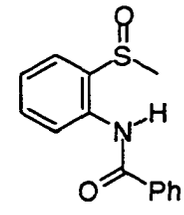

9

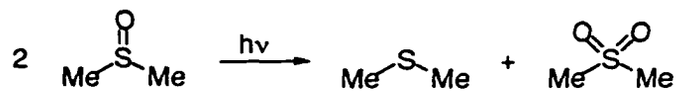

Figure 1. Disproportionation reaction of DMSO

Several mechanisms for the photo-deoxygenation of sulfoxides had been proposed in the literature prior to this investigation. However, even though there were some unanswered questions about each of these mechanisms, little work was done to support or refute them. Thus, they provided a good starting point for the current research. Each of the proposed mechanisms will be discussed individually in the following sections.

2.2 Dimer mechanism

The first mechanism for the photo-deoxygenation of sulfoxides was suggested almost simultaneously by Posner *et al.*[3] and Shelton *et al.* [2] in 1973. It consisted of a triplet excited state sulfoxide coupling with a ground state sulfoxide to form a triplet, peroxide type, diradical intermediate **10**. The diradical **10** then decomposed to form molecular oxygen and the corresponding sulfide. This mechanism will be referred to as the dimer mechanism and is illustrated in Figure 2.

Although not explicitly stated, Posner and Gurria suggested the photodeoxygenation of dibenzothiophene sulfoxide **6** (DBTO) proceeded through a triplet dimer **10**. This dimer than decomposes to form dibenzothiophene **11** and singlet oxygen (Figure 3). The assignment of singlet oxygen was based on the isolation of cyclohexenol **12** when **6** was photolyzed in the presence of cyclohexene as a singlet oxygen quencher. Treatment of the resulting reaction mixture with sodium iodide was suggested to cause the decomposition of

the peroxide to the alcohol. However, it was shown later that the NaI reduction was not needed to isolate the alcohol.[11] The suggestion that the NaI reduction was necessary was based on the premise that cyclohexene was a good chemical quencher of singlet oxygen and a hydroperoxide was formed. However, it was shown some ten years later that the cyclohexene is in fact not a particularly good chemical quencher ($k_r = 3 \times 10^3\ M^{-1}s^{-1}$), but it is a fairly good physical quencher ($k_q = 1.6 \times 10^5\ M^{-1}s^{-1}$).[12]

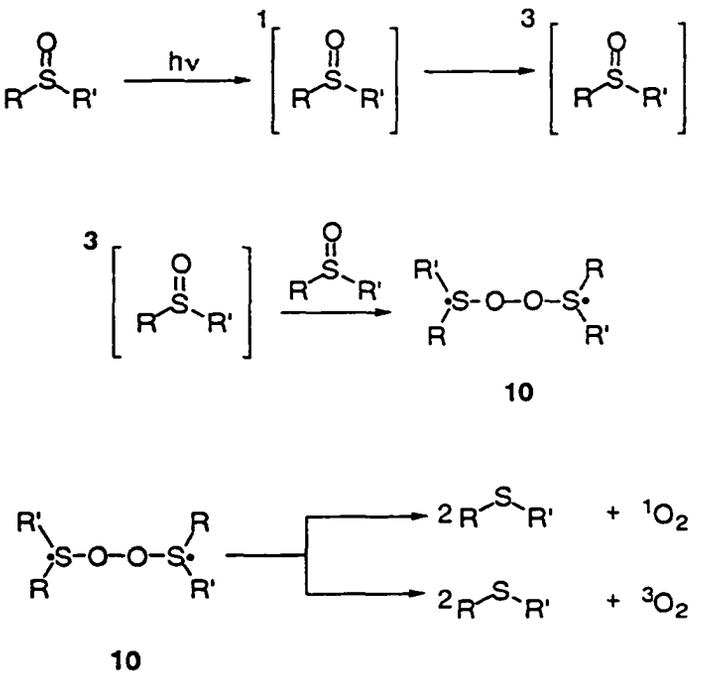

Figure 2. Photo-deoxygenation by the dimer mechanism

The assignment of an excited triplet state being the reactive state in the photo-deoxygenation of DBTO was based on the observation that sensitized experiments lead only to the corresponding sulfide. This was further supported by the fact that piperylene (a good triplet quencher) could stop the deoxygenation of diphenyl sulfoxide.

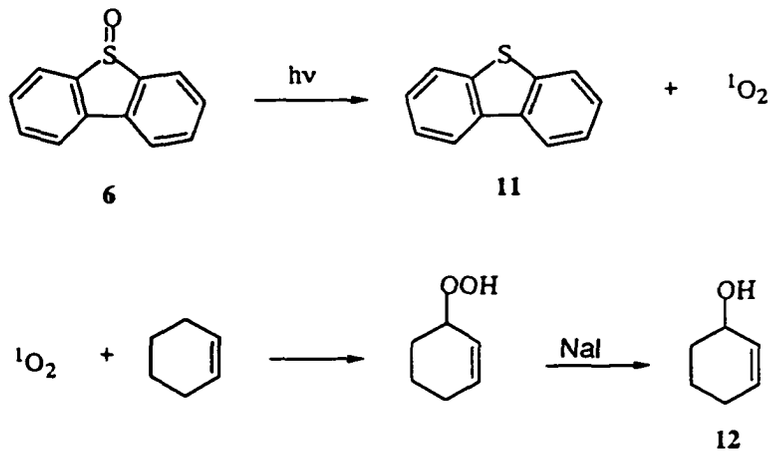

Figure 3. Trapping of singlet oxygen with cyclohexene

Shelton[2] also suggested that, because addition of benzophenone as a sensitizer in the photolysis of diallyl sulfoxide led to an increase in yield of the sulfide, the reaction was taking place out of the triplet state. It is now clear that benzophenone does not have sufficient energy for straightforward triplet energy transfer to diallyl sulfoxide. Based on the observation that all of the sulfides isolated from the photolysis of *t*-butyl methyl sulfoxide contained the same alkyl groups, Shelton suggested that removal of the oxygen from the sulfoxide proceeds without cleavage of either of the C-S bonds. The possibility of the direct transfer of the oxygen atom to an alkyl radical to form alkoxyl and sulfinyl radicals was also considered. However, if this was the major mode of deoxygenation, one would expect to observe an increase in the cross coupling of the sulfinyl radical and alkoxyl radical; such an increase was not observed. This led the authors to explicitly suggest the formation of a triplet diradical intermediate similar to **10**. However, unlike Posner's suggestion, intermediate **3** was suggested to decompose to form the corresponding sulfide and ground state (triplet) molecular oxygen.

The results of work done by Geneste and coworkers[9] on 2-methyl benzothiophene sulfoxide **13** in low yield also led to the suggestion of a dimer mechanism. This suggestion was based on the observation that a plot of $1/\phi$ vs. 1/C yielded a linear relationship as would be expected for a dimer mechanism. An increase in the quantum yield (ϕ) with the concentration of the sulfoxide is consistent with the notion of two sulfoxide molecules forming a dimer which can then decompose to form the sulfide and molecular oxygen. All attempts to trap the liberated oxygen as had been done by Posner were not successful. Sensitized experiments did not allow for the elucidation of any relationship between the quantum yield and the sulfoxide concentration.

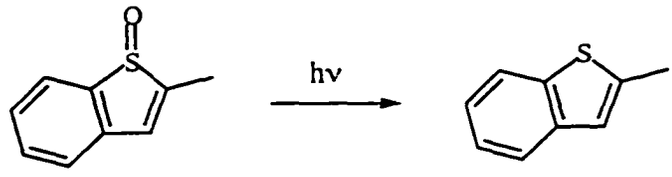

13 **14**

2.2.1 Evidence against the dimer mechanism for DBTO

There are several different aspects in which the dimer mechanism can be experimentally tested. These aspects were investigated using dibenzothiophene sulfoxide (see Section 2.5). First, because the reaction is proposed to take place out of an excited triplet state, the photolysis of the sulfoxide in the presence of a triplet quencher should decrease the quantum yield of deoxygenation. Since the triplet excited state sulfoxide must form a dimer with another ground state sulfoxide, one would expect the lifetime of the triplet

state would be sufficiently long to allow for triplet quenching. However, photolysis of DBTO in the presence of several triplet quenchers such a isoprene, cyclopentadiene, and oxygen did not lead to a decrease in the quantum yield of deoxygenation.[11]

Another aspect pertaining to the dimer mechanism that can be investigated has to do with the formation of the dimer. Because the mechanism above requires the excited sulfoxide to couple with a ground state sulfoxide, either pre-association of the sulfoxides or mobility in the solvent matrix is required. Preassociation seems unlikely. Mislow has shown that dialkyl sulfoxides do form dimers in solution, but the extent of this dimerization is strongly dependent on the solvent.[13] In ethanol, for example, essentially no dimerization of dimethyl sulfoxide occurs. However, when the solvent is changed to cyclohexane a significant amount of dimerized sulfoxide is observed. Despite this observation for dialkyl sulfoxides, alkyl aryl and diaryl sulfoxides did not show any significant association in either solvent. The observations by Mislow coupled with the insensitivity of the deoxygenation quantum yield to solvent polarity and sulfoxide concentration give strong evidence against preassociation.

The importance of mobility of the sulfoxide in the solvent matrix was investigated by photolyzing the sulfoxide in a frozen glass matrix. Phosphorescence of DBT **11** at 77 K allowed for its detection in a frozen EPA glass, even at very low concentrations. Again, preassociation seems unlikely given the fact that EPA is polar in nature (with a significant amount of ethanol) and the starting concentration of the sulfoxide is very dilute $\sim 10^{-6}$ M. Photolysis of DBTO in a glass matrix led to the formation of DBT. Thus, it was concluded

that mobility in the solvent matrix is not essential for the photodeoxygenation reaction of dibenzothiophene sulfoxide to occur.[1]

Finally, the dimer mechanism requires an excited state sulfoxide to couple with a ground state sulfoxide to form the dimer intermediate **10**. This suggests that if DBTO was photolyzed in the presence of another sulfoxide, which remained in the ground state, one would expect both of the sulfides would be formed. To investigate this, DBTO was photolyzed (2 mM) at 340 nm in the presence of diphenyl sulfoxide **7** at a wide range of concentrations (0-96 mM). Analysis of the reaction mixture showed the dibenzothiophene **12** was the only sulfide formed. Thus, the formation of sulfoxide dimers seems unlikely.[1]

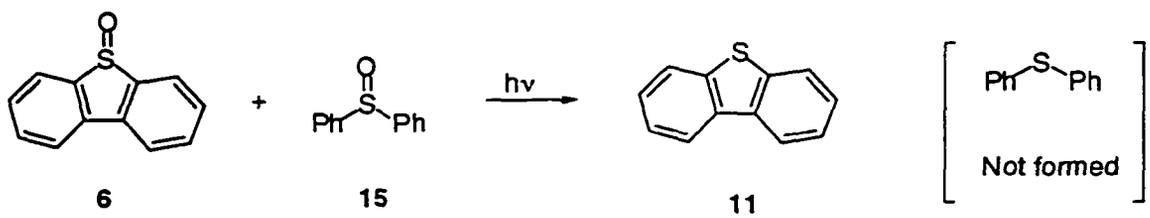

6 15 11

From these experiments it can be concluded that preassociation of the sulfoxides as well as mobility in the solvent matrix are not required for the photo-deoxygenation of dibenzothiophene sulfoxide. This, coupled with the fact that the photolysis of DBTO in the presence of diphenyl sulfoxide led only to the formation of DBT, suggests the dimer mechanism is not the predominant mechanism for the photo-deoxygenation of DBTO.

2.3 Sulfinyl mechanism

A second mechanism for the photo-deoxygenation of sulfoxides was suggested by Lüdersdorf,[14,15] in the early 1980's and will be referred to as the sulfinyl mechanism. The sulfinyl mechanism (Figure 4) was based on a series of CIDNP (chemically induced nuclear polarization) experiments on substituted phenyl methyl sulfoxides **16**. Because the methyl radical showed polarization in the nmr and the phenyl group did not, it was suggested that the first photochemical event was scission of the sulfur methyl bond to form a sulfinyl radical **17** and a methyl radical. This is the very common α-cleavage reaction observed in the photochemistry of many sulfoxide systems. The sulfinyl radical then transfers the oxygen to another radical in solution. The sulfenyl radical **18** resulting from this oxygen transfer then couples with a methyl radical to form the sulfide **19**.

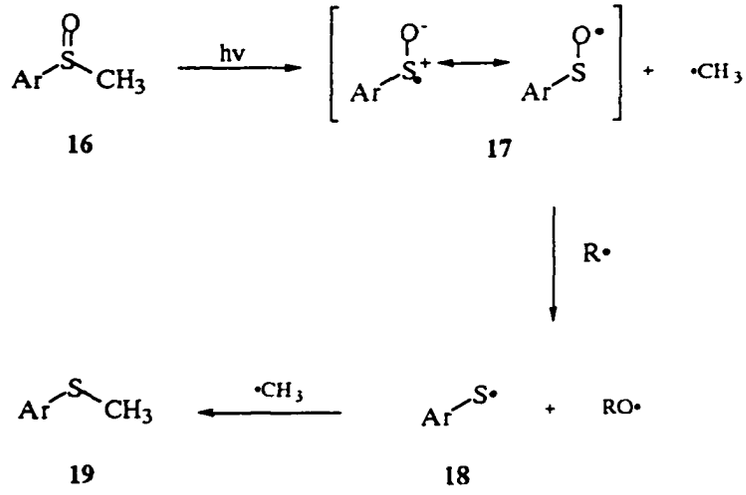

Figure 4. Deoxygenation of a sulfoxide by the sulfinyl mechanism.

2.3.1 Evidence against the sulfinyl mechanism

The major problem with the sulfinyl mechanism has to do with the energetics of the sulfinyl reduction. For phenyl methyl sulfoxide the bond dissociation energy of the S-Me bond (< 55 kcal/mol) is lower than the dissociation energy for the S-C_6H_6 bond (≈66 kcal/mol). Thus, one would expect cleavage of the S-Me bond before the S-Ph bond. However, the transfer of the oxygen atom from the sulfinyl radical to some molecule in the solution is where this mechanism breaks down. Although it was not pointed out explicitly which molecule was oxidized in the reaction, the most reasonable candidate is another methyl radical. The heat of formation for the phenylsulfinyl radical was estimated by Benson at ≈13 kcal/mol.[16] The heats of formation for the methyl radical, methoxy radical, triplet oxygen atom and the sulfenyl radical are all known experimentally.[17] From these values it can be shown that transfer of an oxygen atom from phenyl sulfinyl radical to the methyl radical is endothermic by ≈12 kcal/mol. The epoxidation of ethene (a reaction whose relevance will become clear below) is endothermic by ≈17 kcal/mol. Furthermore, the S-O bond energy for the phenyl sulfinyl radical is estimated at 102 kcal/mol and the C-S bond energy is estimated at 67 kcal/mol. Thus, one might expect SO transfer rather than O transfer in such reactions. Based on these estimates, the sulfinyl mechanism does not seem to be a viable mechanism. The T_1 for the PhSO• is expected to ≤ 10 μs and thus one would not expect these reaction would be fast enough to still yield nuclear polarized products.

2.4 Hydrogen abstraction

Another possible mechanism for the photo-deoxygenation of sulfoxides is referred to as the hydrogen abstraction mechanism and is shown in Figure 5. In this mechanism, which draws an analogy from ketone photochemistry, the excited sulfoxide abstracts a hydrogen from the solvent to form radical **20**. Subsequent decomposition of radical **20** forms the sulfide and a hydroxyl radical or the R• can attack the oxygen atom in an S_H2 type reaction. The hydroxyl radical can then undergo further reaction with the solvent. Regardless of the mechanism, the final products would be dibenzothiophene and oxidized solvent.

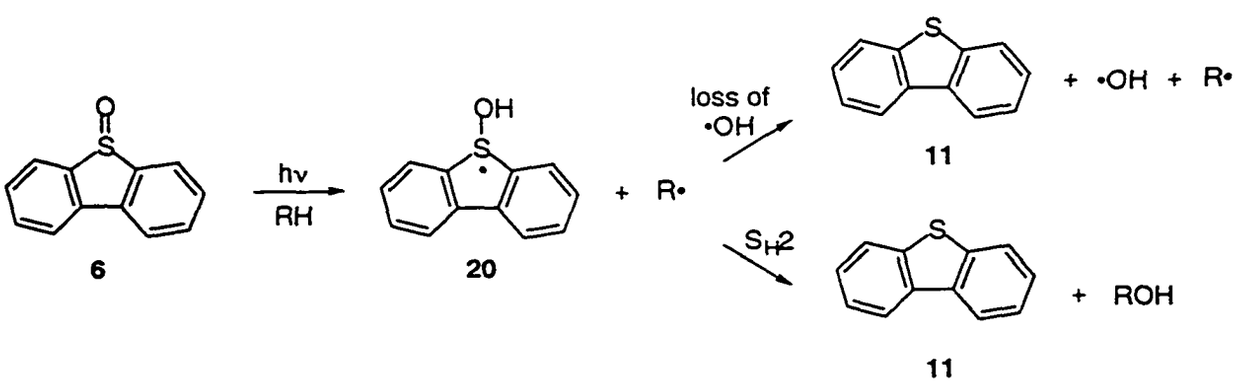

Figure 5. Hydrogen abstraction mechanism.

2.4.1 Evidence against hydrogen abstraction

The hydrogen abstraction mechanism implies that the quantum yield for deoxygenation should be dependent on the hydrogen donating ability of the solvent. One would expect the quantum yield for deoxygenation would be higher in solvents that can donate a hydrogen atom easily. However, as shown in Table 1, the quantum yield of deoxygenation of DBTO is essentially constant in a very wide variety of solvents with

Table 1. Quantum yield for the Formation of DBT in photolysis of DBTO. Uncertainties are ≤ 20%.

Solvent	Quantum yield
acetonitrile	0.0026
benzene	0.0030
cyclohexane	0.0030
cyclohexene	0.0100
2,2-dimethylbutane	0.0029
dimethyl sulfoxide	0.0079
Freon 113(CCl_2FCF_2Cl)	0.0024
hexane	0.0029
2-methylbutane	0.0031
tetrahydrothiophene	0.0085
tetrahydrofuran	0.0028
2-propanol	0.0034

different hydrogen donating abilities. This is taken to the extreme with freon 113, which does not have any hydrogens to abstract. While it is possible to rationalize an increased reactivity in cyclohexene, and tetrahydrothiophene (perhaps electron transfer), it is hard to understand the presence of DMSO in the "high quantum yield" group of solvents for this class of mechanisms. Nonetheless, based on this, the hydrogen atom abstraction mechanism does not seem to explain the experimental results sufficiently. It is important to keep in mind that because back reaction of the reactive intermediates must compete with the path that leads to products, the quantum yield is not always a good indication of the reactivity of the excited state. Wagner and Hammond have shown, at least for the photo-elimination reaction in ketone chemistry, that the quantum yield is not a good indicator of the reactivity of the

ketone excited states because of the variable partitioning of biradical intermediates between starting material and products.[18] In the present system, however, the range of the hydrogen donating ability of the solvents is broad enough to allow one to draw tentative conclusions pertaining to the mechanism somewhat more confidently.

The experimental results presented thus far have raised doubts in all of the previously suggested mechanisms discussed above. The photolysis of DBTO in the presence of several triplet quenchers does not affect the quantum yield for deoxygenation, and the photolysis of DBTO in the presence of Ph_2SO leads only to the formation of DBT. This coupled with the deoxygenation of DBTO in a glass matrix makes the dimer mechanism seem unlikely. The sulfinyl mechanism can be dismissed based on the energetics of the oxygen transfer from the sulfinyl radical. The hydrogen abstraction mechanism seems unlikely based on the consistency of the quantum yield for deoxygenation in a variety of solvents with different hydrogen donating abilities. These results led to another mechanism being suggested that will be referred to the direct cleavage mechanism. The remainder of this chapter will describe the direct cleavage mechanism and discuss the results of experiments designed to gain a better understanding of it.

2.5 Dibenzothiophene sulfoxide

The system chosen as a prototype for the mechanistic work on the photodeoxygenation of sulfoxides was dibenzothiophene sulfoxide (DBTO) **6**. There are several characteristics about DBTO which make it attractive for this study. First, neither dibenzothiophene sulfone nor its photoproducts are produced upon photolysis of DBTO.[19]

This eliminates the possibility of a disproportionation reaction. Although the quantum yield is fairly low, it is possible to get nearly quantitative deoxygenation of DBTO. This shows that, unlike many systems, deoxygenation is the primary photochemical reaction of DBTO. The sulfide produced from the deoxygenation dibenzothiophene (DBT) **11** is photo-inert under the reaction conditions and its absorption spectrum is to the blue (higher in energy) of DBTO. This ensures the products isolated in the photolysis of DBTO do not originate from secondary photolysis of DBT. The disproportionation product (dibenzothiophene sulfone) was also shown to be photoinert under the reaction conditions.[19] The quantum yield for deoxygenation is nearly constant over a wide concentration range. This is important when investigating the photolysis of DBTO at low concentrations.

The UV absorption spectrum corrected for the extinction coefficient for DBTO is shown in Figure 6. The spectrum shows there are three maxima at 240, 280, and 320 nm. The quantum yield for deoxygenation as a function of wavelength is also included in Figure 6. There is an increase in the quantum yield of deoxygenation when moving from the 320 nm to 280 nm maximum. However, a similar increase is not observed when moving from the 280 to 240 nm band. Nonetheless, the quantum yield for deoxygenation is very low over the whole range. Even though the photodeoxygenation of DBTO is an inefficient process, it is essentially the only observable photochemistry and, therefore, it is still photonically useful in terms of a mechanistic product study. Even though the quantum yield for deoxygenation is higher over the 280 nm band than the 320 nm band, most of the experiments were done with light in the 320 nm band. This ensures the DBTO is the major absorber of light. From fluorescence and phosphorescence experiments the singlet energy of DBTO was estimated at

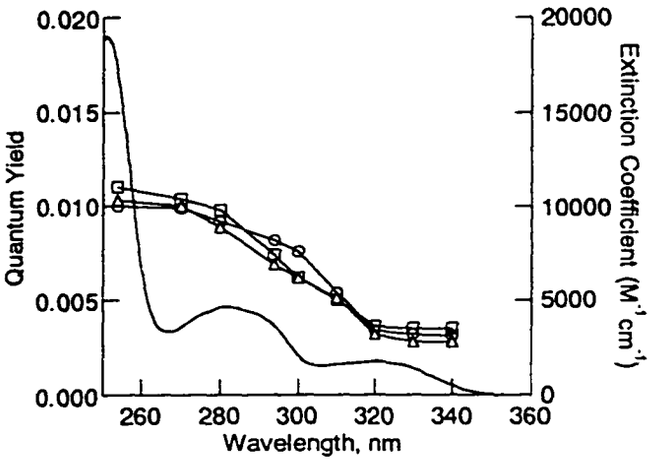

Figure 6. Quantum yield as a function of excitation wavelength and absorption spectrum in THF. Initial concentrations for quantum yields: 0.24 mM in hexane (circles), 1.5 mM in acetonitrile (squares), 3.0 mM in THF (triangles). The line without illustrated points is the absorption spectrum

≈81 kcal/mol and the triplet energy is ≈61 kcal/mol respectively and is slightly variable with solvent.[20]

2.6 Direct cleavage of the S-O bond

The experimental results eliminating the mechanisms discussed in Section 2.1-2.4 led to the suggestion of the direct cleavage mechanism outlined in Figure 7. In this mechanism the S-O bond is cleaved directly to the form the corresponding sulfide and a triplet oxygen atom O(^{3}P). The triplet oxygen then undergoes further chemistry to form oxidized solvent. The direct cleavage mechanism is consistent with all of the experimental data discussed thus far. An important observation not yet discussed is the observed oxidation of the solvents in the reaction. It is clear that an active oxidizing species is produced, which is consistent with an O(^{3}P) atom. The direct cleavage mechanism does not require preassociation or mobility in

the solvent matrix, and the quantum yield for deoxygenation is not expected to depend on the hydrogen donating ability of the solvent. The remainder of this chapter will focus on reviewing the reactivity of the triplet oxygen atom and testing the direct cleavage mechanism experimentally.

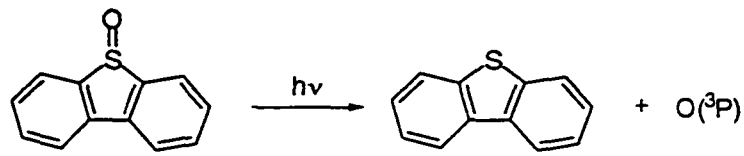

6 11

Figure 7. Direct homolysis of the S-O bond of dibenzothiophene sulfoxide to form a triplet oxygen atom.

2.7 Chemical reactivity of O (^{3}P)

The oxygen atom both in its ground state, O(^{3}P), and first excited state, O(^{1}D), has been suggested to play an important role in both atmospheric and combustion chemistry.[21-23] As a result, the reactivity of both species have been studied extensively in the gas phase,[24,25] but their reactivity in solution has not been well established. The majority of the work done on the O(^{3}P) atom in solution has been limited to water as the solvent.[26-28] The major reason for the lack of O(^{3}P) reactivity data in organic solvents is an organic system that generates triplet oxygen atoms cleanly has not been discovered. Nonetheless, there are several systems that produce low yields of triplet oxygen in solution and have allowed for a partial characterization of its reactivity. These systems include the photolysis of N_2O and organic N oxides.

2.7.1 Photolysis of N_2O

Mazur and coworkers have investigated the reactivity of $O(^1D)$ and $O(^3P)$ in simple alkane solutions by photolyzing N_2O.[29] Photolysis of N_2O with high energy light (184 nm) leads to the formation of $O(^1D)$ as the major form of oxygen and $O(^3P)$ as the minor form (Figure 8). The $O(^1D)$ is formed directly from the excited state N_2O molecule, and the $O(^3P)$ is suggested to form by either collisional deactivation of $O(^1D)$ or by intersystem crossing in the excited N_2O molecule.

$$N_2O \xrightarrow{h\nu} O(^1D) + N_2$$
$$N_2O \xrightarrow{h\nu} O(^3P) + N_2$$
$$O(^1D) \longrightarrow O(^3P)$$

Figure 8. Formation of singlet and triplet oxygen atoms form N_2O.

The observed chemistry of $O(^1D)$ in solution is very similar to that observed in the gas phase. The three major pathways $O(^1D)$ can follow are direct insertion into a C-H bond, hydrogen atom abstraction, and H_2 elimination (Figure 9). In general, the reactivity of $O(^1D)$ is dominated by direct insertion into C-H bonds. Because $O(^3P)$ is in a triplet electronic state, the direct addition to lone pairs and the insertion into C-H bonds are prohibited by a spin barrier. Thus, the hydrogen abstraction reaction is the only reaction available to the $O(^3P)$.

Because $O(^1D)$ is highly energetic, no discrimination between different types of C-H bonds is observed in its reactions with alkanes.[30] This can be seen in the product distribution

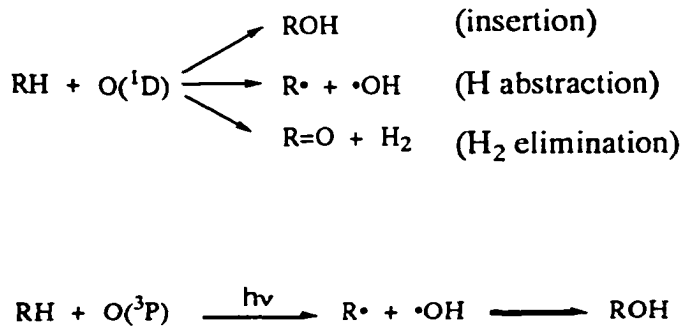

Figure 9. Typical reactions of singlet and triplet oxygen atoms.

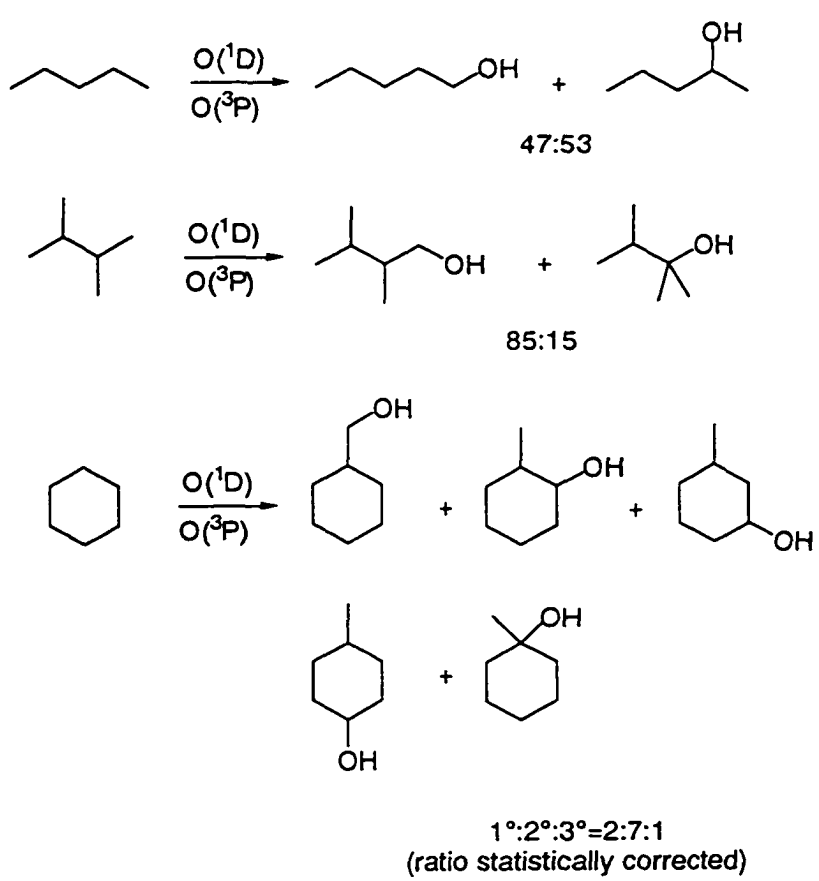

Figure 10. Reactivity of the triplet oxygen atom with alkanes.

of the alcohols formed in the photochemical reaction of N_2O with several alkanes shown in Figure 10.

The small selectivity observed in the product distributions was attributed to the formation of a small amount of $O(^3P)$ and not to $O(^1D)$ reactivity.[30] Another interesting observation is the retention of the *cis* configuration when *cis*-decalin is oxidized with $O(^3P)$. Although this is not surprising with the singlet oxygen atom, where oxidation can occur via C-H insertion, this suggests the oxidation by the triplet oxygen atom may proceed through a tight radical pair which undergoes geminate recombination before inversion to the more stable *trans*-decalin system.

2.7.2 Photolysis of pyridine N-oxide.

Other systems that have been shown to form triplet oxygen upon photolysis are N-oxides.[30] Although photo-deoxygenation of N-oxides is not the main reaction in most systems, several systems have been shown to undergo enough deoxygenation to allow for the investigation of triplet oxygen atom reactivity. There have been several different mechanisms proposed for the deoxygenation of N-oxides (Figure 11). Path **A** was proposed based on results which showed the ratio of deoxygenation vs. rearrangement products were dependent on the concentration of the oxygen acceptor.[31] This suggests both the deoxygenation and rearrangement reactions occur from the same oxaziridine intermediate **21**. Path **A** was also supported by the work of Iwasaki *et al.*[32] who showed the product ratios obtained from photolyses of several N-oxides in dueterated anisole did not compare well with those obtained from the microwave discharge of N_2O. Boyd *et al.* also suggested triplet

atomic oxygen was not produced based on the effect sterics and solvent had on the reaction product mixture.[33] Despite these observations, the dependence of the ratio of deoxygenation vs. rearrangement products on the oxygen acceptor concentration was not observed for several pyridazine and pyridine N-oxides. This led to the suggestion that the photo-deoxygenation of these systems proceeded from the direct cleavage of the N-O bond to form $O(^3P)$.[32] Scaiano and Bücher, at least for pyridine N-oxides, gave further support for the direct cleavage mechanism.

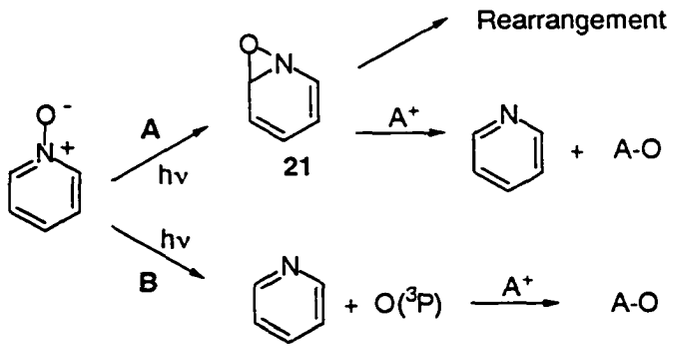

Figure 11. Two proposed mechanisms for the deoxygenation of N-oxides.

Recently, Scaiano and Bücher have investigated the deoxygenation of pyridine N-oxides using laser flash photolysis.[34] When pyridine N-oxide was photolyzed at 308 nm in cyclohexane or toluene no transient was detected and only the simultaneous formation of products was observed. However, when acetonitrile was used as the solvent, a weak transient was observed at 330 nm with a lifetime of ~ 60 μs. It was suggested the species leading to the transient was a complex between the triplet oxygen atom and acetonitrile **22**.

$$O(^3P) + CH_3CN \longrightarrow CH_3CNO$$
22

There are several pieces of evidence that supports the hypothesis of the formation of an $O(^3P)$/acetonitrile complex in the photolysis of pyridine N-oxides. First, no transient with a decay rate corresponding to the formation of the oxaziridine intermediate **21** was detected. This is consistent with an $O(^3P)$, which is not expected to have an absorption. Second, the reactivity of the oxidizing species is very high. The reaction rate constants of the transient species with Br^- and triethyl phosphite were estimated at 2.0×10^{11} and 3.8×10^{10} M^{-1} s^{-1} respectively. Although the diffusional constants for atomic oxygen are not known, estimates using neon suggest they should be 2-3 times larger than an oxygen molecule and 5-10 times larger than typical organic molecules. Thus, one would expect the rate constant given above would be too fast for molecular oxygen and even very small organic molecules. Third, the selectivity and reactivity of the complex with acetonitrile compares very well with gas phase and aqueous data for $O(^3P)$. Rate constants for the reaction of $O(^3P)$ with several organic substrates were estimated by the transient decay of the complex when photolyzed in several solvents. The estimated reaction rate constants of $O(^3P)$ with several organic molecules are shown in Table 2.

Several general trends can be established from this data. First, a primary kinetic isotope effect can be observed for cyclohexane/cyclohexane-*d*-12. This is consistent with hydrogen atom abstraction by the $O(^3P)$ as the rate limiting step. Second, an inverse secondary kinetic isotope effect is observed in the aromatic systems such as benzene and

Table 2. Rate constants of triplet oxygen atom reaction with organic molecules.[34]

Substrate	k, 10^9 $M^{-1}s^{-1}$	Substrate	k, 10^9 $M^{-1}s^{-1}$
cyclopentene	16	pyridine	0.11
1-octene	8.7	pyridine-d_5	0.10
chloroform	0.0019	cyclohexane	0.34
chloroform-d	0.00035	cyclohexane-d_{12}	0.057
dichloromethane	0.0020	cyclopentane	0.38
benzene	0.30	*n*-pentane	0.25
benzene-d_6	0.38	acetonitrile	0.0001

pyridine. This is consistent with the addition of the oxygen atom into the π system as the rate limiting step. The addition of $O(^3P)$ into the π system of aromatic molecules supports the electrophilic nature observed in gas phase reactions of $O(^3P)$. A comparison of rate constants between $O(^3P)$ and the hydroxyl radical show that the triplet oxygen atom is a slightly more selective oxidizing agent than the hydroxyl group.

2.8 Energetics of S-O homolysis in DBTO

This first point of interest in terms of establishing the deoxygenation mechanism for the dibenzothiophene sulfoxide is its feasibility energetically. As mentioned earlier the singlet energy of DBTO was estimated at ~82 kcal/mol and the triplet at ~61 kcal/mol. Experimental bond dissociation energies for sulfoxides are limited. However, the S-O bond dissociation energies of Me_2SO, Et_2SO and Ph_2SO have been estimated at 87, 89, and 89

kcal/mol respectively.[16] This suggests that in fact the energy of the singlet state is not enough to afford an S-O bond scission. However, a recent computational study has shown that, at the MP2 level of theory, the aromaticity of the resulting thiophene lowers the S-O bond strength in DBTO to ~78 kcal/mol.[35] Based on these results, the direct cleavage mechanism is expected to be energetically feasible.

2.9 Electronic state of dibenzothiophene sulfoxide

A very important aspect when establishing a photochemical mechanism is the electronic state of the active species. The quenching experiments (section 2.2.2) are consistent with either a short lived (unquenchable) triplet or a singlet state of DBTO. If the S-O bond cleavage mechanism is correct, an excited state energy of the order of 80 kcal/mol or greater is necessary. This eliminates the phosphorescent triplet of **6**, whose fluorescence energy is about 82 kcal/mol. If the electronic state is not a triplet, it must recognized that we are postulating a formally spin-forbidden process. On the other hand, the quantum efficiencies are quite low, which seems to be consistent with the notion of spin-forbiddeness. Another possibility is that a short-lived upper triplet state is involved. The unusual dependence of the quantum yield on the excitation wavelength may support this idea, particularly in combination with the observation that the hydroxylation selectivity is independent of the excitation wavelength (see below). The latter suggests (but does not prove) that a common oxidizing intermediate is produced at all photolysis wavelengths, simply with a higher efficiency with higher energy excitation.

2.10 Observed oxidations

The oxidations that accompany the deoxygenation of DBTO are fairly extensive and imply a robust oxidizing agent. Shown in Table 3 are the products obtained from the photolysis of DBTO in several different organic substrates. The ratios of the oxidized products are also included. Several important points can be made about the oxidations.

Table 3. Oxidized products identified in the photolysis of DBTO. Total yields represent the yield of oxygen recovered in the products .

Substrate	Total Yield	Product Ratio
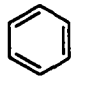	0.60-0.65	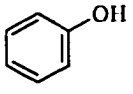
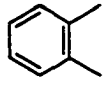	0.55-0.60	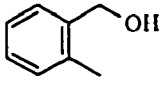 1.0 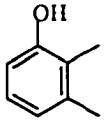 0.15-0.17 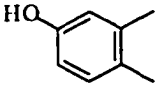 0.15-0.17
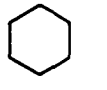	0.95-1.0	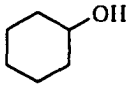 1.9-2.2  1.0
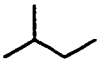	0.40-0.45	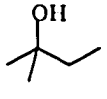 1.0 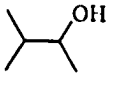 0.3-0.4 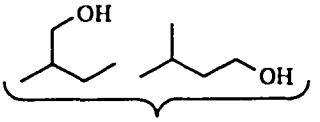 0.2-0.3
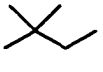	0.45-0.50	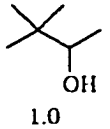 1.0 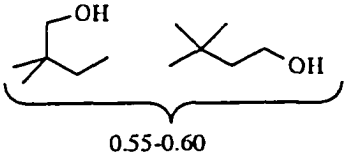 0.55-0.60
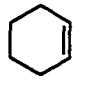	0.97-1.00	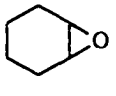 1.0-1.4 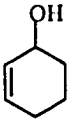 1.0 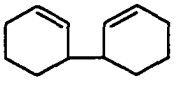 0.2-0.3

Benzene is oxidized to phenol, which suggests the oxidizing agent has significant electrophilic character. Among hydroxylations, a significant preference of tertiary over secondary and primary positions is observed for branched alkanes. When DBTO is photolyzed in alkene solvents, the epoxide is the major isolated product followed by the allylic alcohol.

Singlet oxygen atom O(^{1}D) is not consistent with this broad range of oxidized products nor with the observed selectivities. As mentioned in section 2.7.2, it is expected that products resulting from O(^{1}D) oxidations will be dominated by insertion into C-H bonds, similar to singlet carbene chemistry, to form alcohols. Also, it has been shown that O(^{1}D) shows only minimal selectivity for tertiary hydrogens which is in marked contrast with experiment. [36] Furthermore, O(^{1}D) is 45 kcal/mol above O(^{3}P), so its formation is not energetically feasible from DBTO. However, all of this chemistry is consistent with O(^{3}P).

2.10.1 Oxidations by the triplet oxygen atom

It is important to establish that a triplet oxygen atom can explain all of the products identified in the experiment. Shown below is the reaction of O(^{3}P) with cyclohexane. In the reaction of cyclohexane, the first step is abstraction of a hydrogen atom to form the hydroxyl radical and the cyclohexyl radical **23**. Geminate recombination of these radicals forms cyclohexanol **24**. Disproportionation of HO• and **23** forms cyclohexene **25** and water. Similar mechanisms are postulated for the reaction with other alkanes. Some reasonable products for substrates in Table 3 (methylbutene from methyl butane) are not reported, but

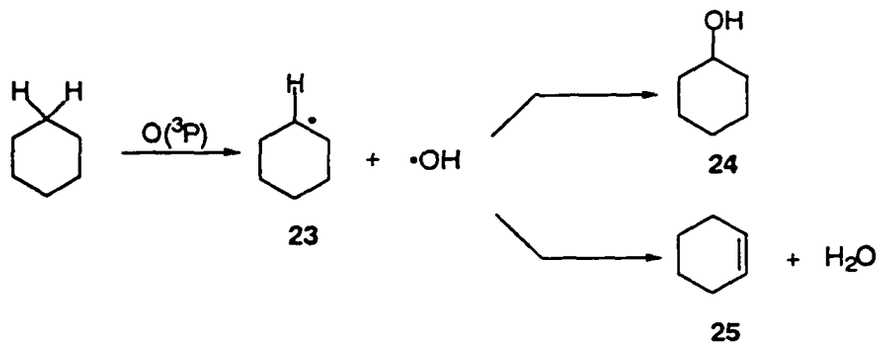

Figure 12. Triplet oxygen oxidations of cyclohexane.

they were not looked for because of analytical difficulty. This may explain some of the "missing" O atom yield.

The reaction of $O(^3P)$ with benzene is expected to proceed via electrophilic attack into the π system to form the arene oxide intermediate **26** (Figure 13). Compound **26** then rearomatizes to form the major product phenol **27** along with other minor products. Although **26** has not been observed in the current study, there is precedence in the literature for its formation and decay under these conditions.[37-39]

Abstraction of an allylic hydrogen from cyclohexene will form the hydroxyl and cyclohexyl radical **30** (Figure 14). Geminate recombination will form the corresponding allylic alcohol **31** (no analysis was done for cyclohexadiene). Recoupling of two

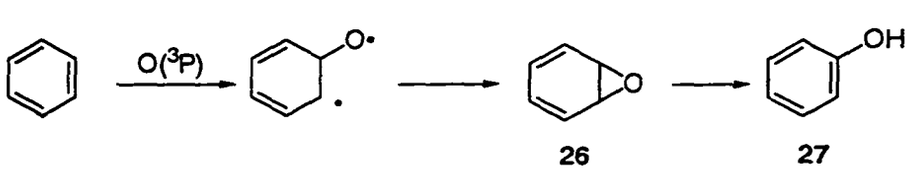

Figure 13. Triplet oxygen reaction with benzene.

cyclohexenyl radical that have escaped from the solvent cage will form the cyclohexenyl dimer **32.** Electrophilic addition of the triplet oxygen atom into the π system of the alkene to form the biradical intermediate **28** followed by recombination will form the epoxide **29** product. Thus, $O(^3P)$ can account for the formation of all of the observed oxidized products.

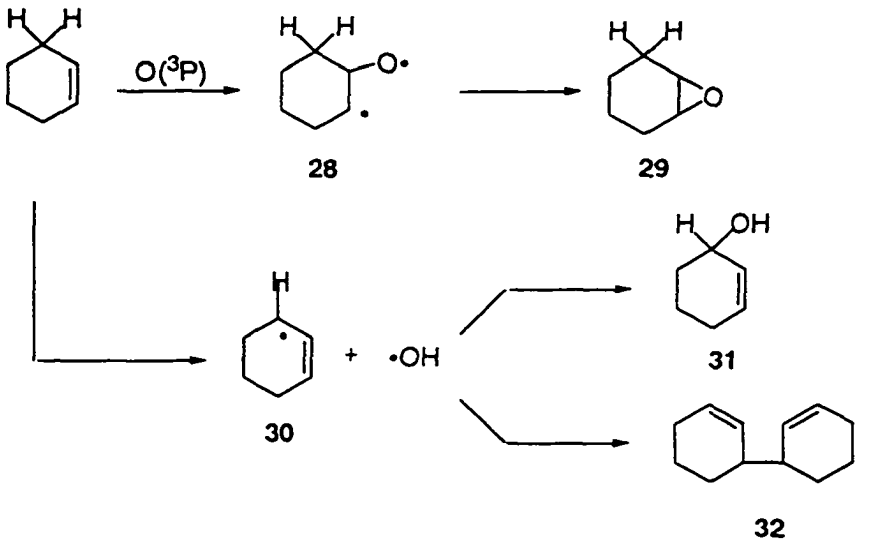

Figure 14. Triplet oxygen oxidation of cyclohexene.

2.11 Origin of the oxygen atom

The origin of the oxygen atom was investigated with $DBT^{18}O$. Using the exchange of the oxygen between DBTO and $H_2{}^{18}O$ a sample of 5.5% ^{18}O enriched DBTO was produced.[40] The enriched DBTO was photolyzed in benzene and resulted in 5.1% enriched phenol, which is essentially identical to the starting $DBT^{18}O$ within experimental error. This implies the oxygen incorporated into the solvent originates from the DBTO.

2.12 Epoxidation of alkenes

There are several different aspects of the oxidation mechanism proposed in section 2.9.2 that can be tested to gain evidence for or against the formation of $O(^3P)$ in the photolysis of DBTO. The first is the insertion of the oxygen atom into the π bond of an alkene. The point of interest here is the following. If the oxidizing agent is in fact a triplet oxygen atom, addition into the double bond will result in a triplet biradical **33**. Before this biradical can close to form the corresponding epoxide, it must undergo inter system crossing (isc). Because the spin slip will take a finite length of time, it allows the once rigid double bond to undergo isomerization. Thus, one would expect both the *cis-* and *trans-* epoxide to be formed in the oxidation of an alkene. If, however, the oxidizing agent is in the singlet state, one would expect a concerted addition into the π system with retention of the *cis-* or *trans-* alkene.

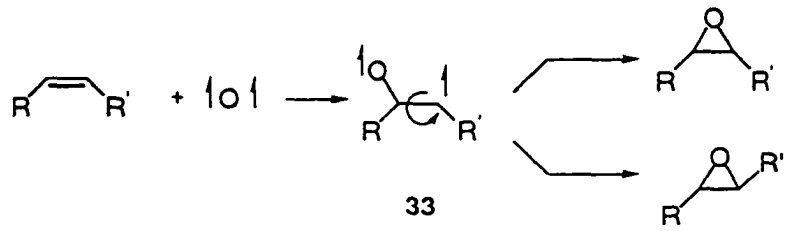

33

To investigate this point, DBTO was photolyzed in the presence of both the *cis-* and *trans-* isomers of 4-octene and ß-methyl styrene. A solution of 5 mM DBTO and 20% *cis-* or *trans-*4-octene w/v in methylene chloride was prepared and degassed with the freeze pump thaw method (3 x 60 mTorr see experimental section). The degassed solution was then photolyzed at 300 nm using a Rayonet photoreactor.

Photolysis in the presence of *cis*- and *trans*-ß-methyl styrene was very similar the that of the 4-octenes. However, in this case, a Xe arc lamp focused on a monomchromater was used to carry out the photolyses at 340 nm. This was done to minimize the isomerization of the alkene during the photolysis.

Although the corresponding alcohols were also formed in the reaction, only the epoxides were of interest here and only their yields are reported in Table 4. There is significant isomerization observed in the resulting epoxides. When starting with *cis*-4-octene and *cis*-ß-methyl styrene, the major product is the more thermodynamically stable trans epoxide in both cases, 52% and 74% respectively. In the case of the *trans* isomer a significant amount of the *cis* isomer is formed: 36% in the 4-octene case and 42% in the ß-methyl styrene case. This is consistent with the oxidizer being a triplet oxygen atom. Some information about the lifetime of the intermediate can also be gained from this data. The differences in the epoxide ratios between the *cis* and *trans* alkenes are indicative of a short lived intermediate, which closes before complete thermodynamic equilibration is achieved.

Table 4. Epoxide formation from *cis*-4-octene in photolysis of **6**. Each run number is an average of three independent experiments.

Alkene	Concentration of Epoxide (mM)		Ratio of Epoxide Concentration	
	Trans	Cis	Trans	Cis
cis-4-octene	0.066	0.064	1.1	1.0
trans-4-octene	0.079	0.042	1.8	1.0
cis-ß-methylstyrene	0.078	0.026	2.8	1.0
trans-ß-methylstyrene	0.042	0.012	3.5	1.0

It is important to establish that the isomerization of the epoxides is taking place with the insertion of the oxygen atom into the alkene and not simply photo-isomerization of the alkene[41,42] followed by a concerted oxidation. The first step taken to minimize the isomerization of the alkene was the selection of the photolysis wavelength. The absorption cut off (the wavelength at which the molecule no longer absorbs A<1) for 4-octene and ß-methyl styrene is approximately 290 nm and 300 nm respectively. Thus, photolysis of the DBTO reported in Table 4 was conducted on the red (lower energy) edge of its absorption band ~ 330 nm to minimize the absorption of the alkenes. To insure the alkene isomerization was in fact minimized under these reaction conditions, the alkenes were analyzed before and after the photolysis. The results are shown in Table 5. None of the alkenes, with the exception of *cis* ß-methyl styrene, showed any significant isomerization.

In the case of the 4-octenes, the alkene ratio was determined by oxidizing the remaining alkenes from the experiment with *m*-CPBA followed by GC analysis. The *m*-CPBA oxidizes alkenes with retention of stereochemistry and thus gives a good estimate of the *cis/trans* alkene ratio.[43] The *cis*- and *trans*-ß-methylstyrenes could be separated in the GC and the *cis/trans* ratio was calculated directly. Even though the *cis* ß-methyl styrene did show significant isomerization, the extent of the *trans*-epoxide is much larger than that of the alkene (75% vs. 17%). Based on these results it can be reasonably concluded that isomerization of the alkenes cannot account for the extent of isomerization observed in the epoxides, and the isomerized epoxide is consistent with the formation of $O(^3P)$.

Table 5. Isomerization of alkenes in photolysis of **6**.
All numbers are averages of three independent experiments.

Alkene	Ratio of alkene concentration	
	Trans	Cis
cis-4-octene	5.0	95.0
trans-4-octene	99.0	1.0
cis-ß-methylstyrene	17.3	82.7
trans-ß-methylstyrene	99.0	1.0

2.13 Oxidation of allyl benzene

Another interesting aspect of the oxidation of alkenes with $O(^3P)$ is the formation of allylic alcohols. The abstraction of an α-hydrogen of an alkene system leads to the formation of a stabilized allylic radical pair **34** (Figure 15). Geminate recombination of the hydroxyl radical and the allylic radical is expected to result in oxidation at both ends of the allylic system. Formation of both alcohols would be strong evidence for a stepwise oxidative process, consistent with expectations for $O(^3P)$.

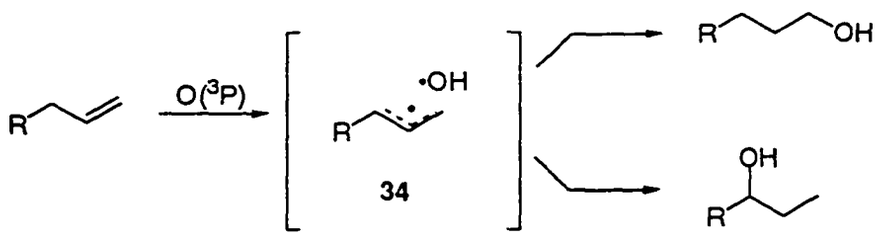

Figure 15. Oxidation of a generic allylic system.

To investigate this reaction DBTO was photolyzed in the presence of allyl benzene. A solution of 10 mM DBTO and 20% w/v allyl benzene in methylene chloride was degassed using argon bubbling. The resulting solution was photolyzed at 320 nm using a Xe arc lamp focused on a monochromator and the results are shown in Table 6a-b. Although as expected the epoxide was the major photoproduct, a significant amount of both alcohols were obtained. This is consistent with the formation of a triplet oxygen atom.

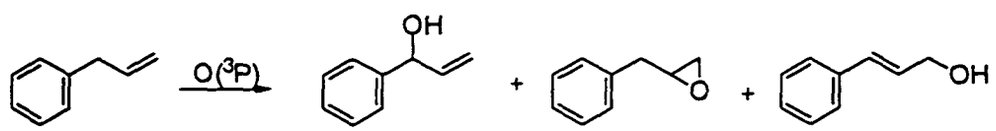

35 36 37

Table 6a. Photolysis of DBTO in 10% allyl benzene and methylene chloride.

% Conversion	[DBT] mM	[35] mM	[36] mM	[37] mM
18	0.56	0.033	0.054	0.017
19	0.66	0.041	0.058	0.014
16	0.52	0.031	0.053	0.015

Table 6b. Photolysis of DBTO in neat allyl benzene.

% Conversion	[DBT] mM	[35] mM	[36] mM	[37] mM
25	0.49	0.043	0.079	0.015
20	0.46	0.044	0.080	0.014
23	0.47	0.039	0.075	0.015

Again, it is important to establish the fact that the allyl benzene is not simply isomerizing to form ß-methyl styrene followed by a concerted oxidation. To check this, allyl benzene was photolyzed under identical conditions in the absence of DBTO and afforded no ß-methyl styrene.

2.14 Competitive oxidations with dueterated solvents.

Currently, there is no clean way to produce $O(^3P)$ in solution. Despite this, several researchers have been able to investigate its reactivity in the solution phase (section 2.7). In an effort to characterize the oxidizing species formed in the photolysis of DBTO, several competition reactions were investigated. The intention of these experiments is to compare the product ratios of the oxidized products with the estimated rate constant ratios of Scaiano (section 2.7.3). A 2 ml solution of 10 mM DBTO and two other substrates was dissolved in methylene chloride. Three different relative ratios for the two substrates were investigated (1:1, 1:3, and 3:1). Each of the samples were degassed using the freeze pump thaw method (3 x 60 mtorr). The solutions were photolyzed at 300 nm using the Rayonet photoreactor and analysis of the oxidized products was done with a GC-MS by analyzing the corresponding mass peaks. The results are shown in Table 7 below.

As is shown in Table 7, the product selectivity ratios obtained from the photolysis of DBTO compare very well with the rate constant ratios estimated by Scaiano. This is particularly interesting considering the fact that the two different types of experiments represent a different stage of the reaction. The rate constant ratios represent the initial interaction of $O(^3P)$ with a substrate, and the product ratios represent the most stable product

formed from this interaction perhaps several chemical steps down the line. The large product selectivity and rate constant ratios observed in the C_6H_{12}/C_6D_{12} case are consistent with hydrogen abstraction as the rate limiting step of the reaction. The C_6H_6/C_6D_6 entry warrants a few words of discussion.

Table 7. Product selectivities compared with predicted rate constant ratios.

Compound A	Compound B	Products	Selectivity A:B	k_A / k_B from Scaiano
		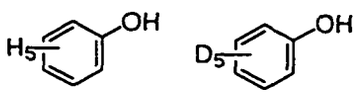	1.4	0.8
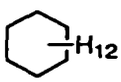	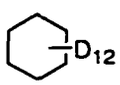	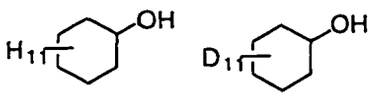	6.5	6.0
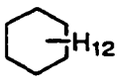	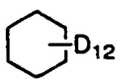		6.2	6.0
		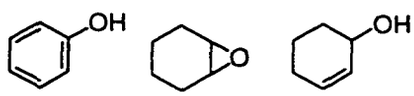	0.019	0.021
		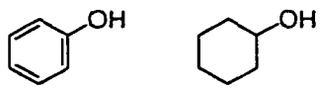	0.52	0.88

The absolute difference between the rate constant ratio (0.8) and the product ratio (1.4) in the C_6H_6/C_6D_6 entry is larger than the differences found in the other entries. Furthermore, if the oxidizing species formed in the photolysis of DBTO is truly a triplet oxygen atom, one would expect the addition of the oxygen atom into the π system of the benzene to be the rate limiting step. If this is indeed the case, the expected product ratio in

the C_6H_6/C_6D_6 entry would be less than one as is the case in the rate constant ratio. This somewhat puzzling result led to the reinvestigation of this entry.

In the original value reported (1.4), the GC-MS response factors for both phenol and phenol-d_5 were assumed to be equal. Surprisingly, this was found to be incorrect, and the correction for the response factors was calculated to be 1.05.

When this correction along with the correction for the differences in molarity between C_6H_6 and C_6D_6 are taken into account the new product ratio becomes 1.1. Although this value is closer to the estimated rate constant ratio (0.8), it is still larger than expected for an inverse secondary isotope effect. It was then discovered that an additional correction was needed in the data. This correction originated from experiments where DBTO was photolyzed in benzene and benzene-d_6, separately but under identical conditions. What was found is the yield of the dueterated phenol was consistently only about 83% of the yield for phenol. This suggests there is an isotope dependant branching step *after* the addition of the oxygen into the π system that leads to the formation of products other than the corresponding phenols. The values for the product ratios, which include each of these corrections, are shown in Table 8a-c.

These data yield an overall product selectivity ratio of 1.1. However, the selectivity for what is presumed to be the first step, oxygen addition into the ring, is 0.9, which is in much better agreement with that of Scaiano's rate constant ratio of 0.8.

Table 8a. Correction for (1:3) benzene:benzene-d_6 product ratios ([C_6H_5OH] / [C_6D_5OH]).

Experiment	[C_6H_5OH]/[C_6D_5OH]	Corrected Molarity & R.F.	Corrected All three corrections
1	0.86	0.90	0.75
2	0.87	0.91	0.76
3	0.91	1.09	0.95
4	1.1	1.13	0.96

Table 8b. Correction for (1:1) benzene:benzene-d_6 product ratios ([C_6H_5OH] / [C_6D_5OH]).

Experiment	[C_6H_5OH]/[C_6D_5OH]	Corrected Molarity & R.F.	Corrected All three corrections
1	0.91	0.95	0.79
2	0.92	0.96	0.80
3	0.92	0.96	0.83
4	0.95	0.98	0.82

Table 8c. Correction for (3:1) benzene:benzene-d_6 product ratios ([C_6H_5OH] / [C_6D_5OH]).

Experiment	[C_6H_5OH]/[C_6D_5OH]	Corrected Molarity & R.F.	Corrected All three corrections
1	0.99	1.00	0.83
2	0.98	1.00	0.83
3	0.90	0.95	0.79
4	0.93	0.97	0.91

2.15 Direct detection of $O(^3P)$

All of the experiments discussed thus far deal with obtaining indirect evidence for the formation of a $O(^3P)$ in the photo-deoxygenation of DBTO. At this point efforts were switched to the direct detection of the $O(^3P)$ using the laser flash photolysis technique discussed in Section 2.7.3. Several solutions of DBTO (O.D. ≈ 0.2 - 0.6 at 266) in CH_3CN were photolyzed at 266 nm using the fourth harmonic of a Nd:YAG laser pulsed at 10 Hz. No transient absorption was observed at 325 nm corresponding to a triplet oxygen atom complexed with acetonitrile in any of the samples. However, it is not unreasonable to expect the signal would not be within the detection limit of the system considering deoxygenation of DBTO occurs with a very low quantum yield (0.01 at 266 nm).

Therefore, efforts to find another sulfoxide system that photo-deoxygenates with a higher quantum yield than DBTO began. The search began with the investigation of the S-O bond strengths with the speculation that a decrease in the S-O bond energy might lead to an increase in the quantum yield of deoxygenation. Recently, the thermodynamics of several sulfoxide systems were characterized computationally.[35] Shown in Figure 16 are the bond dissociation energies of several thiophene derivatives based on MP2 level calculations of isodesmic reactions. The trend of interest is the decrease in the S-O bond energies with the removal of the benzene moieties from the thiophene ring. The S-O bond dissociation energy for DBTO is estimated at 74 kcal/mol. The S-O bond dissociation energy for thiophene, however, is lowered to 61 kcal/mol.

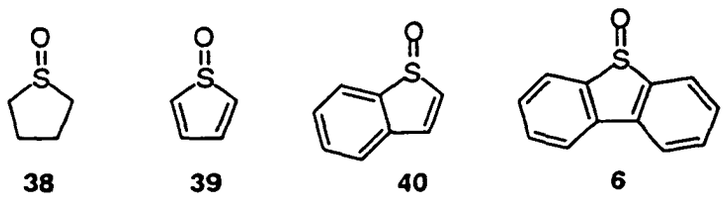

	38	39	40	6
S-O Bond Energy (kcal/mol)	86	61	69	78

Figure 16. Bond dissociation energies in kcal/mol predicted by MP2/6-31G(d,p).

Ideally, based on the S-O bond energies presented in Figure 13, one would chose thiophene oxide **39** as the most likely candidate for the laser flash photolysis experiment. The problem with this choice has to do with the chemical reactivity of the thiophene S oxide. It was shown by Evans that sterically unhindered thiophene sulfoxides could not be isolated due to a Diels-Alder dimerization which forms compound **41** (Figure 17).[44] This chemistry is also observed with the corresponding thiophene sulfone.

One can imagine two possible structures for the thiophene sulfoxide Figure 18. The first, compound **A**, which would maximize the contribution of electrons to the aromatic sextet, can be visualized as the sulfur atom being sp^2 hybridized with the lone pair electrons occupying a pure 3p orbital. The second, compound **B**, puts the sulfur atom in the more traditional sp^3 hybridization.

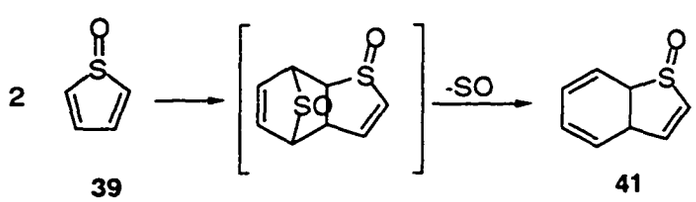

39 41

Figure 17. Diels-Alder dimerization of thiophene S-oxide.

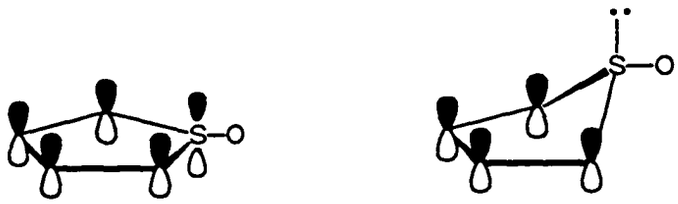

A B

Figure 18. Two proposed structures for thiophene S-oxide.

Mock has shown the Diels-Alder dimerization can be retarded considerably by the increasing the sterics at the 2 and 5 position of the thiophene ring, and he was able to investigate the structures of several substituted thiophene sulfoxides using NMR and UV-vis techniques.[45] What was found was the data for both 2,5-di-*tert*-butylthiophene sulfoxide and 2,5-di-*tert*-octylthiophene sulfoxide supported a structure similar to compound **B**, where the sulfoxide is sp^3 hybridized. This conclusion was later supported by the work of Mansuy and co-workers who were able to characterize 2,5-di-phenylthiophene sulfoxide using X-ray diffraction and the computational work by Jenks.[35,46] The instability of the thiophene sulfoxide can be understood in terms of the removal of aromaticty of thiophene ring upon oxidation. Substitution of the thiophene ring at the 2 and 5 positions stabilizes the sulfoxide by hindering this dimerization. It is assumed that the addition of the *tert*-butyl groups will not have a major affect on the S-O bond energy or on the photophysics. Thus, efforts to synthesize several 2,5 disubstituted thiophene sulfoxides began.

Due to their relative instability, there have been very few reported syntheses of substituted thiophene sulfoxides reported in the literature. Most of the work reported on thiophene sulfoxides deal with their characterization as transient species,[47,48] or as the Diels-

Alder products.[49-52] Mock reported the synthesis of several di-alkylthiophene sulfoxides (5% yield) and their characterization in solution.[45] Later the synthesis and characterization of 2,5-di-phenylthiophene sulfoxide was reported (40% yield).[46] The systems chosen for the current study were 2,5-diphenylthiophene sulfoxide **42**, 2,5-di-*tert*-butylthiophene sulfoxide **43** and are shown in Figure 19. Both compound **42** and **43** have both been characterized spectroscopically.

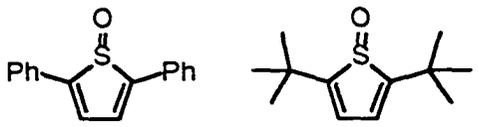

42 **43**

Figure 19. Three sulfoxides with possible increased deoxygenation quantum yield.

2.16 Synthesis of 2,5-di-phenylthiophene sulfoxide

Because it had been synthesized and isolated as a pure compound, 2,5-diphenylthiophene sulfoxide was investigated first.[46] Mansuy and coworkers synthesized 2,5-diphenylthiophene using the technique of closing the diketone with Lawesson's reagent.[53] The 2,5-diphenylthiophene was then oxidized to afford 2,5-diphenylthiophene sulfoxide (40%) via 30% H_2O_2 catalyzed by CF_3CO_2H.[46]

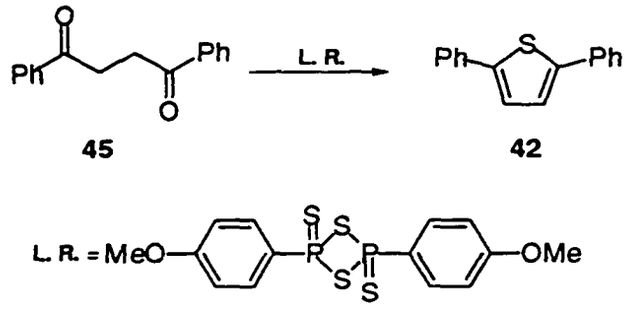

There have been several reported methods for the synthesis of 1,2-dibenzoyl ethane **45**, all of which afforded the diketone in low yields 5-25%.[54-57] However, because both the closure of the diketone with Lawesson's reagent and the oxidation of the thiophene to the sulfoxide are fairly inefficient reactions (15% and 40%, respectively) and a relatively large amount of the sulfoxide was needed, several preliminary reactions were run using simple unreported methods. The first method investigated was a Friedel-Crafts reaction of succinic anhydride and benzene.

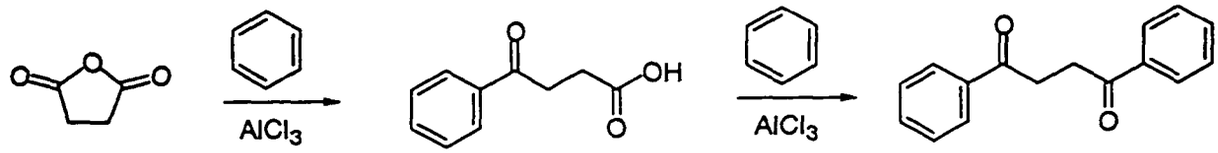

46 **45**

To a 30 ml aliquot of benzene was added 2.0 g of succinic anhydride and 2.5 equivalents of $AlCl_3$. Work up of the reaction after 14 hours of reflux afforded white crystals. Analysis by nmr showed the crystals were the ß-keto acid **46** formed by the addition of one benzene ring into the anhydride. The addition of the second phenyl ring into

the system proved to be more challenging. An attempt to increasing the electrophilic character of acid carbonyl was done by changing the acid functional group to an acid chloride. Addition of acid **46** to neat $SOCl_2$ led to the evolution of HCl. The reaction was continued until this had ceased. The remaining $SOCl_2$ was removed under reduced pressure and the acid chloride was used in a second Friedel-Crafts reaction without further purification. The resulting reaction mixture contained many different products, none of which matched the R_f of 1,2-dibenzoyl ethane on TLC. Although the reaction of the acid chloride with benzene produced several products, it is reasonable that at least one product was the intramolecular product **48**.[58,59]

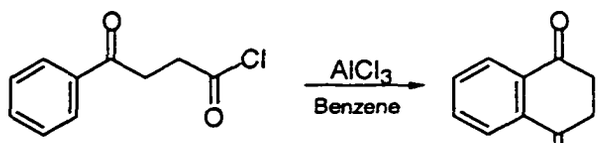

47 **48**

The focus of the preparation of 1,2-dibenzoyl ethane was then shifted to a coupling reaction where two enolates of acetophenone were coupled in the presence of copper (II) chloride, Figure 20.[60] The enolate of acetophenone was produce by treatment with lithium diisopropyl amine. A solution of anhydrous $CuCl_2$ dissolved in dry DMF was then added. Work up of the reaction showed the major component in the mixture was recovered starting material. However, approximately 25% was the diketone **45** was obtained. Purification, followed by closure of the diketone using Lawesson's reagent, afforded 2,5-diphenylthiophene in 10% overall yield.

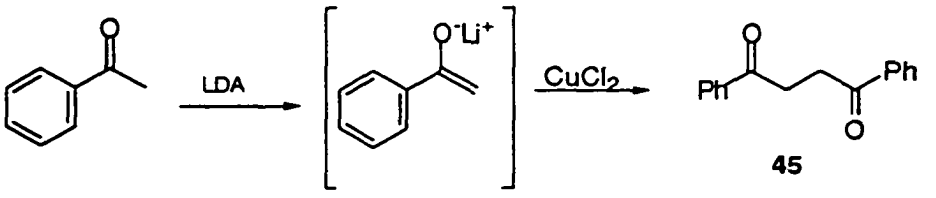

Figure 20. Coupling of the enolate with copper(II) chloride.

Due to the inefficiencies of the enolate coupling reaction and the closure reaction, another method that would produce the thiophene directly, was investigated. Although the palladium catalyzed coupling of 2,5-diiodothiophene with phenyl magnesium bromide had not been reported earlier, several related systems had been investigated.[61] Oxidative addition of the palladium (Pd^0) into the carbon halogen bond followed by reductive elimination with the phenyl Grignard leads to the formation of a new carbon-phenyl bond. The organo-zinc analog of the Grignard was used to minimize the cross coupling byproduct biphenyl. Using this method, 2,5-diphenyl thiophene **42** was produced in 53% yield. The oxidation was then carried out using H_2O_2/ CF_3CO_2H to yield 2,5-diphenylthiophene sulfoxide in ~40% yield.

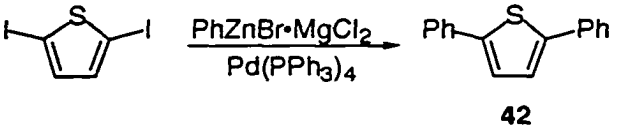

42

2.17 Photolysis of 2,5-di-phenylthiophene sulfoxide

Before the sulfoxide was photolyzed, the photostabilitiy of two potential products (2,5-diphenyl thiophene **42** and 2,5-diphenyl thiophene sulfone) was investigated. This was done to ensure the products isolated from the photolysis of the sulfoxide were not secondary

photolysis of the sulfide or sulfone. Several samples of 2,5-diphenylthiophene sulfide (10-25 mM) were photolyzed over a range of wavelengths (230-380 nm). The sulfide did not decompose, as indicated by a constant peak area in the HPLC traces, under any of the conditions investigated. Several samples of the 2,5 diphenylthiophene sulfone (10-25 mM) were also investigated. Figure 21 shows the peak area ratio of the sulfide/sulfone vs. the photolysis time. The ratio of sulfide/sulfone remains constant over a wide time scale. This coupled with the fact that photolysis of 2,5-diphenylthiophene did not lead to a decrease in the sulfide peak area in the HPLC shows the sulfone is also inert under the reaction conditions.

The 2,5-diphenyl sulfoxide was then photolyzed at 260 nm. Figure 22 shows the sulfide grows in at the expense of the sulfoxide, which is consistent with the photo-

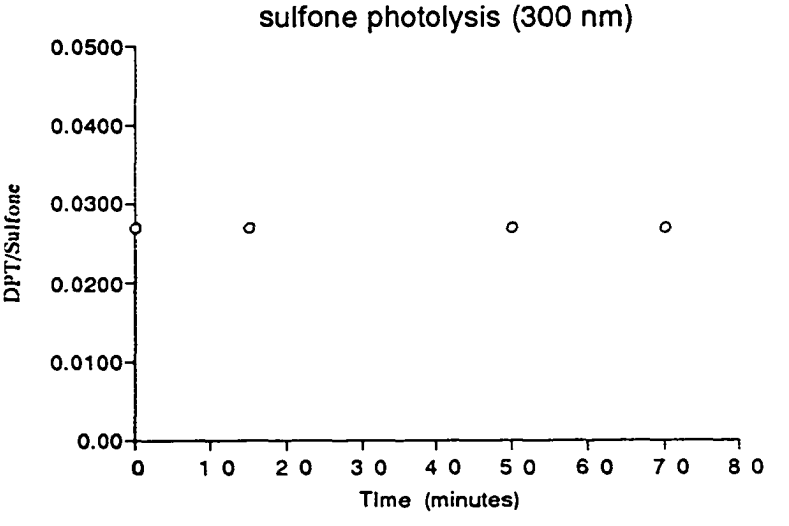

Figure 21. Photolysis of 2,5-di-*tert*-butylthiophene sulfone at 380 nm

deoxygenation of the sulfoxide. However, several unidentified peaks were formed along with the sulfide. The quantum yield for deoxygenation was not calculated quantitatively, but the time required for this deoxygenation indicates that it is not a major improvement over that of DBTO. Thus, further experiments were not carried out with this compound.

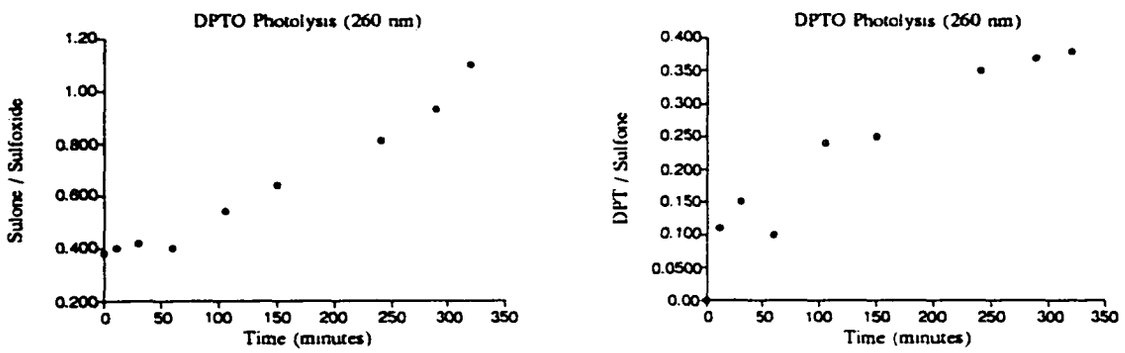

Figure 22. Photolysis of 2,5-di-*tert*-butylthiophene sulfoxide at 260 nm

Next, we move on to the to the synthesis and photolysis of the second compound 2,5-di-*tert*-butylthiophene sulfoxide. One advantage of using this system is it better lends itself to a computational investigation see section (2.16.3).

2.18 Synthesis of 2,5-di-*tert*-butylthiophene sulfoxide (DTBTO)

Unlike 2,5-diphenyl thiophene sulfoxide, very little work on 2,5-di-*tert*-butylthiophene sulfoxide **43** has been reported. Originally, Wynberg and Wiersum synthesized 2,5-di-tert-butylthiophene (DTBT) in 30% yield by closing the corresponding di-*tert*-butyl diketone with P_2S_8.[62] However, in the mid 1980's, Hojo and coworkers[63]

synthesized 2,5-di-*tert*-butylthiophene (78% yield) via a Friedel-Crafts reaction of thiophene and *tert*-butyl bromide on a silica gel support, Figure 23. The major disadvantage in the Hojo synthesis is the possibility of the formation of both the 2,4 and 2,5 isomer. However, the 2 and 5 positions are expected to be activated by the sulfur.

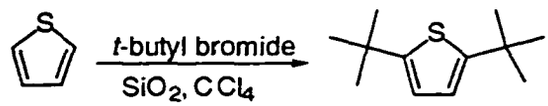

43

Figure 23. Synthesis of 2,5-di-*tert*-butylthiophene

To a flask charged with carbon tetrachloride as the solvent was added dry EM Science Silica Gel 60 (230-400 mesh), sodium carbonate, and thiophene. The reaction was heated to 78° for 40 hours at which point the thiophene peak was absent from the GC trace. The 2,5-di-*tert*-butylthiophene was isolated in 75% yield with less than 1% of the 2,4 isomer. Attempts to separate the two isomers via silica gel were unsuccessful. The 2,5-di-*tert*-butylthiophene S-oxide (DTBTO) was produced by oxidation of the thiophene with H_2O_2/CF_3COOH as before. Despite the small amount of the 2,4 isomer impurity, preliminary photolysis was done on the compound.

2.19 Photolysis of 2,5-di-*tert*-butylthiophene sulfoxide

The photo-stability of the 2,5-di-*tert*-butylthiophene (DTBT) and 2,5-di-*tert*-butylthiophene sulfone ($DTBTO_2$) under the reaction conditions was investigated. A 10 mM solution of DTBT in CH_3CN was photolyzed at 320 nm for 3 hours using the Xe arc lamp

focused on a monochromator. No decomposition of the thiophene was observed under these conditions. Next, a 10 mM solution of $DTBTO_2$ in CH_3CN was photolyzed at 320 nm. Even though a small amount of the sulfone decomposed under these reaction conditions, about 3% over 3 hours, it is assumed this decomposition is not important for the photolysis times used for the sulfoxide. The products of the photodecomposition of 2,5-di-*tert*-butylthiophene sulfone were not isolated or identified. However, no sulfone was ever identified in the photolysis of the sulfoxide.

Photolysis of a 10 mM solution of 2,5-di-*tert*-butylthiophene sulfoxide in methylene chloride at 320 nm showed the sulfoxide disappeared very quickly. The quantum yield for disappearance of the sulfoxide was estimated at 0.6 from a plot of the concentration of the DTBTO vs. Time, Figure 24.

HPLC shows the disappearance of the DTBTO peak with a retention time ~2.0 min led to the formation of second peak with a retention time ~5.8 minutes. Although a retention

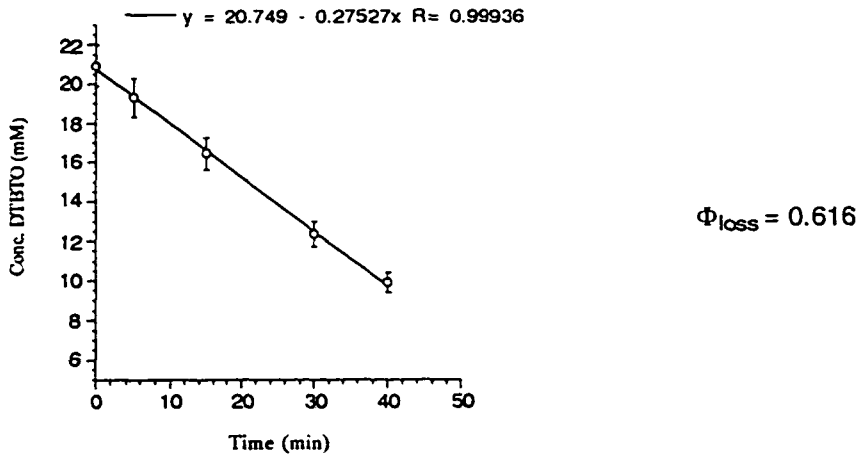

Figure 24. Quantum yield for the disappearance of DTBTO

time of 5.8 minutes is very close to that of the sulfide (5.9 minutes), the λ_{max} in the absorption spectra is blue shifted by ~20 nm from ~240 nm to ~220 nm. Conclusive proof that the new peak formed in the HPLC was not 2,5-di-*tert*-butylthiophene came from the formation of a new peak when the reaction mixture was spiked with a small amount of 2,5-di-*tert*-butylthiophene.

Because the UV absorption spectra and the retention time in the HPLC is very similar to that of the thiophene, one would expect the structure of this compound to also be very similar. One possibility would be the 2,5-di-*tert*-butylfuran **56** produced by the photo desulfurization of the thiophene as shown in Figure 26. To test this, the furan was synthesized using the same method as that used for the 2,5-di-*tert*-butythiophene.[63] Both the retention time and the UV absorption spectra of the synthesized 2,5-di-*tert*-butylfuran matched those of the new peak being formed in the photolysis of 2,5-di-*tert*-butylthiophene S-oxide. It should be noted that the 2,5-di-*tert*-butylfuran slowly decomposed into unidentified products when photolyzed at 320 nm.

Although rare, the photo-desulfurization of sulfoxides has been observed by Schlessinger and Schultz.[64-68] These authors have shown the photolysis of several substituted naphthalene sulfoxides **49** leads to the formation of one of two possible desulfurized products **51** and **54** (Figure 25). Under sensitized photolysis, the major product is the ketone. This has been proposed to result from α-cleavage of the S-C bond to form the triplet diradical, which forms the corresponding sulfine **53**. The sulfine then undergoes an additional photochemical reaction to form the resulting ketone **54**. Under direct photolysis conditions, however, both the ketone **54** and the pyran **51** are formed. The pyran is

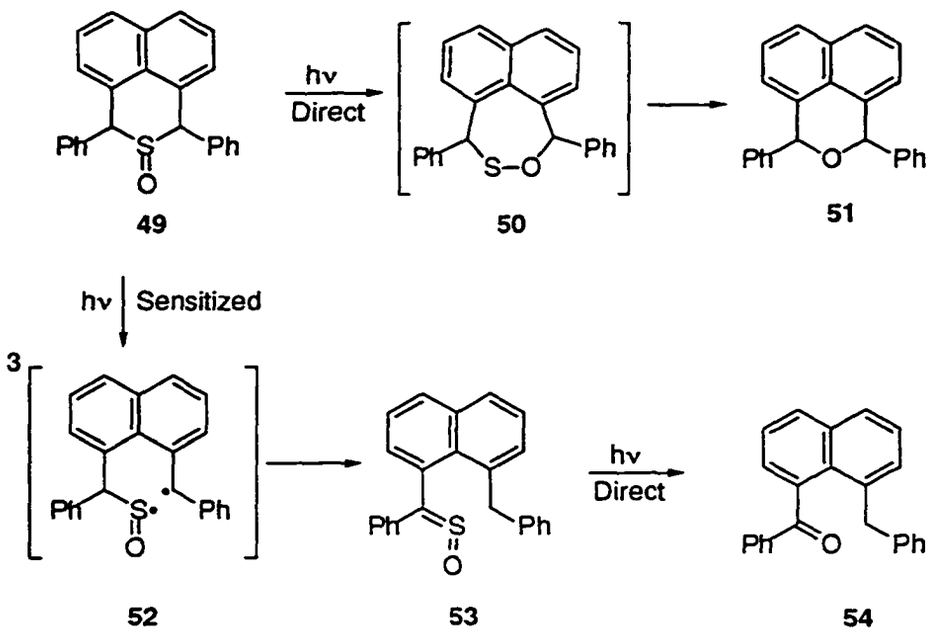

Figure 25. Proposed mechanism for the photolysis of substituted naphthalene Sulfoxides.

suggested to form by the photo-decomposition of the sultene **50**. The sultene can be formed by an α-cleavage reaction, followed by O-C closure. Schlessinger was able to characterize both the sulfine **53** and the sultene **50** intermediates from the product mixture.

However, formation of the analogous sulfine in the 2,5-di-*tert*-butylthiophene sulfoxide is not possible due to the unsaturation of the ring. Thus, within the Schlessinger model, one would expect the reaction to follow the pathway involving the formation of the sultene (Figure 26).

Direct evidence for the existence of the sultene intermediate **55** has not yet been obtained from the photolysis of 2,5-di-*tert*-butylthiophene sulfoxide, Figure 26. Schlessinger was able to maximize the formation of the sultene **51** by lowering the polarity of the solvent,

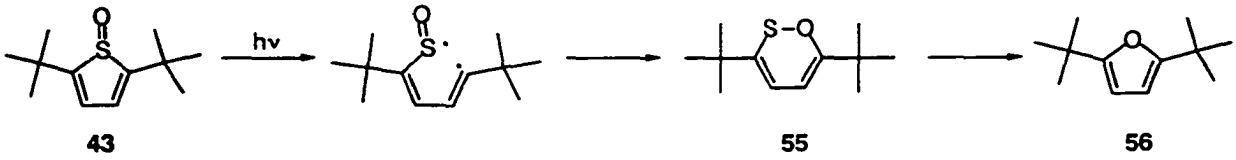

Figure 26. Formation of 2,5-di*tert*-butylfuran from the thiophene sulfoxide

but attempts to lower the polarity of the solvent to give **55** in the reaction failed to produce any new signals in the HPLC or NMR.

This is not completely surprising considering the work done by Block[69,70] and Schroth[71] on the thermodynamics and reactivity of dithiins. For the 3,6 disubstituted 1,2-dithiins, large aryl substituents stabilized the formally antiaromatic molecules and allowed for their isolation. However, the 3,6-di-*n*-butyl dithiin was isolated and characterized as an unstable molecule that is extremely susceptible to sulfur extrusion to form the corresponding thiophene. The 3,6 di-*tert*-butydithiin was not detectable even at –50°C. It is not clear if this is because it is so unstable or the large *tert*-butyl groups block its formation in during the synthesis. Nonetheless, based on the computational work (Chapter 3) the sultene is expected to be more unstable, in terms of S-O vs. S-S homolysis, than the corresponding disulfide. Thus, at this point the isolation of the 3,6-di-*tert*-butyl sultene **55** seems unlikely. It is then reasonable that **55** is formed in this photolysis reaction, but that is simply too short lived to be detected.

Attempts were made to quench the deoxygenation reaction of DTBTO using several triplet quenchers including isoprene and oxygen. A solution of 20 mM DTBTO and 0.4 M isoprene in acetonitrile was photolyzed at 320 nm. The isoprene did not decrease the rate of formation of 2,5-di-*tert*-butylfuran. A solution of 20 mM DTBTO in acetonitrile bubbled

with O_2 for 15 minutes was photolyzed at 320 nm. The photolysis of DTBTO in the presence of molecular oxygen also did not lead to a decrease in the rate of 2,5-di-*tert*-butylfuran formation. However, an interesting observation of this experiment was that molecular oxygen increased the rate of secondary photo-decomposition of the furan (Figure 27). The exact implications of this result are currently not known. Regardless, it would appear that the photochemistry of **43** originates from either a singlet or a very short-lived triplet.

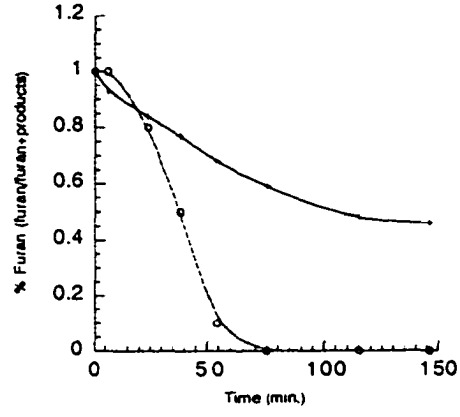

Figure 27. Photolysis of 2,5-di-*tert*-butyl furan in oxygen and argon. The + is without O_2 and the o are with O_2 added.

It is possible that the DTBTO does undergo photo-deoxygenation followed by a very fast reaction of the triplet oxygen atom with the thiophene ring. To test for the formation of any oxidized product, 2,5-di-*tert*-butylthiophene sulfoxide was photolyzed in the presence of tetrahydrothiophene. A solution of 20 mM DTBTO in neat tetrahydrothiophene was photolyzed at 320 nm. No tetrahydrothiophene sulfoxide was detected with either HPLC or GC in the photolysis. This suggests that, if the triplet oxygen atom is formed, it is not

captured by the tetrahydrothiophene. However, based on the evidence thus far, deoxygenation seems unlikely.

Several unanswered questions remain pertaining to the photochemistry of the 2,5 substituted thiophene sulfoxides. First, preliminary results show the 2,5 diphenylthiophene sulfoxide does undergo deoxygenation along with other reactions while the 2,5-di-*tert*-butylthiohene sulfoxide undergoes very fast desulfurization. One can postulate this may be due to electronic effects caused by the phenyl rings, but at this time it is only speculation. Another interesting question pertains to the desulfurization of the 2,5-di-*tert*-butylthiophene sulfoxide. Based on the work of Schlessinger and coworkers a reasonable mechanism would proceed through the sultene **55**.[64-68] Based on earlier work on related dithiins,[69,70] this intermediate may be very hard to detect and up to now remains only speculative for this system.

2.20 Excited state of thiophene sulfoxide

As a supplement to the experimental work on the photodeoxygenation of substituted thiophene sulfoxides, a computational study aimed at developing the excited state of the thiophene sulfoxide was initiated (for a complete review of computational methods and basis sets see appendix A).

The thiophene sulfoxide was optimized at the RHF/6-31G(d) level, and a CASSCF(14,10) was done on this geometry to get a reliable representation of the molecular orbitals. Because the molecule is C_s symmetry, each of the orbitals is symmetric (A') or unsymmetric (A") with respect to the mirror plane. The orbitals included in the active space

consisted of the four π molecular orbitals from the thiophene ring, the 3 lone pairs of electrons on the oxygen along with the one lone pair of electrons on the sulfur, and the S-O σ bond. Analysis of the orbitals produced from this calculation showed that two of the lone pairs on oxygen residing in two oxygen 3 p orbitals were converted to C-C and C-H bonds. Because of this, these orbitals were removed form the active space thus changing the calculations to a CASSCF(10,8).

The orbitals generated from this calculation showed the LUMO was consistent with promoting an electron into the π^3 (2 nodes) orbital of the thiophene ring. However, a configuration interaction calculation CIS/6-31G(d,p) revealed that there was really two excited states very close in energy (ΔE_{CIS} = 2.1 kcal/mol). These states were consistent with a n$\rightarrow$ π^* (A'$\rightarrow$A') and $\pi \rightarrow \pi^*$ (A" $\rightarrow$ A') transitions. The n$\rightarrow$ π^* transition represents the promotion of an electron from the lone pair of electrons on the sulfur to the π^3 orbital of the thiophene ring. The $\pi \rightarrow \pi^*$ transition represents the promotion of an electron from the π^2 orbital of the thiophene ring to the π^3 orbital. The CIS calculation predicted the n$\rightarrow$ π^* transition was lower in energy.

A series of CASSCF calculations were done to better characterize the two close excited states predicted by the CIS. Both the singlet and triplet electronic states were examined for each of the two promotions. The active space for the excited state calculations was identical to the one used above CASSCF(10,8). The results of these calculations are shown in Figure 28. For the singlet electronic state, the n $\rightarrow$ π^3 transition is favored over the $\pi \rightarrow \pi^3$ state by ~2 kcal/mol. This is consistent with the observed photochemistry of

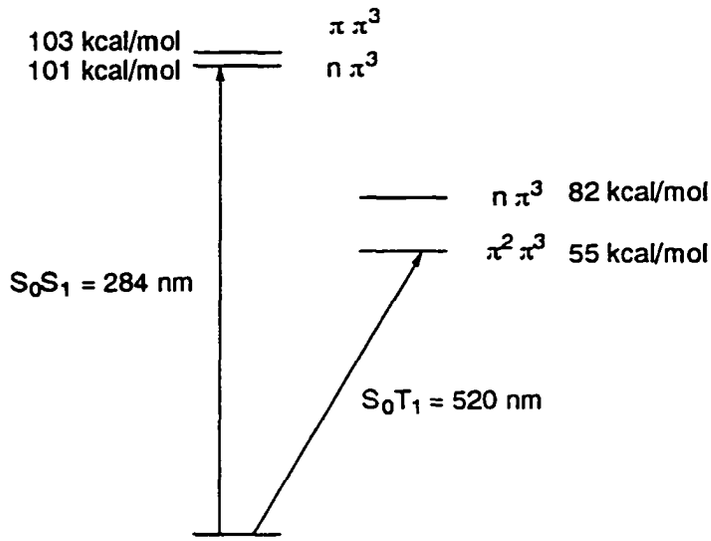

Figure 28. Energetics of the vertical singlet and triplet states of thiophene sulfoxide calculated at CASSCF(10,8).

thiophene sulfoxides. In the triplet state, however, the $\pi \rightarrow \pi^3$ transition is lower in energy by ~28 kcal/mol.

2.21 Conclusions

Photolysis of dibenzothiophene sulfoxide produces dibenzothiophene in very high chemical yield and low quantum yield. The quantum yield is independent of sulfoxide concentration. This and other experiments rule out the formation of any sort of sulfoxide dimer as part of the mechanism for formation of **11**. A proposed mechanism for deoxygenation based on O-atom transfer by sulfinyl radicals is ruled out on an energetic basis. Mechanisms based on direct interaction between solvent and the excited state of **6** in a reaction analogous to carbonyl photochemistry cannot be ruled out, but seems unlikely due to the pattern of quantum yields in different solvents.

In addition to **11**, photolysis of **6** produces a species that is capable of oxidizing benzene to phenol and hydroxylating alkanes. The yield of such oxidized products ranges from modest to nearly quantitative. The pattern of reactivity is consistent with intuitive expectations for $O(^3P)$ or a similar substance, and it is suggested that this is the mechanism for the formation of **11**. Dehydrogenation of alkanes has also been demonstrated. The stepwise nature of the hydroxylation reaction has been demonstrated by formation of both alcohols derivable from a 1-phenylallyl radical. The stepwise nature of epoxidations is demonstrated by the partial loss of stereochemistry in acyclic substrates. Product competition studies are consistent with kinetic comparisons to rate constants for removal of $O(^3P)$, as determined by Scaiano.

It should be emphasized that our data are merely *consistent with* the formation of $O(^3P)$. We have made no observation that directly implies the existence of this or any other short-lived intermediate. Nonetheless, it is exceedingly clear that photolysis of **6** produces a transient of some sort that is a very powerful oxidizing agent. Circumstantial evidence described herein suggests that the oxidizing agent may be $O(^3P)$ or a solvated complex with similar reactivity.

The photolysis of 2,5-diphenyl thiophene sulfoxide leads to the formation of the sulfide along with other products. However, the quantum yield for deoxygenation is not significantly increased over that of DBTO. The photolysis of 2,5-di-*tert*-butylthiophene sulfoxide leads to very fast desulfurization. It may be possible the difference in the observed photochemistry between these molecules is due to electronic effects of the phenyl rings, but further work is needed before any definitive conclusions can be drawn.

2.22 Experimental

Photolysis systems. There were two different systems used in the photolysis experiments. The first was a Southern New England Ultraviolet Rayonet mini-reactor that had been modified to have both a fan and magnetic stirring. The fans kept the operating temperature of the solution at ambient and stirring the solution assured uniformity of exposure to light. All photolyses were done at room temperature with stirring. Either clear quartz low pressure mercury bulbs, which utilize the 253.7 nm emission band of mercury, or coated bulbs with an emission band centered at 300 nm ± 24 nm were used. The second system was a Photon Technologies, Inc., 150 W Xe arc lamp focused directly on a LPS-220 monochromator. The monochromator was used to select the wavelengths of irradiation, and generally slit widths which allowed for ± 12 nm linear dispersion of the set wavelengths were utilized. The samples were placed in a permanently mounted cell holder that was placed in such a way that all of the light was focused directly on the sample. All samples were deoxygenated with either argon bubbling for 30 minutes or a freeze pump thaw (FPT) method. Quantum yields were calculated using valerophenone as the actinometer.[72] All products formed in the photolysis were compared with authentic samples with either GC or HPLC.

General instrumentation. ^{1}H- and ^{13}C-NMR were obtained on a Varian VXR-300 MHz spectrometer. The GC-MS data were recorded on a VG Magnum ion trap instrument equipped with a 25 m DB-5 GC column. Gas chromatography data were obtained with a HP 5890 Series II gas chromatograph equipped with an FID detector. Either a 10 m HP-1, HP-

20, DB-5 or 15m DB-1701 column was used. HPLC data were collected with a HP 1050 liquid chromatograph with a diode array detector. An ODS Hypersil reverse phase column (5 μm, 200 x 2.1 mm) was used. The elution of compounds was achieved with acetonitrile/water gradients. Response factors (± 10%) for each of the compounds were calculated against an internal standard for all GC and HPLC experiments. All purifications done by flash chromatography or preparative TLC were done using EM Science Silica Gel 60 (230-400 mesh). The preparative TLC plates were produced in the lab by mixing 9:1 ratio of EM Science Silica Gel 60 (230-400 mesh) and Aldrich Silica Gel (TLC grade with fluorescent indicator, particle size 2-25μm). The silica was placed on the plate without binder and smoothed with a glass rod. Typical thickness of the silica gel was 2.5 mm. After the plate was loaded with sample, it was developed using a typical preparative TLC developing chamber tilted at ~45°. The portion of silica that contained the desired product was removed and washed with ethyl acetate with vacuum filtration. Analytical TLC was performed on EM Science Silica Gel 60 F_{254} precoated plates with a film thickness of 0.25 mm.

Photolysis of dibenzothiophene sulfoxide in the presence of oxidizable solvents. The general procedure for the photolysis of dibenzothiophene sulfoxide is as follows. All solutions ranged in DBTO concentration between 4-10 mM depending on the solubility. Except in the alkene cases, all photolyses was done with the Rayonet system and the 300 nm bulbs in quartz test tubes. In all cases that required a cosolvent, methylene chloride was used. Typically, the substrate:cosolvent ratio was 20% v/v. It was shown the presence of the

cosolvent did not effect the oxidation results for cyclohexane or cyclohexene. The reactions were generally continued until ~20-25% of the sulfoxide was converted. Dissolved oxygen was removed from all samples by using the FPT (3 x 60 mtorr) method or Ar degassed. All products formed in the photolysis were compared to authentic samples by GC, GC-MS or HPLC. Hexadecane was used as an internal standard for the GC analysis, and mesitylene was used as an internal standard for HPLC analysis.

Photolysis of DBTO in cis- and trans –octenes. The cis- and trans-4-octenes were individually purified by distillation from $LiAlH_4$. Freshly distilled alkenes were used to prepare the solutions, which contained 10 mM DBTO, 10% (v/v) alkene, and either acetonitrile or dichloromethane. No significant difference in results was observed between the two solvents. Photolyses were carried out using the Rayonet system with the 300 nm bulbs in quartz test tubes. The resulting allylic alcohols were not separated from one another, but all other products were. These products were characterized by GC with hexadecane as the internal standard.

Photolysis of DBTO in cis- and trans-ß-Methylstyrene. The trans-ß-methylstyrene was purified by two successive distillations from $LiAlH_4$. The purified alkene was used in the preparation of a solution containing 6 mM DBTO, 10% (v/v) alkene, and 1 mM hexadecane in benzene or methylene chloride. This solution was photolyzed in a quartz cell at 320 nm with the Xe arc lamp. Both the epoxides and cinnamyl alcohol were identified with the GC.

The purified cis-ß-methylstyrene was obtain as discussed below. A mixture of 10 mM DBTO, 10% (v/v) cis-ß-methylstyrene, and 1 mM hexadecane was photolyzed at 340 nm using the Xe arc lamp. Again, the products were identified using the GC.

Photolysis of DBTO in allyl benzene. The DBTO was photolyzed with allyl benzene with a cosolvent and as a neat solution. The allyl benzene (Aldrich Chemical Co.) was purified by distillation over CaH_2. A solution of 8mM DBTO, 1 mM hexadecane (internal standard), 10% (v/v) allyl benzene and methylene chloride as the cosolvent was prepared and degassed with Ar. The solution was photolyzed in a quartz cell to ~20% conversion of the sulfoxide at 320 nm using the Xe arc lamp. Product analysis was done by GC (10 m HP-1 column). The photolysis of DBTO in neat allyl benzene was exactly the same as this procedure except the methylene chloride is not present.

Photolysis of DBTO in benzene and benzene-d_6. Benzene-d_6 (Wiley Chemical) was analyzed for phenol and used as received. The benzene was purified by distillation from CaH_2. Mixtures of 1:3, 1:1, and 3:1 of the benzene:benzene-d_6 respectively were used to establish selectivities. The solutions of 10 mM DBTO, 10mM hexadecane and the corresponding mixtures of benzene:benzene-d_6 were photolyzed with the Rayonet 300 nm bulbs. The solutions were photolyzed to ~20% conversion of the sulfoxide. Quantification of the phenols was done by analysis of the molecular ions using an ion trap GC-MS.

Photolysis of 2,5-di-phenylthiophene sulfoxide (16). Stock solutions of 4-8 mM 2,5-diphenylthiophene sulfoxide in CH_3CN or CH_2Cl_2 were prepared. Generally, the stock solutions were split into several samples and used in subsequent runs. Because 2,5-di-phenylthiophene sulfoxide decomposed over the course of several days, stock solutions were stored only at low temperatures and no longer than 2-3 days. All samples were degassed by Ar bubbling for 15 minutes to remove any dissolved oxygen. Each of the samples consisted of ~2-3 ml in a quartz cells. Photolyses were carried out using the Xe arc lamp and monochromator with constant stirring. Photolysis was carried out to ~20% conversion of the sulfoxide. Products were characterized by HPLC and GC. Hexadecane was used as an internal standard for the GC analysis, and mesitylene was used as an internal standard for HPLC analysis.

Photolysis of 2,5-di-*tert*-butylthiophene sulfoxide. Stock solutions of 4-9 mM 2,5-diphenylthiophene sulfoxide in CH_3CN or CH_2Cl_2 were prepared in a quartz cell. Again, the stock solutions were generally split into several samples and used in subsequent runs. Because the sulfoxide decomposed over the course of couple of days at room temperature, the stock solutions were be prepared and photolyzed immediately after its synthesis and purification. All photolyses were carried out using the Rayonet system with the 300 nm bulbs and constant stirring. All samples were degassed with Ar bubbling to remove any dissolved oxygen. Products resulting from the photolysis were characterized with HPLC with mesitylene as an internal standard.

Laser flash photolysis of DBTO. The laser flash photolysis experiments on DBTO were carried out using a computer-controlled nanosecond transient absorption spectrometer. Samples of DBTO were irradiated with the fourth harmonic of a Continuum Surelite Nd:YAG laser (266 nm, 5ns, 2-25 mJ/pulse, 3mm beam radius). The spectroscopic detection system included a 75 W xenon lamp, an ISA H10 monochromator, an IP-28 photomultiplier (R_l = 50 Ω), and a Tetronix TDS-250 200 MHz transient digitizer. Control of the experiment, data collection, and processing were carried out using a Macintosh Quadra 640 with Labview 3 software. The laser beam was used at 90° with respect to the probe beam. Investigations were carried out in a standard 1 cm quartz cell. The optical densities of the DBTO solutions ranged from 0.2-0.8 at 266 nm. All solutions were degassed with Ar before the experiments, and all experiments were conducted at room temperatures.

Dibenzothiophene sulfoxide (1). Dibenzothiophene sulfoxide was obtained by the oxidation of Dibenzothiophene (Aldrich Chemical Co.) by $Bu_4N^+IO_4^-$ and catalytic (5,10,15,20-tetraphenylporphine)iron(III) chloride.[73,74]

***cis*-4-Octene.** A 25 ml round bottom flask equipped with a septum and balloon was charged with 5 ml of methanol, 0.73 ml of 4-octyne and 0.01 g of Pd/C at room temperature. The system was evacuated by aspiration and charged with hydrogen gas (98 %, Aldrich Chemical Co.). This procedure was repeated 3 times to ensure the atmosphere in the system was mostly hydrogen. Hydrogen gas was then bubbled through the solution via an 8 inch needle. The reaction was monitored with GC and quenched when *n*-octane began to appear.

The reaction was filtered, quenched with water, extracted with diethyl ether, dried over sodium sulfate, and concentrated under reduced pressure. Purification by distillation under argon afforded *cis*-4-octene (B.P. = 65°) in 65 % yield. Both the ^{1}H- and ^{13}C matched those reported in the literature.[75]

***m*-CPBA Oxidations of alkenes.** A solution of 0.5 g of 85% *m*-chloroperbenzoic acid in 25 ml of methylene chloride was cooled to 0°C with a cryocool and acetone bath. The corresponding alkene was added slowly over 5 minutes and allowed to react at 0° for 30 minutes. The acetone bath was then removed and the reaction was warmed to room temperature and allowed to react for 4 hours. The reaction was monitored with TLC and allowed to react until all of the starting alkene had disappeared. The solution was then quenched with 5% NaOH and saturated aqueous NaCl, dried over magnesium sulfate, and concentrated under reduced pressure. Purification via column chromatography afforded ~92% of the corresponding epoxide. The NMR spectra of all of the epoxides matched those reported in the literature.

***trans*-4-Octene-3-ol.** Coupling of *trans*-2-hexenal with ethyl Grignard produced the desired alcohol. A 0.14 g sample of magnesium along with 25 ml of dried ether was added to a flame dried round bottom flask equipped with a dropping funnel and stir bar. The system was kept under positive Ar pressure to ensure anhydrous conditions. A 0.42 ml aliquot of iodoethane was added dropwise at room temperature and allowed to react until all of the magnesium had disappeared. The solution was then cooled to 0° and 0.35 ml of 2-hexenal

(Aldrich Chemical Co.) was added dropwise and allowed to react for 30 minutes. The solution was then warmed and refluxed for 30 minutes. The reaction was washed with aqueous 3M HCl until acidic, extracted with ether, dried over sodium sulfate, and concentrated under reduced pressure. Purification via a silica gel column (70:30 hexane :ethyl acetate) afforded the corresponding alcohol in 55% yield. The NMR matched those reported in the literature for both epoxides.[76]

***trans*-3-Octene-4-ol.** The alcohol was prepared by coupling *trans*-2-pentenal (Aldrich Chemical Co.) and propyl Grignard (Aldrich Chemical Co.). The method used to prepare this enol was very similar to that described above. However, in this case the bromopropane and magnesium mixture had to heated slightly in the preparation of the Grignard. The ^{1}H and ^{13}C NMR matched previously reported spectra.[77]

***cis*- and *trans*-ß-Methylstyrene.** The *trans*-ß-methylstyrene was purchased from Aldrich Chemical Co. and used without further purification. The *cis*-ß-methylstyrene was produced by the reduction of the corresponding alkyne similar to the method used in the 4-octene case. However, the Pd/C catalyzed reaction gave poor yields of the desired alkene. Thus, several different variations of the reduction were investigated in order to establish the most efficient route. The results are shown below. The overall reaction conditions, such as temperature, concentration of the alkyne and isoquinoline were held constant and only the backing of the palladium was altered. The palladium backed on barium carbonate gave the best results and, therefore, this was the catalyst used in the reaction. Purification via silica

gel column afforded pure *cis*-ß-methylstyrene in 60% overall yield. The setup for this reaction was also modified from that of the 4-octyne experiments. Increased control of the hydrogen gas flow was obtained by pumping it through a glass vessel equipped with a needle valve. This, coupled with changing the reaction vessel from a flask to a test tube, led to greatly increased efficiencies. All reactions included in this investigation started with 0.5 ml of the 1-phenylpropyne.

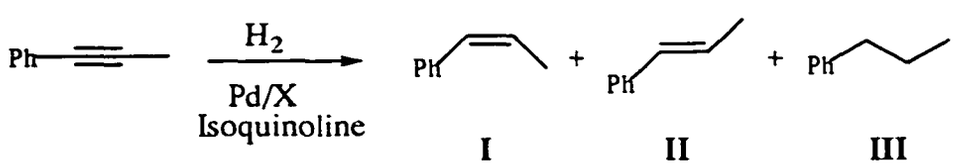

I II III

Catalyst	% I	% II	% III
Pd/C	30	5	50
$Pd/CaCO_3$ + Pb	60	20	11
$Pd/BaCO_3$	80	4	11

1-Phenyl-3-propene-1-ol. A solution of freshly distilled THF and 15 mmol vinyl magnesium bromide (Aldrich Chemical Co.) was cooled to –20°C under a constant flow of argon. Benzaldehyde (20 mmol) in THF was added dropwise over the course of 15 minutes. The reaction was allowed to react for 1 hour at –20°C and 1 hour at room temperature. The solution was then quenched in ammonium chloride, extracted with ether, dried over sodium sulfate, and concentrated under reduced pressure. Purification with preparative TLC yielded pure product in 80% yield. The ^{1}H- and ^{13}C-NMR matched those previously reported.[78]

$AlCl_3$ Catalyzed Friedel-Crafts of succinic anhydride and benzene. A 50 ml round bottom flask was charged with 30 ml of benzene, 2.0 g of succinic anhydride and 2.5 x mol/mol excess of $AlCl_3$. The reaction was heated to 90° and refluxed for 14 hours. The resulting solution was quenched in 25 ml of concentrated HCl in crushed ice, extracted with methylene chloride, dried over sodium sulfate and concentrated with reduced pressure. Purification was not necessary and 87% of the keto acid was isolated. The NMR matched that published in the literature.

Preparation of γ-keto acid chloride (44). To a sample of 2.0 g of the corresponding carboxylic acid was added 1.8 ml of $SOCl_2$. The evolution of HCl was monitored through a bubbler with litmus paper and the reaction was heated until this evolution stopped. The $SOCl_2$ was removed under reduced pressure. The resulting residue was dissolved in methylene chloride and used in a second Friedel-Crafts reaction identical to the one above. A TLC of the reaction mixture showed the formation of 5-6 new compounds. The major product was isolated and identified as the diphenyl methane formed in a Friedel-Crafts reaction with methylene chloride. Attempts to modify the reaction conditions by changing the acid, solvent, reaction time and temperature produced only a minimal amount of the diketone.

Friedel-Crafts on succinyl dichloride. Another attempt at synthesizing the diketone **43** using an acid catalyzed Friedel-Crafts reaction between benzene and succinyl chloride (Aldrich Chemical Co.) was made. A sample of 0.71 ml of succinyl dichloride was added to

a dry, argon flushed 50 ml round bottom flask with 30 ml of benzene. The addition of 134 mg of $AlCl_3$ made the reaction turn dark red in color. The reaction was refluxed for 2 hours. Subsequent work up and analysis by TLC showed the formation of a large number of products. Additional reactions in which 1,1,2,2,tetrachloroethane was used as a solvent all produced minimal amounts of the desired product.

Coupling of the enolate of acetophenone. The coupling of acetophenone enolates with $CuCl_2$ was reported by Yoshikiko and coworkers.[79] A solution of 30 ml of THF (freshly distilled from Na) and 30 mmoles of diisopropyl amine (freshly distilled) was cooled to –78°C. A solution of 30 mmoles of *n*-butyl lithium (Aldrich Chemical Co.) in methylene chloride was added dropwise and allowed to react for 30 minutes. A solution of 28 mmol of acetophenone in THF was added dropwise and allowed to react for 15 minutes. A solution of 30 mmol of anhydrous $CuCl_2$ dissolved in dry DMF was added to the enolate solution. The reaction turned green and was allow to react for 30 minutes at which time the solution was slowly warmed to room temperature and allowed to react for 1 hour. The resulting reaction was quenched in aqueous ammonium chloride and extracted with hexane. Purification with a silica gel column yielded 1,2-dibenzoylethane in 30% yield. The ^{1}H- and ^{13}C-NMR matched those previously reported.[79]

Palladium catalyzed synthesis of 2,5-diphenylthiophene. A 15 mmol sample of anhydrous $ZnCl_2$ (dried with $SOCl_2$) was dissolved in dried THF and added to a flame dried, argon flushed round bottom flask. The solution was cooled to 0°C and 15 mmol of phenyl

magnesium bromide (2.0 M solution in tetrahydrofuran Aldrich Chemical Co.) was added dropwise with stirring. The solution was held at 0° for 15 minutes and warmed to room temperature at which time a white precipitate formed (magnesium salts). The resulting solution was added dropwise to a cooled solution of 5.0 ml THF, 5 mmol of 2,5-dibromothiophene (Wiley Organics), 10 mg $Pd(PPh_3)_4$. The organo-zinc compound was added slowly to minimize the cross coupling reaction. The reaction was then heated to 50 °C for 14 hours. A second aliquot of the organo-zinc compound was added and the reaction was continued for an additional 3 hours. The product was then filtered, extracted with hexane, and concentrated under reduced pressure. Purification with a silica gel column afforded 53% pure 2,5-di-phenylthiophene. The ^{1}H- and ^{13}C-NMR matched those previously reported.[46]

2,5-di-*tert*-butylthiophene To a flask containing 1 g of silica gel, 1.2 g of sodium carbonate and 10 ml carbon tetrachloride was added 0.32 ml of thiophene and 1.38 ml of *tert*-butylbromide. The reaction was warmed to 78°C and allowed to react for 40 hours. Filtration of the resulting solution followed by three successive washes separated the product from the silica gel and sodium carbonate. Unreacted starting material along with the solvent were removed under reduced pressure leaving a mixture of 99% of the 2,5 isomer and 1% of the 2,4 isomer in 75% overall yield. The NMR matched those previously reported.[63]

Oxidation of 2,5-di-substituted thiophenes. Several different methods for oxidizing the thiophene were investigated. The general procedure for the most efficient route is as follows. To a solution of 1 mmol of the corresponding thiophene in methylene chloride

cooled to 0°C was added 0.18 equivalents 30% hydrogen peroxide and 3 equivalents of trifluoroacetic acid. The reaction mixture was allowed to react for 30 minutes at 0°C at which time it was warmed to room temperature and stirred for an additional 4.5 hours. Analysis of the reaction by TLC and HPLC showed remaining starting material and very little sulfone. Therefore, an additional full equivalent of hydrogen peroxide was added and the reaction mixture was allowed to react for an additional 2 hours. TLC and HPLC showed the sulfone was beginning to form and thus the reaction was quenched in sodium carbonate. The product was extracted with methylene chloride, dried over sodium sulfate, and concentrated under reduced pressure. Purification with a 2 successive preparative TLCs afforded pure 2,5-di*tert*-butylthiophene sulfoxide in 35% yield. The NMR and UV-vis spectra match those previously reported.[45] The oxidation of 2,5-diphenylthiophene was accomplished in a very similar manner as that for the *tert*-butyl case with a yield of 30%. The ^{1}H and ^{13}C NMR spectra matched those reported in the literature.[46] Both of the sulfoxides should be used on the same day they were prepared for purity reasons.

Due to the relative inefficiencies of the peroxide/trifluoroacetic acid oxidations, several different methods were investigated. The results of these experiments are shown below in Table 9. None of the other methods produced any detectable product, probably due the fact that oxidation of the thiophene removes the ring out of aromaticity and the other methods are less aggressive than the peroxide and acid.

Both the 2,5 diphenyl and 2,5-di-*tert*-butyl thiophene sulfones were isolated as by-products from the preparation of the corresponding sulfoxide reactions discussed above. The ^{1}H and ^{13}C NMR spectra matched those reported in the literature.[45,46]

Table 9. Oxidation of 2,5-di-*tert*-butythiophene with several methods.

Oxidant	Acid	Solvent	Temperature	% Yield of 15
H_2O_2	CF_3COOH	CH_2Cl_2	0°C	20
H_2O_2	CF_3COOH	CH_2Cl_2	R.T.	35
m-CPBA	-	CH_2Cl_2	0°C	-
m-CPBA	-	CH_2Cl_2	R.T.	-
H_2O_2-Urea	-	CH_3CN	0°C	-
H_2O_2-Urea	-	CH_3CN	R.T.	-
H_2O_2-Urea	-	CH_3OH	0°C	-
H_2O_2-Urea	-	CH_3OH	R.T.	-
$(CH_3)_3COOH$	CH_3COOH	CH_2Cl_2	0°C	-
$(CH_3)_3COOH$	CH_3COOH	CH_2Cl_2	R.T.	-
$(CH_3)_3COOH$	CH_3COOH	CH_2Cl_2	0°C	-
$(CH_3)_3COOH$	CH_3COOH	CH_2Cl_2	R.T.	-

References

(1) Gregory, D. D.; Wan, Z.; Jenks, W. S. *J. Am. Chem. Soc.* **1997**, *119*, 94-102.

(2) Shelton, J. R.; Davis, K. E. *Int. J. Sulfur Chem.* **1973**, *8*, 217-228.

(3) Gurria, G. M.; Posner, G. H. *J. Org. Chem.* **1973**, *38*, 2419-2420.

(4) Still, I. W. J.; Arora, P. C.; Chauhan, M. S.; Kwan, M. H.; Thomas, M. T. *Can. J. Chem.* **1976**, *54*, 455-470.

(5) Still, I. W. J.; Cauhan, M. S.; Thomas, M. T. *Tetrahedron Lett.* **1973**, 1311-1314.

(6) Still, I. W. J.; Thomas, M. T. *Tetrahedron Lett.* **1970**, 4225-4228.

(7) Still, I. W. J.; Arora, P. C.; Hasan, S. K.; Kutney, G. W.; Lo, L. Y. T.; Turnbull, K. *Can. J. Chem.* **1981**, *59*, 199-209.

(8) Still, I. W. J. In *The Chemistry of Sulfones and Sulfoxides*; S. Patai; Z. Rappaport and C. J. M. Stirling, Ed.; John Wiley & Sons Ltd.: New York, 1988; pp 873-887.

(9) El Amoudi, M. S. E. F.; Geneste, P.; olive, J. L. *J. Org. Chem.* **1981**, *46*, 4258-4262.

(10) Kharasch, N.; Khodair, A. I. A. *J. Chem. Soc., Chem. Commun.* **1967**, 98-100.

(11) Wan, Z.; Jenks, W. S. *J. Am. Chem. Soc.* **1995**, *117*, 2667-2668.

(12) Ando, W.; Takata, T. *Singlet Oxygen*; CRC Press: Boca Raton, 1983; Vol. III.

(13) Mislow, K.; Green, M. M.; Laur, P.; Melillo, J. T.; Simmons, T.; Ternay, A. L. J. *J. Am. Chem. Soc.* **1965**, *87*, 1958-1976.

(14) Khait, I.; Lüdersdorf, R.; Muszkat, K. A.; Praefcke, K. *J. Chem. Soc., Perkins Trans 2* **1981**, 1417-1429.

(15) Lüdersdorf, R.; Khait, I.; Muszkat, K. A.; Praefcke, K.; Margaretha, P. *Phosph. and Sulfur* **1981**, *12*, 37-54.

(16) Benson, S. W. *Chem. Rev.* **1978**, *78*, 23-35.

(17) Stein, S. E.; Lias, S. G.; Liebman, J. F.; Levin, R. D.; Kafafi, S. A. In U.S. Department of Commerce, NIST: Gaithersburg, MD, 1994; pp .

(18) Wagner, P. J.; Hammond, G. S. *J. Am. Chem. Soc.* **1966**, *88*, 1245-1251.

(19) Jenks, W. S.; Taylor, L. M.; Guo, Y.; Wan, Z. *Tetrahedron Lett.* **1994**, *35*, 7155-7158.

(20) Jenks, W. S.; Lee, W.; Shutters, D. *J. Phys. Chem.* **1994**, *98*, 2282-2289.

(21) Levine, J. S. *The Photochemistry of Atmospheres*; New York, 1985.

(22) Wayne, R. P. *Chemistry of Atmosphere*; Oxford University Press: New York, 1991.

(23) Warneck, P. *Chemistry of Natural Atmosphere*; Academic Press Inc.: New York, 1988.

(24) Singleton, D. L.; Cvetanovic, R. J. *J. Phys. Chem. Ref. Data* **1988**, *17*, 1420-1435.

(25) Francisco, L. T.; Ureña, A. G. *J. Chem. Soc., Faraday Trans, 2* **1985**, *81*, 1395-1405.

(26) Kläning, U. K.; Sehested, K.; Wolff, T. *J. Chem. Soc., Faraday Trans.1* **1984**, *80*, 2969.

(27) Brown, W. G.; Hart, E. J. *J. Phys. Chem.* **1978**, *82*, 2539.

(28) Sauer, M. C., Jr.; Brown, W. G.; Hart, E. J. *J. Phys. Chem.* **1984**, *88*, 1398.

(29) Varkony, T. H.; Pass, S.; Mazur, Y. *J. Chem. Soc. Chem. Commun.* **1975**, 457-458.

(30) Albini, A.; Alpegiani, M. *Chem. Rev.* **1984**, *84*, 43-71.

(31) Kaneko, C.; Yamamori, M.; Yamamoto, A.; Hayashi, R. *Tetrahedron Lett.* **1978**, 2799.

(32) Ogawa, Y.; Iwasaki, S.; Okuda, S. *Tetrahedron Lett.* **1981**, *22*, 3637-3640.

(33) Akhatar, N. M.; Boyd, D. R.; Neill, J. D.; Jerina, D. M. *J. Chem. Soc. Perkin Trans. 1* **1980**, 1693-1699.

(34) Bucher, G.; Scaiano, J. C. *J. Phys. Chem.* **1994**, *98*, 12471-12473.

(35) Jenks, W. S.; Matsunaga, N.; Gordon, M. G. *J. Org. Chem.* **1996**, *61*, 1275-1283.

(36) Varkony, T. H.; Pass, S.; Mazur, Y. *J. Chem. Soc. Chem. Commun.* **1975**, 457-458.

(37) Kaubisch, N.; Jerina, D. M.; Daly, J. W. *Biochemistry* **1972**, *11*, 3080-3086.

(38) Bruice, P. Y.; Kasperek, G. J.; Bruice, T. C.; Yagi, H.; Jerina, D. M. *J. Amer. Chem. Soc.* **1973**, *95*, 6041-6048.

(39) Vogel, E.; Günter, H. *Angew. Chem., Int. Ed. Engl.* **1967**, *6*, 385-401.

(40) Tillett, J. G. *Chem. Rev.* **1976**, *76*, 747-772.

(41) Gilbert, A.; Baggott, J. *Essentials of Molecular Photochemistry*; Blackwell Scientific Publications: Oxford, 1991.

(42) Turro, N. J. *Modern Molecular Photochemistry*; Benjamin/Cummings Publishing Co.: Menlo Park, 1978, pp 628.

(43) Smith, M. B. *Organic Synthesis*; McGraw-Hill, Inc.: New York, 1994, pp 1595.

(44) Bailey, W. J.; Cummins, E. W. *J. Am. Chem. Soc.* **1954**, *76*, 1932-1940.

(45) Mock, W. L. *J. Am. Chem. Soc.* **1970**, *92*, 7610-7612.

(46) Pouzet, P.; Erdelmeier, I.; Ginderow, D.; Mornon, J. P.; Dansette, P.; Mansuy, D. *J. Chem. Soc., Chem. Commun.* **1995**, 473-474.

(47) Procházka, M. *Collect. Czech. Chem. Commun.* **1965**, *39*, 1158-1168.

(48) Treiber, A.; Dansette, P. M.; El Amri, H.; Girault, J. P.; Ginderow, D.; Mornon, J. P.; Mansuy, D. *J. Am. Chem. Soc.* **1997**, *119*, 1565-1571.

(49) Rosell, K. *Acta Chim. Scand.* **1976**, *B30*, 353-357.

(50) Naperstkow, A. M.; Macauley, J. B.; Newlands, M. J.; Fallis, A. G. *Tetrahedron Lett.* **1989**, *30*, 5077-5080.

(51) Thiemann, C.; Thiemann, T.; Li, Y. Q.; Sawada, T.; Nagano, Y.; Tashiro, M. *Bull. Chem. Soc. Jpn.* **1994**, *67*, 1886-1893.

(52) Li, Y. Q.; Thiemann, T.; Sawada, T.; Tashiro, M. *J. Chem. Soc., Perkin Trans.* **1994**, 2323-2329.

(53) Scheibye, S.; Shabana, R.; Lawesson, S. O. *Tetrahedron* **1982**, *38*, 993-1001.

(54) Yates, C. *J. Am. Chem. Soc.* **1952**, *74*, 5376-5380.

(55) Mcleod, M.; Boudreault, N.; Leblanc, Y. *J. Org. Chem.* **1996**, *61*, 1180-1183.

(56) Wagner, P. J.; Frerking, H. *Can. J. Chem.* **1995**, *73*, 2047-2061.

(57) Lee, Y. J.; Ling, R.; Mariano, P. S.; Yoon, U. C.; Kim, D.; Oh, S. W. *J. Org. Chem.* **1996**, *61*, 3304-3314.

(58) Schuber, R.; Sweeney, G. *J. Am. Chem. Soc.* **1954**, *76*, 5462-5470.

(59) Agranat, S. *J. Chem. Educ.* **1976**, *53*, 488.

(60) Kobayashi, Y.; Taguchi, T.; Tokuno, E. *Tetrahedron Lett.* **1977**, *42*, 3741-3742.

(61) Minato, A.; Tamao, K.; Hayashi, T.; Suzuki, K.; Kumada, M. *Tetrahedron Lett.* **1980**, *21*, 845-848.

(62) Wynberg, H.; Wiersum, U. E. *J Org Chem* **1964**, *30*, 1058-1060.

(63) Kamitori, Y.; Hojo, M.; Ryoichi, M.; Tatsuo, I.; Tsukamoto, S. *J. Org. Chem.* **1984**, 4161-4165.

(64) Schultz, A. G.; DeBoer, C. D.; Schlessinger, R. H. *J. Am. Chem. Soc.* **1968**, *90*, 5314-5315.

(65) Schultz, A. G.; Schlessinger, R. H. *Tetrahedron Lett.* **1973**, 4787-4890.

(66) Schultz, A. G.; Schlessinger, R. H. *J. Chem. Soc. Chem. Commun.* **1970**, 1294-1295.

(67) Schultz, A. G.; Schlessinger, R. H. *J. Chem. Soc. Chem. Commun.* **1969**, 1483-1484.

(68) Schlessinger, R. H.; Schultz, A. G. *Tetrahedrom Lett.* **1969**, *52*, 4513-4515.

(69) Block, E.; Page, J.; Toscano, J. P.; X., W. C.; Zhang, X.; DeOrazio, R.; Guo, C.; Sheridan, R. S.; Towers, N. *J. Am. Chem. Soc.* **1996**, *118*, 4719-4720.

(70) Block, E.; Guo, C.; Thiruzazhi, M.; Toscano, P. J. *J. Am. Chem. Soc.* **1994**, *116*, 9403-9404.

(71) Schroth, W.; Dunger, S.; Billig, F.; Spitzner, R.; Herzschuh, R.; Vogt, A.; Jende, T.; Israel, G.; Barche, J.; Ströhl, D. *Tetrahedron* **1996**, *52*, 12677-12698.

(72) Wagner, P. J.; Kelso, P. A.; Kemppainen, A. E.; McGrath, J. M.; Schott, H. N.; Zepp, R. G. *J. Am. Chem. Soc.* **1972**, *94*, 7506-7512.

(73) Takat, T.; Ando, W. *Tetrahedron Lett.* **1983**, *24*, 3631-3534.

(74) Suter, C. M.; Maxwell, C. E. *Org. Synth. Collective Volume 2* **1943**, 485-486.

(75) Hatings, D. J.; Weedon, A. C. *Can. J. Chem.* **1991**, *69*, 1171-1182.

(76) Roth, W. R.; König, J.; Stein, K. *Chem. Ber.* **1970**, *103*, 426-439.

(77) Mordini, A.; Rayana, E.; Margot, C.; Schlosser, M. *Tetrahedron* **1990**, *46*, 2401-2410.

(78) Fisher, G. B.; Fuller, J. C.; Harrison, J.; Alvarez, S.; Burkhardt, E. R. *J. Org. Chem.* **1994**, *59*, 6378-6385.

(79) Yoshihiko, I.; Konoike, T.; Sagusa, T. *J. Am. Chem. Soc.* **1975**, *97*, 2912-2914.

CHAPTER III
THERMOCHEMISTRY OF SULFENIC ESTERS (RSOR'): NOT JUST ANOTHER PRETTY PEROXIDE

This chapter is partially based on a paper published in the *Journal of Organic Chemistry*[1]

Daniel D. Gregory and William S. Jenks

Abstract: A computational study on the thermochemistry of several simple sulfenic acids (RSOH) and esters (RSOR') is reported. The enthalpies of R-S, S-O, and O-R' homolytic cleavage are calculated at the G2 level of theory and compared to related peroxides and disulfides. Less expensive B3LYP calculations were unsatisfactory. When R and R' are both alkyl, the O-C bond is expected to be the weakest in the molecule; for CH_3SOCH_3, C-S, S-O, and O-C bond dissociation enthalpies of 67, 64, and 49 kcal/mol are predicted by G2. Compared to peroxides, sulfenic esters are predicted to have weaker O-C bonds and S-O bonds that are stronger than the analogous O-O bonds. The C-S bonds of sulfenic esters are predicted to be somewhat stronger than those of disulfides. A rationalization is given for these observations that radical stabilization is greater for RSO• than ROO•, RSS•, or ROS•.

3.1 Introduction

As discussed in chapter one, the sulfenic ester **3** has been suggested to be an intermediate in the photolysis of several different sulfoxide systems.[2-9] This class of compounds is isomeric to the sulfoxide, but with a linear connectivity that reminds one of peroxides or disulfides. As a point of nomenclature, however, they are esters of sulfenic acids (RSOH). More commonly known organic sulfur acids are the sulfonic (RSO_3H) and sulfinic (RSO_2H) classes, in which sulfur is at a higher oxidation state.

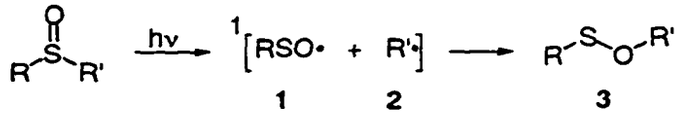

Sulfenic acids are not especially common in natural products, but they are extraordinarily important in the kitchen, being the first enzymatically produced compounds on crushing or slicing of onions, garlic and other members of the *Allium* genus.[10] The actual onion lacrymator is a sulfine, $CH_3CH_2CH{=}S{=}O$, formed by an electrocyclic isomerization of the enzymatically produced 1-propenesulfenic acid.[11]

As another point of interest, the sulfenic acid is essentially unique among organic acids in that the equilibrium in aqueous solution favors its anhydride, called a thiosulfinic ester.[12]

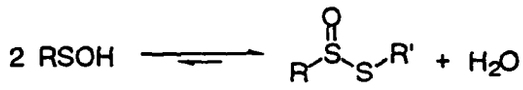

As a result, less is known about sulfenic acids than the more highly oxidized sulfur acids.

In sulfoxide photochemistry, the sulfenic ester is generally proposed to be formed from an α-cleavage reaction followed by recombination of the sulfinyl radical **1** at the oxygen terminus with the carbon radical **2**.[13-16]

Recently, Guo and Jenks investigated the photolysis of phenyl benzyl sulfoxides to gain a better understanding of the mechanism of the α-cleavage reaction.[2] The general reaction scheme proposed is shown below in Figure 1. Absorption of a photon by the sulfoxide leads to the formation of a radical pair via the α-cleavage reaction. The radical pair can then undergo several different reactions. These include the geminate recombination at the sulfur atom to form starting material, escape from the solvent cage to form the corresponding dimer products, and recombination at the oxygen atom to form the sulfenic ester. The sulfenic ester then undergoes secondary photolysis resulting in products consistent with S-O homolysis. Indeed, Guo and Jenks showed the photolysis of several substituted benzyl arene-sulfenic esters led exclusively to S-O homolysis without the observation of O-C homolysis.[2] This mechanism is supported by the results of Pasto and coworkers, which showed the photolyses of several alkyl nitrobenzenesulfenic esters is an excellent source of alkoxy radicals.[17-21] The nitro group was used to make the sulfenic ester easier to handle in the laboratory and shift the absorption into a more convenient range.

At first, the homolysis of the S-O bond in sulfenic esters seems completely reasonable drawing an analogy from the peroxide where the O-O bond is the weakest bond. However, a Benson type thermodynamic analysis of the phenyl benzyl sulfenic ester suggests this is not

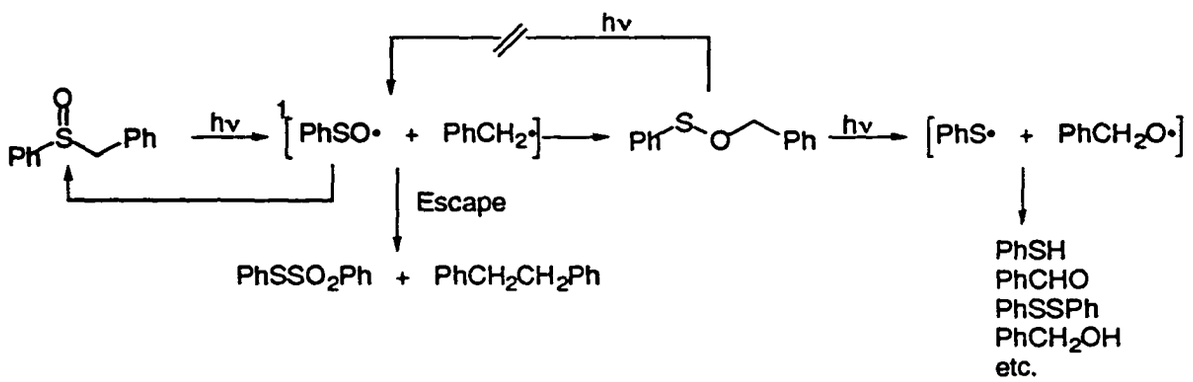

Figure 1. Proposed mechanism for the photolysis of phenyl benzyl sulfoxide.

the weakest bond in the molecule. By using estimates[22] of the heats of formation for all of the appropriate radicals it was shown that the S-O bond was in fact about 20 kcal/mol stronger than the O-C bond, despite the photochemical results. This surprising result justified further investigation.

Because of their relative instability, very little experimental thermodynamic data exists for sulfenic esters in the literature. The heterolysis of several highly substituted sulfenic esters has been investigated in solution.[23-26] However, it was proposed that the solution-phase thermal decomposition of benzyl *p*-toluenesulfenate went mainly to the sulfoxide via a concerted mechanism.[27] No gas phase data could be found in the literature regarding the thermolysis of sulfenic esters. The heat of formation has been estimated for the methyl sulfinyl radical (MeSO•),[28] but not for any other organic sulfinyl radical.

Because of the relatively small amount of experimental data a computational study was started. The major goal of this investigation was to better establish both the ground state thermodynamics and excited states of sulfenic esters and acids. This knowledge could then

be used to gain an intuitive understanding of the surprising bond strengths projected for the sulfenic ester by the Benson estimates.

3.2 General plan of attack and computational methods

One of the main points of interest in this study was the development of the ground state thermodynamics of a series of sulfenic esters. The bond dissociation energy was estimated for each of three cleavages shown below by taking the energy difference between the closed shell structure and the corresponding radicals formed from the cleavage. The structural effects on these bond dissociation energies were investigated.

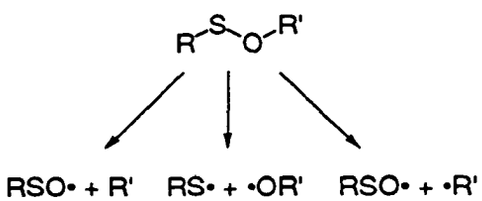

Because the calculated bond dissociation energies rely on the energies calculated for both closed shell molecules and radicals, it is important to use a computational method that can predict heats of formation of both types of systems accurately. The Gaussian 2 (G2) method is a computational method designed specifically for estimating accurate heats of formation.[29]

The G2 method was developed by Pople and coworkers and was designed to calculate heats of formation of a wide range of molecules to within ±2 kcal/mol of experimental values.[29-32] It was designed to approximate the result of a QCISD(T)/6-311+G(3df,2p)//

MP2(full)6-31G(d) calculation. The procedure starts with a geometry optimization at the MP2(full)/6-31G(d) level. A series of MP2 and MP4 single point energies are then calculated at this geometry and used in the approximation of the overall energy. The G2 method can be divided into the six individual corrections shown below.

1) A correction for the addition of diffuse functions into the basis set is evaluated as shown below.

$$\Delta E(+) = E[MP4/6\text{-}311+G(d,p)] - E[MP4/6\text{-}311G(d,p)]$$

2) A correction for higher polarization on nonhydrogen atoms is evaluated as

$$\Delta E(2df) = E[MP4/6\text{-}311G(2df,p)] - E[MP4/6\text{-}311G(d,p)]$$

3) A correction for the inclusion of a third d-function on nonhydrogen atoms and a second p-function on hydrogens is obtained by

$$\Delta = E[MP2/6\text{-}311+G(3df,2p)] - E[MP2/6\text{-}311G(2df,p)]$$
$$- E[MP2/6\text{-}311+G(d,p)] + E[MP2/6\text{-}311G(d,p)]$$

4) A correction of correlation effects beyond the fourth order perturbation theory is represented as

$$\Delta E(QCI) = E[QCISD(T)/6\text{-}311G(d,p)] - E[MP4/6\text{-}311G(d,p)$$

5) A higher level correction (HLC) which takes into account any remaining basis set deficiencies is then added to the energy in the form,

$$HLC = An_\beta - Bn_\alpha$$

where A = 4.81 mhartree, B = 0.19 mhartree, n_β = number of beta electrons, and n_α = number of alpha electrons. The value of A was derived to give the minimum mean deviation from experiment of the calculated atomization

energies of 55 molecules having well established experimental values.[29] The value for B is the error in the hydrogen atom energy.[33] The HLC is thus an empirical correction designed to help the calculated data better fit experimental results.

6) The last correction is the zero-point energy correction. It is obtained from the scaled (0.893) HF/6-31G(d) frequencies.

The final G2 energy is given by the summation of these corrections as shown below.

$$E_o = E[MP4/6\text{-}311G(d,p)] + \Delta E(+) + \Delta E(2df) + \Delta + \Delta E(QCI)$$
$$+ HLC + E(ZPE)$$

Because the G2 method requires several extensive single point calculations, its computational demands increase rapidly with the size of the system. Within current limitations, molecules with 5-6 non-hydrogen atoms seem to be about the limit for the G2 method. Nonetheless, the G2 method has been shown to perform very well at predicting the thermodynamic data of a variety of smaller molecules.[29,34,35] To get around both of these obstacles, several variations of the G2 method have been suggested including G2(MP2), G2(MP2,SVP), and G2(MP3). Only the G2(MP2) and G2(MP2,SVP) were used in this investigation and each of the calculations are outlined below.

In the G2 method, the most demanding calculation is the MP4/6-311G(2df,p). This calculation is eliminated in the G2(MP2) protocol which replaces the first 3 MP4 corrections in the G2 method (diffusional functions, polarization functions, and additional d and f shell corrections) with one correction obtained at the MP2 level.

$$\Delta_{MP2} = E[MP2/6\text{-}311+G(3df,2p)] - E[MP2/6\text{-}311G(d,p)]$$

Thus, the G2(MP2) energy is represented by the following.

$$E_o = E[QCISD(T)/6\text{-}311G(d,p)] + \Delta_{MP2} + HLC + E(ZPE)$$

By replacing the more extensive single point correction of the G2 method with the Δ_{MP2} correction the computational rigor of the G2(MP2) is greatly reduced. Objective experience shows that this causes only a minor loss in accuracy.[30]

The simplification of the G2 method is taken one step farther in the G2(MP2,SVP) method. Even though the G2(MP2) method is much less demanding than the G2 method, it still requires the calculation of the QCISD(T)/6-311G(d,p) which is in itself a fairly large calculation. The G2(MP2,SVP) protocol was develop to lower the computational demands of the G2(MP2) method by replacing the QCISD(T)/6-311G(d,p) with a less expensive QCISD(T)/6-31G(d) calculation.[36]

$$\Delta_{MP2,SVP} = E[MP2/6\text{-}311+G(3df,2p)] - E(MP2/6\text{-}31Gd$$

Thus, the G2(MP2,SVP) energy is given by the following.

$$E_o = E[QCISD(T)/6\text{-}31G(d)] + \Delta_{MP2,SVP} + HLC + E(ZPE)$$

In reality, the G2(MP2,SVP) protocol requires only two calculations; namely a QCISD(T)/6-31G(d) and MP2/6-311+G(3df,2p). The MP2/6-31G(d) energy is obtained in the QCISD(T) calculation.

Recent work by Curtiss and coworkers was done to establish the reliability of both the G2(MP2) and G2(MP2,SVP) methods compared to the G2 method.[36] Calculated dissociation energies, ionization energies, electron affinities and proton affinities were compared to experimental values for all of the molecules included in a test bank of 125 different systems. The mean absolute deviation from experimental values for the G2,

G2(MP2) and G2(MP2,SVP) were found to be 1.21, 1.58, and 1.63 kcal/mol respectively. The mean absolute deviations of the G2(MP2,SVP) relative energies from G2 and G2(MP2) values were 0.88 and 0.50 kcal/mol respectively. Despite the very good overall agreement, those molecules that contained sulfur consistently had a higher deviation than most of the other molecules, with the G2 method performing better than the other two methods. Thus, all three methods were investigated in this study.

As mentioned above, the G2 method is very demanding and is the limiting factor to the size of systems that can be investigated computationally. Because the recent experimental work by Pasto and Jenks involved alkyl esters of arenesulfenic esters, the direct comparison of the computational work to experimental results were of limited value.[18,19,21,37] Thus, along with establishing the ground state thermodynamics of several model sulfenic esters with the G2 protocols, other less expensive methods were investigated in hopes to find one that would give comparable values to the G2 method for the systems of interest. The less expensive method would then be applied to larger sulfenic esters, which would better model experimental results.

3.3 Model sulfenic acid and ester systems

The model systems investigated are shown in Figure 2. The first molecule is the simplest of the sulfenic acids HSOH **4**. The interest in this molecule stems from the fact that several of the radicals produced by homolysis (HSO• and HOS•) are suspected to play a very important role in atmospheric sulfur chemistry (see section 4.1.1). The effects of adding a heavy atom into the sulfenic ester and acid systems were investigated with compounds **5-7**.

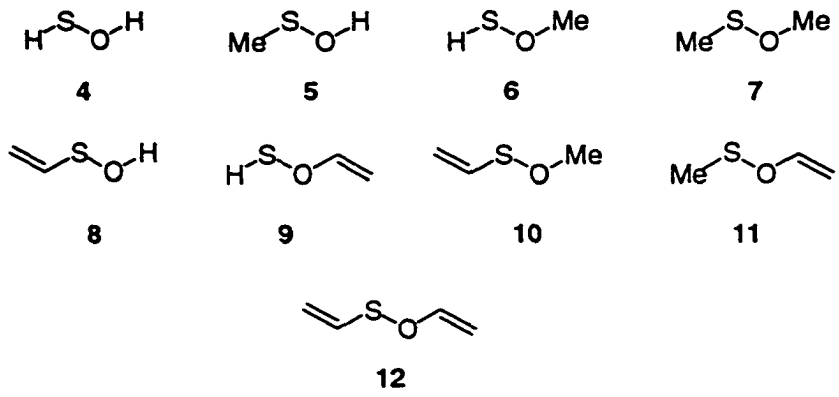

Figure 2. Model Sulfenic Acids and Esters.

Finally, the effects of bringing these systems into conjugation with a π system were investigated with molecules **8-12**.

The MP2(full)/6-31G(d) optimized geometries are shown in Table 1. All optimized geometries are local minima as indicated by the absence of imaginary frequencies in the calculated Hessian. A Hessian is a calculated vibrational analysis of the molecule. As shown in Table 1, the structures of the sulfenic acids have comparable bond lengths and angles. This is also the case for the sulfenic esters.

It should be noted that the spin contamination on all radicals not containing the vinyl group was quite modest ($S^2 \leq 0.76$). For the vinyl-substituted radicals, however, the spin contamination was more significant ($S^2 \approx 0.80$), and the spin-projected energies were used, though the variation between the projected and unprojected G2 energies was less than 0.5 kcal/mol.

Table 1. MP2(full)/6-31G(d) optimized geometries for model compounds.

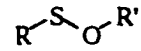

R	R'	R-S (Å)	S-O (Å)	O-R (Å)	∠RSO	∠SOR	∠RSOR'
H	H	1.35	1.69	0.98	98.6	106.2	93.4
H	Me	1.35	1.68	1.43	98.6	113.0	83.3
Me	H	1.79	1.69	0.98	99.6	106.4	92.2
H	C_2H_3	1.34	1.69	1.38	97.7	117.8	75.5
C_2H_3	H	1.75	1.69	0.98	100.3	106.3	86.3
Me	C_2H_3	1.79	1.69	1.38	99.2	113.8	81.2
C_2H_3	Me	1.75	1.69	1.43	100.0	112.6	80.5
Me	Me	1.80	1.69	1.43	99.6	112.9	88.9
C_2H_3	C_2H_3	1.75	1.69	1.44	100.0	112.6	80.5

3.4 Results

Though not necessary to calculate BDEs, heats of formation are quite useful for comparison of theory and experiment, and computed ΔH_f° values were obtained. Different methods have been advocated for arriving at computed heats of formation, generally using either atomization[32] or bond separation[35] approaches. It has been shown, however, that for larger systems an accumulation of small component errors can lead to heats of formation that are unacceptably large when calculated from atomization energies.[38] The bond separation method, which uses isodesmic reactions and molecular rather than atomic reference compounds, has some advantages, but it requires that there be appropriate reference

compounds with experimentally known $\Delta H_f°$ values. Among the sulfenic acids and esters, there is only one experimental estimate of ΔH_f (for HSOH), so the atomization method was used instead. The calculated heats of formation, shown in Table 2, were corrected to 298 K (see appendix A).[35] They are compared to available experimental values and all three models perform well.[36] It was found that G2 ΔH_f values reproduced previous computational reports to within less than 1 kcal/mol for species which did not contain sulfur. Such minor differences were attributed to slightly different geometries obtained from structural optimizations and the use of a modified basis set on the sulfur atom. (see Appendix A) The G2 heats of formation obtained for sulfur-containing compounds varied slightly more than the non-sulfur molecules (< 1.5 kcal/mol) when compared to previous computations.

Bond dissociation energies, obtained by the three G2-type methods are shown in Table 3, and agreement is generally very good. Nonetheless, only the G2 values will be used in the Discussion section.

Computing resource limitations did not allow for calculation of G2 energies for the largest sulfenic esters: $CH_3SOC_2H_3$, $C_2H_3SOCH_3$, and $C_2H_3SOC_2H_3$. Relative bond dissociation energies were obtained by comparing the sums of energies of the three pairs of products; these are reported in parentheses in Table 3. Examination of the rest of the table (and previous work on sulfur thermochemistry[22]) suggested that C-S bond enthalpies would be nearly stable for these larger sulfenic esters. This allowed the estimation of the S-O and O-C bond enthalpies for the largest sulfenic esters, and the results are shown in italics.

In addition to those necessary for the sulfenic ester BDEs, heats of formation for a few other species were obtained. A few are as noted in Table 4 for the standards. Also

calculated were energies of dimethyl sulfoxide, the "sulfoxide" isomer of H_2SO, and the transition state which connects dimethyl sulfoxide and CH_3SOCH_3 in a concerted rearrangement.

It is important to establish what is to be considered a significant effect when comparing BDEs for similar bonds in different compounds and a lower limit of 4 kcal/mol is rationalized here. The absolute average deviation for heats of formation in the expanded G2 test set, which includes many molecules of this size, is 1.6 kcal/mol. The spread of BDEs calculated by the three G2 variants is generally small ($\leq$ 2 kcal/mol), but ranges up to 4 kcal/mol. Further, three compounds are used to calculate any given BDE. Therefore, it is concluded that 4 kcal/mol is probably a reasonable limit below which BDE differences were not considered significantly different.

3.5 Discussion

A major portion of this discussion is dedicated to the BDEs of the sulfenic acids and esters, compared to other related compounds, with the object of assessing the bond strengthening or weakening by particular structural units. In order to facilitate this comparison, the G2 BDEs for the current compounds are collected in Table 4 along with experimental BDEs for representative standard compounds. A very useful compilation of measured and estimated bond enthalpies for many other types of sulfur containing compounds has been published previously.[22]

Any given homolytic bond dissociation can be described by the following equation:

$$A—B \rightarrow A^{\bullet} + B^{\bullet}$$

Table 2. Heats of formation ΔH_f° (298 K), kcal/mol

Species	G2	G2(MP2)[c]	G2(MP2,SVP)[d]	experiment[a]
H•	51.6	51.6	51.6	52.1 ± 0.0
HO•	9.1	8.9	9.3	9.4 ± 0.1
HS•	34.6	32.9	32.9	34.2 ± 0.7
HSO•	-4.0	-7.6	-6.4	
HOS•	-0.3	-2.7	-1.7	-0.5 ± 2[b]
CH_3•	35.1	35.6	35.8	35.0 ± 0.1
CH_3O•	4.7	4.9	5.0	4.1 ± 0.9
CH_3S•	30.0	28.6	28.4	29.8 ± 0.4
CH_3SO•	-15.5	-18.8	-17.8	-14.8 ± 2[c]
CH_3OS•	2.6	0.4	1.4	
C_2H_3•	72.7	73.5	71.7	71.6 ± 0.8
CH_2=CHO•	4.1	3.8	3.5	2.5 ± 2.2
CH_2=CHS•	49.3	48.1	46.4	
CH_2=CHSO•	9.5	7.1	6.3	
CH_2=CHOS•	26.6	24.7	23.7	
HSOH	-26.4	-29.5	-26.4	-27. ± 3.5[b]
CH_3SOH	-33.6	-36.4	-35.6	
$HSOCH_3$	-23.2	-26.1	-25.1	
CH_3SOCH_3	-29.5	-32.1	-31.4	
CH_2=CHSOH	-8.1	-10.9	-11.8	
HSOCH=CH_2	-1.1	-3.8	-4.6	

[a]Experimental heats of formation taken from reference 47 unless otherwise noted; [b]Reference 20; Reference 19. [c]The average deviation between G2 and G2(MP2) was -1.7 kcal/mol, and the average absolute deviation was 1.9 kcal/mol. [d]The average deviation between G2 and G2(MP2,SVP) was -1.6 kcal/mol, and the average absolute deviation was 1.7 kcal/mol.

Table 3. Computed Cleavage Enthalpies for Sulfenic Acids and Esters (298 K, kcal/mol)

		R-SOR'	RS-OR'	RSO-R'
HSOH	G2	77	70	73
	G2(MP2)	74	71	69
	G2(MP2,SVP)	74	71	70
	Experiment	79 ± 3.5[a]		
$HSOCH_3$	G2	76	63	54
	G2(MP2)	74	64	54
	G2(MP2,SVP)	74	63	54
CH_3SOH	G2	68	73	69
	G2(MP2)	69	74	65
	G2(MP2,SVP)	70	73	65
CH_3SOCH_3	G2	67	64	49
	G2(MP2)	68	66	49
	G2(MP2,SVP)	69	65	49
$HSOCH{=}CH_2$	G2	78	40	70
	G2(MP2)	76	41	70
	G2(MP2,SVP)	76	41	70
$CH_2{=}CHSOH$	G2	81	67	68
	G2(MP2)	82	68	66
	G2(MP2,SVP)	82	68	66
$CH_3SOC_2H_3$[b]	G2	(27) *67*	(0) *40*	(23) *63*
$C_2H_3SOCH_3$[b]	G2	(21) *80*	(0) *59*	(-10) *49*
$C_2H_3SOC_2H_3$[b]	G2	(46) *80*	(0) *34*	(29) *63*

[a]Reference 20; [b]Values in parentheses are G2 *relative* cleavage energies in kcal/mol, with the S-O cleavage arbitrarily set to 0, derived only from the radical energies. Values in italics are crude estimates of the absolute BDEs, based on absolute H-S and C-S cleavage energies for the related species. This assumption was justified based on previous collections of data. [37]

Table 4. Bond dissociation energies

	BDE, kcal/mol					
Compound	O–H	O-C(sp3)	O-C(sp2)	S-H	S-C(sp3)	O-O S-S S-O
HOH	119	-	-	-	-	-
CH_3OH	104	93	-	-	-	-
CH_2=CHOH	85	-	103	-	-	-
CH_3OCH_3	-	83	-	-	-	-
CH_2=$CHOCH_3$	-	62	91	-	-	-
CH_2=CHOCH=CH_2	-	-	69	-	-	-
HOOH[a]	87	-	-	-	-	51
CH_3OOH[b]	85	67	-	-	-	44
CH_3OOCH_3[c]	-	67	-	-	-	37
HSH	-	-	-	90	-	-
CH_3SH	-	-	-	91	74	-
PhSH	-	-	-	80	-	-
CH_3SCH_3	-	-	-	-	77	-
$PhSCH_3$	-	-	-	-	67	-
HSSH[a]	-	-	-	76	-	71
CH_3SSH[f]	-	-	-	79	64	68
CH_3SSCH_3	-	-	-	-	57	72
HSOH	73	-	-	79[a], 77[e]	-	70
CH_3SOH	69	-	-	-	68	73
$HSOCH_3$	-	54	-	76	-	63
CH_2=CHSO-H	68	-	-	-	-	67
HSOCH=CH_2	-	-	70	78	-	40
CH_3SOCH_3	-	49	-	-	67	64
CH_3SOCH=CH_2[d]	-	-	*63*	-	*67*	*40*
CH_2=$CHSOCH_3$[d]	-	*49*	-	-	-	*59*
CH_2=CHSOCH=CH_2[d]	-	-	*63*	-	-	*34*

Unless otherwise indicated, BDEs for sulfenic acids and esters are G2 values from Table 2. Unless otherwise noted, all others are taken from $\Delta H_f°$ values from the NIST database. [47]
[a]Reference 20; [b]$\Delta H_f°$ of $CH_3OO•$ taken as the G2 value of 1.7 kcal/mol; [c]ΔH_f of $CH_3OO•$ = 1.7 kcal/mol taken from G2 calculation; [d]See Table 3 and text; [e]This work; [f]$\Delta H_f°$ for CH_3SSH from reference 49.

Though this is self-evident, it is useful to consider when discussing BDEs, because it makes the following point clear. Structural effects that stabilize one or more of the product radicals to an extent greater than the starting material lower the BDE. (This could also be put as destabilizing the products less than the starting material.) This is illustrated in Table 4, for instance, in the O-H BDEs for CH_3OH and CH_2=CHOH. The CH_2=CHO• is expected to be stabilized by the π system and thus the O-H bond dissociation energy for CH_2=CHOH is lower than for the CH_3OH molecule.

Conversely, structural effects that selectively stabilize A-B lead to increased BDEs. An example of this type of interaction is electronegativity differences between the bonding atoms in A-B. When the electronegativity difference is large, a stabilizing bond dipole ensues in response. Of course, this bond dipole is unavailable to the separated radicals A• and B•. As a result, a larger electronegativity difference between two bonded atoms generally leads to a stronger bond than for analogous compounds whose atoms of interest have more similar electronegativity. This, for instance, contributes to the extraordinary bond strength for O-H.

3.5.1 Comparison of the weakening of the O-H, O-C, S-H, and S-C bonds by peroxides, disulfides and sulfenic esters.

The three functional groups under consideration (now designated RYY'R' where Y is S and/or O) are isoelectronic, and their respective homolytic cleavages yield isoelectronic radicals. All are expected to have weakened H-Y or C-Y bonds, relative to RYR', because the RYY• radicals have a new electronic structure that is stabilized, compared to alkoxyl or

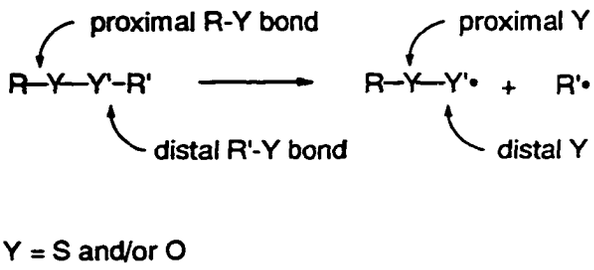

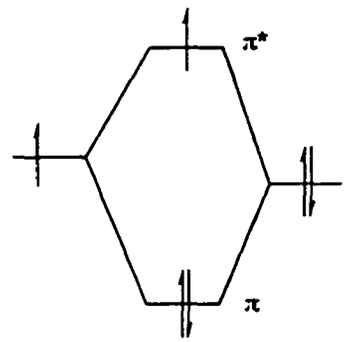

thiyl radicals. For purposes of discussion, we define "proximal" and "distal" bonds and atoms in relationship to the alkyl group of RYY' as shown below.

In RYY'•, the orbital containing the unpaired electron on Y' (which used to be involved in the distal sigma bond) overlaps with a lone pair orbital on Y, giving a 3-electron π system consisting of a doubly occupied π orbital and singly occupied π* orbital. Overall, this stabilizes the system. In support of this interpretation, peroxyl, perthiyl and sulfinyl radicals are all known experimentally to be π-type radicals.

It is reasonable to inquire whether the radical stabilization exerted by this π interaction will be the same for peroxyl radicals, perthiyl radicals, and the two radicals available from sulfenic ester cleavage, RSO• and ROS•. This can be addressed in a traditional organic chemistry sense by examination of resonance forms. Under this analysis, there are two important structures that can be drawn for each of the four radicals, one neutral, and one dipolar (Figure 3). The extent to which the dipolar form contributes to the correct overall structure is an expression of the extent to which the 3-electron π stabilization is effective. An expectation of no dipolar contribution is related to the expectation that the 3-electron π system does not stabilize the radical at all.

Underneath the dipolar structures in Figure 3 are qualitative judgments on their value as contributing structures. Charge separation in the peroxyl case is expected to be energetically expensive. Sulfur, on the other hand, is more polarizable than oxygen, so the charge separated species is seen as more viable for the perthiyl radical. Oxygen is more electronegative than sulfur; thus it is expected that the dipolar structure for ROS• will probably be the least important among all four radicals.

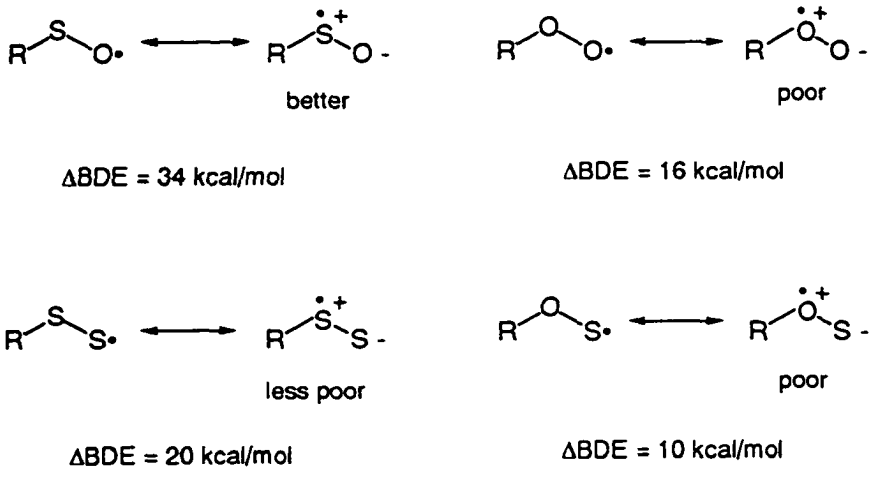

Figure 3. Resonance forms for the RYY'• radicals. ΔBDE represents the difference in O-C or S-C BDE between CH_3OCH_3 or CH_3SCH_3 and the appropriate molecule $CH_3YY'CH_3$ which produces the given radical.

However, the dipolar resonance form will be important for the sulfinyl radical RSO•, where both polarizability and electronegativity are favorable for the charge-separated form. Thus we arrive at the expectation that, while all four systems should cause weakening of the distal Y'-R' bond, the greatest destabilization should be for the O-R' bond of sulfenic acids and esters. The least bond destabilization is expected for the R-S bond of these same compounds. Confirming this expectation are the ΔBDE data shown in Figure 3, which

compare the C-O or C-S BDE of the CH_3-Y-Y'-CH_3 compound to that of dimethyl ether or dimethyl sulfide as appropriate.

The best computational surrogate to probe for the contribution of the dipolar resonance forms in the electronic structure calculations is the amount of unpaired spin on the proximal and distal Y atoms for all four radicals. This is shown in Table 5, using the Natural Population Analysis of Reed and Weinhold.[39] The delocalization is qualitatively smaller for ROO• and ROS• than for the other two, and is clearly the greatest for RSO•. Thus the sulfinyl radical (RSO•) appears to be the best radical stabilizing group of the four, with the rest in the following order:

$$RSO\bullet > RSS\bullet > ROO\bullet > ROS\bullet.$$

Other effects impinge on the BDEs as well. The O-H bond of hydrogen peroxide is weaker than that of water and alcohols. However, the fraction of the weakening due to the fractional π bond of HOO• is difficult to extract because of the large electronegativity contribution to the bond strength changes. However, this is less difficult for the destabilization of O-C(sp^3) bonds by the ROO function compared to RO. A value of about 16 kcal/mol is probably reasonable for any simple alkyl system.[22,40]

Since the H-S BDE differs so much less for H_2S and CH_3SH, one can presume that the 12-20 kcal/mol BDE drop observed on substitution of SS for S in Table 4 is due largely to the partial bond in the perthiyl radical. Benson had estimated a nearly universal bond destabilization for $RS_{n>1}$-H of about 21 kcal/mol, but the recent results of O'Hair, *et al.*

Table 5. Natural Population Analysis for CH_3YY' Radicals[a]

Species	Proximal spin density	Distal spin density
$CH_3OO\bullet$	0.10	0.90
$CH_3SS\bullet$	0.18	0.82
$CH_3SO\bullet$	0.39	0.62
$CH_3OS\bullet$	0.10	0.91

[a]All data taken from UMP2(full)/6-31(d) optimized structures.

make revision of ΔH_f° of HSS• seem necessary and the O'Hair value is used to calculate the H-S bond strength in Table 4.[41] The G2 calculations on HSS• (data not shown) are in very good agreement the O'Hair datum. A further consequence of this revision is an increase in the HSS-CH_3 bond strength, compared to the Benson value. The BDE of 57 kcal/mol and bond destabilization of about 20 kcal/mol (relative to the corresponding sulfide) for the distal alkyl-SS bond is probably still general as long as the proximal substituent is also an ordinary alkyl group.

The sulfenic esters are considered next. Compared to CH_3O-CH_3, the CH_3SO-CH_3 bond is weaker by some 34 kcal/mol. A similarly astounding O-H bond weakening of 35 kcal/mol is observed for methanesulfenic acid, relative to methanol. On the other hand, the BDEs for CH_3S-CH_3, CH_3SS-CH_3, and CH_3OS-CH_3 are 77, 57, and 67 kcal/mol, respectively. They suggest a bond weakening of 20 and 10 kcal/mol for the disulfide and S

face of the sulfenic ester. For S-H bonds, similar bond destabilizations of 12 and 15 kcal/mol are observed for disulfides and HSOR.

Finally, examination of Table 4 yields the conclusion that distal RYY'-R' BDEs are less sensitive to the proximal substituent than are the single heteroatom functional analogs. Because of the extra "insulation" of the proximal Y atom, proximal substituents have less influence on the effective electronegativity of the distal Y' atom. Since larger electronegativity differences lead to higher BDEs, it stands to reason that such "insulation" will decrease variability in the proximal Y'-R' bond BDE. Furthermore, the aforementioned radical stabilization occurs whether or not the peroxide, disulfide or sulfenic ester is conjugated on the proximal side.

3.5.2 Comparison of O-O, S-S, and S-O bond enthalpies

Among peroxides, disulfides, and sulfenic esters, peroxides have the weakest Y-Y' bonds (Table 4). The destabilization of these bonds is usually ascribed to lone pair repulsion. This effect is smaller for the second row elements than for the first row elements because the lone pairs are more diffuse and the bond lengths are naturally longer.

The S-O bond enthalpies for HSOH and CH_3SOCH_3 are much closer to those of the analogous disulfides than the peroxides. It can reasonably be assumed that the inherent lone pair repulsion energy for S-O will be larger than that of S-S and smaller than that of O-O, leading to an intermediate BDE. However, the electronegativity difference between S and O is expected to increase the bond strength. No quantitative expectation can be given, but the observed values similar to the disulfide BDEs are certainly reasonable.

The peroxide BDEs are sensitive to H/CH_3 substitution, much more so than the disulfides.[42] The O-O BDE drops about 7 kcal/mol for each H that is substituted by CH_3. This effect is virtually negligible for disulfides. This contrast between S and O behavior carries over into the sulfenic compounds. Substitution of CH_3 for H on the sulfur terminus has a small effect on the S-O enthalpy, perhaps slightly increasing it. The effect of the same substitution on the oxygen atom is more dramatic, lowering the S-O BDE by about 10 kcal/mol.

Last, there is the effect of substituting vinyl groups for methyls. Such substitutions will be reflected in the special stability of the allyl-like $C_2H_3S\bullet$ and $C_2H_3O\bullet$ radicals, causing a weakening in the S-O bond. Benson has estimated the allylic stabilization energy for $C_2H_3S\bullet$ to be about 8 kcal/mol.[22] A stabilization of 5-6 kcal/mol is observed here, but the magnitude is clearly comparable. A much larger allylic stabilization is observed for $C_2H_3O\bullet$, approximately 24 kcal/mol. The larger allylic stabilization for $C_2H_3O\bullet$ than for $C_2H_3S\bullet$ is also qualitatively in line with trends for PhO• versus PhS• and C-O versus C-S π-bonds in general.[22]

3.6 Isomerization of sulfenic esters to sulfoxides

Mislow and coworkers experimentally studied the isomerization of benzyl *p*-toluenesulfenate to benzyl *p*-tolyl sulfoxide in benzene.[27] They obtained $\Delta H^{\ddagger}$ = 30 kcal/mol and $\Delta S^{\ddagger}$ = -2 e.u. Isotopic labeling experiments indicated a partial retention of configuration at the benzyl carbon during the rearrangement. Thus it was proposed that the reaction was concerted.

Calculations at the G2 level are out of the question for molecules of that size, but a transition state was obtained for the concerted conversion of CH_3SOCH_3 to dimethyl sulfoxide. Its geometry, if not energy, is quite similar to that obtained at lower levels of theory.[43] As shown in Figure 4, the concerted transition state is expected to be about 21 kcal/mol above the radical cleavage pathway in this case. Thus a concerted rearrangement pathway does not seem likely for any simple alkyl case.

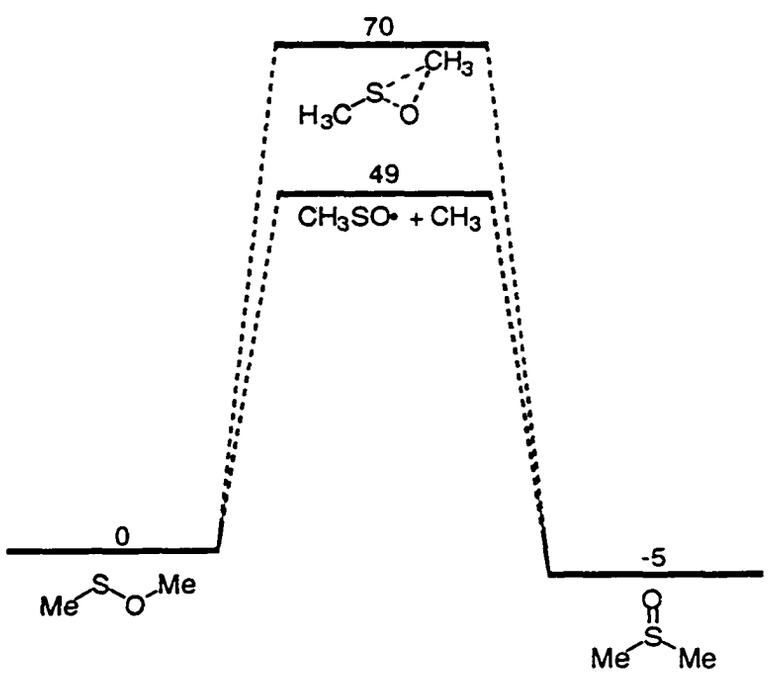

Figure 4. Relative energies of CH_3SOCH_3 structures. All energies are in kcal/mol relative to the sulfenic ester CH_3SOCH_3 and are G2 values at 298 K.

3.7 Comparison of less expensive computational methods to G2

As mentioned in Section 3.2, the G2 protocol is a very expensive calculation. Thus several other methods were investigated to see if there was a less expensive method that

could be used to investigate larger systems with an acceptable degree of reliability. It was discovered very early on that, not surprisingly, electron correlation was necessary to get reliable energies for the types of systems of interest. The methods chosen to compare with the G2 results were Møller-Plesset perturbation theory truncated at the second (MP2) and fourth (MP4) orders and the density functional method (Becke3) with the Lee-Yang-Parr exchange functional (B3LYP). (For a brief discussion of density functional theory see Appendix A).

Of some importance here is the choice of the basis set used in each of the methods. The energies for the MP2 and MP4 methods were taken directly out of the G2 calculations and, thus, the basis sets used were determined by the G2 protocol. However, the basis set for the B3LYP calculations were chosen by comparing results of several calculations with G2 results (Table 6).

Table 6. Relative cleavage energies for CH_3SOCH_3 as a function of basis set in B3LYP calculations[a]

Basis Set	CH_3-$SOCH_3$	CH_3S-OCH_3	CH_3SO-CH_3
6-31G(d,p)	9.2	1.1	0
6-31+G(d,p)	8.8	3.2	0
6-311G(d,p)	7.3	5.8	0
6-311+G(3df,2p)	5.7	11.5	0
G2	1.9	16.1	0

[a] The smallest bond dissociation energy is set to zero. Energies in kcal/mol.

The bond dissociation energies for the CH_3SOCH_3 were calculated using the B3LYP method with several different basis sets. In general, the basis sets were chosen to model the same basis sets found in the G2 protocol. As is shown in Table 6, the most complete basis set leads to the most comparable bond dissociation energy to the G2 value. Although this is not surprising, it shows that a fairly extensive basis set is needed with the density functional method in order to describe the chemistry of interest even reasonably accurately.

The relative bond dissociation energies calculated for the HSOH, CH_3SOCH_3, and $C_2H_3SOC_2H_3$ using the methods above were compared to the G2 energies (Table 7a-c). Relative cleavage energies are used to allow for easy comparison of the bond dissociation energies, and the energy of the divinyl sulfenic ester could not be calculated using the G2 method. Although the values for the MP2 and MP4 methods vary with the different systems, the density functional theory with the large basis set consistently compares reasonably well with the G2 energies in all of the molecules investigated. Thus it was decided to apply this method to the larger systems.

The two sulfenic esters chosen as test systems for the B3LYP method were phenyl benzyl sulfoxide **13** and diphenyl sulfoxide **14**.

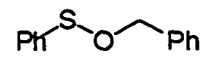

13

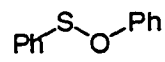

14

Table 7a. Relative bond dissociation energies for HSOH in kcal/mol

Method	Basis Set	H-SOH	HS-OH	HSO-H
UMP2	6-311+G(3df,2p)	3	0	3
UMP4	6-311G(2df,p)	8	0	10
B3LYP	6-311+G(3df,2p)	11	0	9
G2	-	9	0	5

Table 7b. Relative bond dissociation energies for CH_3SOCH_3 in kcal/mol

Method	Basis Set	CH_3-$SOCH_3$	CH_3S-OCH_3	CH_3SO-CH_3
UMP2	6-311+G(3df,2p)	17	18	0
UMP4	6-311G(2df,p)	13	10	0
B3LYP	6-311+G(3df,2p)	19	17	0
G2	-	18	16	0

Table 7c. Relative bond dissociation energies for $C_2H_3SOC_2H_3$ in kcal/mol

Method	Basis Set	C_2H_3-SOC_2H_3	C_2H_3S-OC_2H_3	C_2H_3SO-C_2H_3
UMP2	6-311+G(3df,2p)	42	0	30
UMP4	6-311G(2df,p)	43	0	34
B3LYP	6-311+G(3df,2p)	47	0	31
G2	-	46	0	29

Because both systems contained a fairly large number of heavy atoms and a large basis set is needed for the density functional method, the phenyl-S cleavage was not considered in the comparison of BDEs. This assumption is at least partially justified by the

fact that none of the smaller sulfenic ester systems investigated showed the C-S cleavage as the lowest energy cleavage, and the cleavage of the C-S bond in either molecule **13** or **14** would lead to the formation of an unstablilized phenyl radical. The relative cleavage energies for S-O and O-R homolysis along with the predicted energies from Benson type calculations are shown in Table 8. Although the cleavage energies from the density functional calculations do not compare quantitatively with those predicted by the Benson type calculations, the general trends are the same. Nonetheless, it is obvious that this method is not going to calculate energies of the larger systems accurately enough to allow for comparison with experimental results.

Table 8. Relative bond dissociation energies predicted by B3LYP and Benson calculations.

Method	Basis Set	R	R'	RS-OR'	RSO-R'
B3LYP	6-311+G3df,2p	C_6H_5	$CH_2C_6H_5$	0	-5
Estimated	Benson	C_6H_5	$CH_2C_6H_5$	0	-21
B3LYP	6-311+G3df,2p	C_6H_5	C_6H_5	0	+11
Estimated	Benson	C_6H_5	C_6H_5	0	+26

3.8 Photochemistry of sulfenic esters

As mentioned in section 3.1, the photochemistry of esters of aromatic sulfenic acids (i.e., Ar-S-O-R) involves S-O homolysis, despite the fact that this bond is predicted to be stronger than the O-R bond. Photoheterolysis has also been observed for certain systems, but this was with very highly substituted compounds which were clearly biased toward that path.[44] An understanding of the photochemistry of a species can often begin from a

qualitative picture of the electronic structure of the excited states. Restricted open shell Hartree-Fock (ROHF) calculations on the lowest triplet state of a compound are straightforward and can provide very useful pictures of the orbitals involved in the excitation from ground state. Single point ROHF/6-31G(d) calculations on the lowest triplet of CH_3SOCH_3 (at the ground state geometry) indicated that the lowest energy transition was the promotion of an electron from a non-bonding lone pair on sulfur to a nearly ideal σ^* orbital between S and O ($n_s \rightarrow \sigma^*_{SO}$). Geometry optimization of this state resulted in separation of $CH_3O\bullet$ and $CH_3S\bullet$ radicals, as expected from the orbital picture.

Single point CASSCF/6-31G(d) calculations were also carried out on the lowest excited singlet and lowest triplet of CH_3SOCH_3 at the ground state geometry to confirm this observation. The active space consisted of 14 electrons in 10 orbitals, representing all the C-S, S-O, and S-C sigma bonds, as well as the sulfur and oxygen lone pairs. The first excited singlet state was found to be 118 kcal/mol above the ground state (not including ZPE), consistent with reports of UV spectra for similar compounds.[44] The CASSCF triplet was 95 kcal/mol above the ground state. The orbital pictures for the two states were virtually identical and confirmed the results of the ROHF calculations. All of the natural orbitals in the active space had occupancies quite close to 0, 1, or 2. For the two singly occupied orbitals, an orbital rotation of 45° (i.e., mixing of the orbitals in equal parts) was performed in order to make interpretation easier. This does not change the overall wave function and provides an equally valid picture of the singly occupied orbitals which fall out of the calculation directly. The σ^*_{SO} orbital is illustrated in Figure 5.

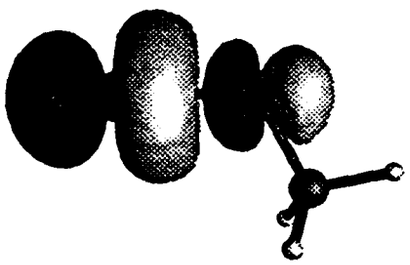

Figure 5. Lowest unoccupied molecular orbital representation of the methyl sulfenic ester

As a model for the experimentally encountered $PhSOCH_2Ph$, computations were carried out on $PhSOCH_3$. After RHF/6-31G(d) optimization of the ground state structure, the vertical ROHF triplet was examined. The triplet obtained from an ROHF/6-31G(d) wavefunction at the ground state geometry was a $\pi \rightarrow \pi^*$ transition predominantly localized on the phenyl ring. Optimization of the triplet had virtually no effect on the SO bond length. CASSCF calculations were not carried out.

Nonetheless, it remains the experimental observation that photolysis of these compounds results in S-O homolysis, despite the apparent availability of a weaker O-C bond. The observation of a stable triplet structure in no way invalidates the computational or experimental results. It merely indicates that there is a barrier to any homolysis in the excited state for the aromatic sulfenic esters. Further conclusions await subsequent work.

3.9 Conclusions

The thermochemistry of the peroxide, disulfide and sulfenic ester functional groups has been compared. G2 calculations were shown to reproduce the experimental ΔH_f° (298 K) data for the sulfur containing species when available, and were used to generate data for sulfenic esters and several radicals whose heats of formation are unknown.

When compared to RY'-R' bonds, RYY'-R' are weaker for the peroxide, disulfide, and sulfenic ester. This is due to the reorganization of the electronic structure of the remaining RYY'• radical by placement of three electrons into a new set of π and π^* orbitals. The sulfinyl radical (RSO•) is the most stabilized of the four types of radicals and its O-C bond is the most destabilized among the set. For any simple alkyl sulfenate, the weakest bond is expected to be the O-C bond. For vinyl or aryl sulfenates, a strong stabilization of the O-centered radical resulting from S-O homolysis is expected to make the S-O bond the most labile. The S-O and O-H bonds of sulfenic acids are expected to have comparable BDEs, depending somewhat on substitution.

The extraordinarily low BDE for O-O bonds in peroxides (~37 kcal/mol) is not reproduced in the sulfenic esters. The S-O bond is much closer to the S-S bond strength (*ca.* 64 kcal/mol for CH_3SOCH_3). This is attributed to less effective lone pair repulsion and the difference in electronegativity between S and O, both of which increase bond enthalpy relative to O-O.

In short, while sulfenic esters are isoelectronic to peroxides, the thermochemistry of the two species stands in distinct contrast. Without allyl-type stabilization of the putative alkoxy radical provided by vinyl or aryl substitution on the O terminus, the O-C bond of a

sulfenic ester will be markedly weaker than the central S-O bond. This makes the photochemistry of sulfenic esters seem all the more interesting.

References

(1) Gregory, D. D.; Jenks, W. S. *J. Org. Chem.* **1998**, *63*, 3859-3865.

(2) Guo, Y.; Jenks, W. S. *J. Org. Chem.* **1995**, *60*, 5480-5486.

(3) Sato, T.; Yamada, E.; Akiyama, T.; Inoue, H.; Hata, K. *Bull. Chem. Soc. Japan* **1965**, *38*, 1225-1225.

(4) Sato, T.; Goto, Y.; Tohyama, T.; Hayashi, S.; Hata, K. *Bull. Chem. Soc. Japan* **1967**, *40*, 2975-2976.

(5) Schultz, A. G.; Schlessinger, R. H. *Tetrahedron Lett.* **1973**, 4787-4890.

(6) Schultz, A. G.; Schlessinger, R. H. *J. Chem. Soc. Chem. Commun.* **1970**, 1294-1295.

(7) Still, I. W. J.; Cauhan, M. S.; Thomas, M. T. *Tetrahedron Lett.* **1973**, 1311-1314.

(8) Still, I. W. J.; Arora, P. C.; Chauhan, M. S.; Kwan, M. H.; Thomas, M. T. *Can. J. Chem.* **1976**, *54*, 455-470.

(9) Still, I. W. J.; Arora, P. C.; Hasan, S. K.; Kutney, G. W.; Lo, L. Y. T.; Turnbull, K. *Can. J. Chem.* **1981**, *59*, 199-209.

(10) Block, E. *Angew. Chem., Int. Ed. Engl.* **1992**, *31*, 1135-1178.

(11) Block, E.; Page, J.; Toscano, J. P.; X., W. C.; Zhang, X.; DeOrazio, R.; Guo, C.; Sheridan, R. S.; Towers, N. *J. Am. Chem. Soc.* **1996**, *118*, 4719-4720.

(12) de Maria, P. In *The Chemistry of Sulphenic Acids and Their Derivatives*; S. Patai, Ed.; John Wiley & Sons: Ltd.: New York, 1990; pp 293-310.

(13) Shelton, J. R.; Davis, K. E. *Int. J. Sulfur Chem.* **1973**, *8*, 217-228.

(14) Kobayashi, K.; Mutai, K. *Tetrahedron Lett.* **1981**, *22*, 5201-5204.

(15) Kobayashi, K.; Mutai, K. *Phosph. and Sulf.* **1985**, *25*, 43-51.

(16) Furukuwa, N.; Fujii, T.; Kimura, T.; Fujihara, H. *Chem. Lett.* **1994**, 1007-1010.

(17) Pasto, D. J.; Cottard, F.; Horgan, S. *J. Org. Chem.* **1993**, *58*, 4110-4112.

(18) Pasto, D. J.; Cottard, F. *J. Org. Chem.* **1994**, *59*, 4642-4646.

(19) Pasto, D. J.; Cottard, F. *Tetrahedron Lett.* **1994**, *35*, 4303-4306.

(20) Pasto, D. J.; Cottard, F. *J. Am. Chem. Soc.* **1994**, *116*, 8973-8977.

(21) Pasto, D. J.; Hermine, G. L. *J. Org. Chem.* **1990**, *55*, 5815-5816.

(22) Benson, S. W. *Chem. Rev.* **1978**, *78*, 23-35.

(23) Hogg, D. R.; Vipond, P. W. *J. Chem. Soc. (C)* **1970**, 60-63.

(24) Hogg, D. R.; Smith, J. H.; Vipond, P. W. *J. Chem. Soc. (C)* **1968**, 2713-2716.

(25) Braverman, S. In *The Chemistry of Sulfenic Acids and Their Derivatives*; S. Patai, Ed.; John Wiley & Sons: New York, 1990; pp 311-359.

(26) Braverman, S. In *The Chemistry of Sulfones and Sulfoxides*; S. Patai; Z. Rappoport and C. J. M. Stirling, Ed.; John Wiley & Sons Ltd.: New York, 1988; pp 717-757.

(27) Miller, E. G.; Rayner, D. R.; Thomas, H. T.; Mislow, K. *J. Am. Chem. Soc.* **1968**, *90*, 4861-4868.

(28) Zhao, H. Q.; Cheung, Y. S.; Heck, D. P.; Ng, C. Y.; Tetzlaff, T.; Jenks, W. S. *J. Chem. Phys.* **1996**, *106*, 86-93.

(29) Curtiss, L. A.; Raghavachari, K.; Trucks, G.; Pople, J. *J. Chem. Phys.* **1991**, *94*, 7221-7230.

(30) Curtiss, L. A.; Raghavachari, K.; Pople, J. A. *J. Chem. Phys.* **1993**, *98*, 1293-1298.

(31) curtiss, L. A.; Raghavachari, K.; Pople, J. A. *J. Chem. Phys.* **1995**, *103*, 4192-4200.

(32) Curtiss, L. A.; Raghavachari, K.; Redfern, P. C.; Pople, J. A. *J. Chem. Phys.* **1997**, *106*, 1063-1079.

(33) Pople, J. A.; Head-Gordon, M.; Fox, D. J.; Raghavachari, K.; Curtiss, L. A. *J. Chem. Phys.* **1989**, *90*, 5622-5630.

(34) Ochterski, J. W.; Petersson, G. A.; Wiberg, K. B. *J. Am. Chem. Soc.* **1995**, *117*, 11299-11308.

(35) Nicolaides, A.; Rauk, A.; Glukhovtsev, M.; Radom, L. *J. Phys. Chem.* **1996**, *100*, 17460-17464.

(36) Curtiss, S. A.; Redfern, P. C.; Smith, B. J.; Radom, L. *J. Chem. Phys.* **1996**, *104*, 5148-5152.

(37) Pasto, D. J.; Cottard, F.; Picconatto, C. *J. Org. Chem.* **1994**, *59*, 7172-7177.

(38) Nicolaides, A.; Radom, L. *Molecular Physics* **1996**, *88*, 759-765.

(39) Reed, A. E.; Weinhold, F. *J. Chem. Phys.* **1983**, *83*, 1736-1743.

(40) Cohen, N.; Benson, S. W. *Chem. Rev.* **1993**, *93*, 2419-2438.

(41) O'Hair, R. A. J.; DePuy, C. H.; Bierbaum, B. M. *J. Phys. Chem.* **1993**, *97*, 7955-7961.

(42) Luo, Y. R.; Benson, S. W. *Acc. Chem. Res.* **1992**, *25*, 375-381.

(43) Wolfe, S.; Schlegel, H. B. *Gazz. Chim. Ital.* **1990**, *120*, 285-290.

(44) Horspool, W. In *The Chemistry of Sulfenic Acids and Their Derivatives*; S. Patai, Ed.; John Wiley & Sons: New York, 1990; pp 517-547.

CHAPTER IV

COMPUTATIONAL STUDY OF SULFINYL RADICAL CHEMISTRY

4.1 Introduction

The sulfinyl radical has been mentioned several times throughout the first three chapters of this dissertation. In this context, its main importance pertained to their role as intermediates in sulfoxide photochemistry. However, the greater historic interest in sulfinyl radicals has been due to their suggested role as intermediates in the oxidation of sulfides, particularly in atmospheric and combustion chemistry.[1-3] This is especially true for smaller sulfinyl radicals such as HSO• and CH_3SO• that are formed by the oxidation of sulfur containing molecules present in the earth's atmosphere.

The hydrosulfinyl radical is produced in the atmosphere by chemical oxidation of HS• and is proposed to be part of the oxidation pathway of H_2S to H_2SO_4.[4] The oxidation of atmospheric H_2S starts with its reaction with a hydroxyl radical to form a molecule of water and the HS• radical.

$$H_2S + \cdot OH \longrightarrow HS\cdot + H_2O$$

The HS• radical is subsequently oxidized to form the sulfinyl radical. There are three major oxidants of atmospheric radicals, namely NO_2, O_3, and O_2, and all three of these molecules are expected to be involved in the formation of sulfinyl radicals to some extent.

$$HS\bullet + NO_2 \longrightarrow HSO\bullet + \text{products}$$

$$HS\bullet + O_3 \longrightarrow HSO\bullet + O_2$$

$$HS\bullet + O_2 \longrightarrow HSO\bullet + \text{products}$$

Although the concentration of NO_2 in the troposphere varies depending on the level of pollution from ~10 ppt (parts per trillion) to ~10 ppb (parts per billion), the concentration of O_3 is more stable and estimated at ~40 ppb.[5,6] The rate of reaction of HS• with NO_2 has been estimated at 3.0×10^{-11} cm^3 $molecule^{-1}$ s^{-1}, and the reaction rate of HS• with O_3 was estimated at 3.2×10^{-12} cm^3 $molecule^{-1}$ s^{-1}. (These rates would be considered diffusion controlled in solution chemistry.[7]) Reactions of RS• radicals with oxygen are slower and will be discussed in detail in Section 4.7.

There has been relatively little work done concerning the chemical reactivity of sulfinyl radicals once they are formed. The majority has focused on the self-coupling reaction, and the reactivity of RSO• with other molecules found in the earth's atmosphere such as O_3 and O_2. The self-coupling reaction of sulfinyl radicals is discussed in detail in Section 4.5.

One reaction that has received some attention is the reaction of sulfinyl radicals with olefins in solution. Fava and coworkers investigated the addition of the phenyl sulfinyl radical into styrene.[8] Phenyl benzenethiosulfinate was thermally decomposed to form PhSO• and PhS• in the presence of styrene. It was intended the PhSO• radical would initiate polymerization of the styrene. However, it was found the phenyl sulfinyl radical did not initiate the polymerization and the final products were the thiosulfonate ($PhS(O)_2SPh$) and

styrene. Quenching experiments showed the rates of thermal decomposition of several aryl arenethiosulfinate esters was decreased in the presence of styrene. This led to the suggestion that the sulfinyl radical adds reversibly into the styrene. It is suggested the radical adducts are likely to be cyclic in nature and are probably too stable to act as the chain carrier in a polymerization reaction. The cyclic adduct is then attacked on the sulfur or oxygen atom by another sulfinyl radical in solution to form the corresponding thiosulfonate and styrene (Figure 1). Experimental evidence for the cyclic adduct is lacking, however, and a short lived acyclic adduct may be a more likely candidate for the reaction of sulfinyl radicals with alkenes (Figure 2).

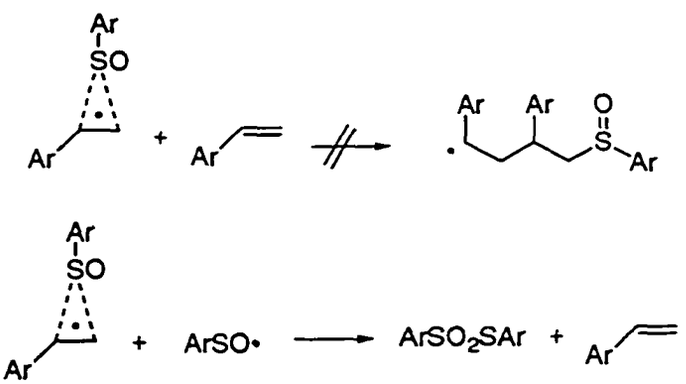

Figure 1. The proposed mechanism for the reaction of aryl sulfinyl radicals with styrene.

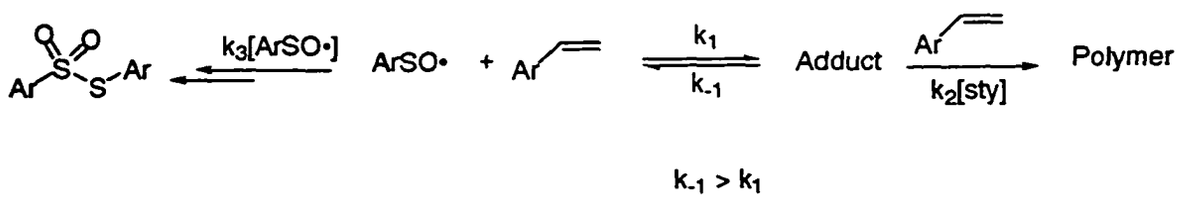

Figure 2. Alternative mechanism for the reaction of aryl sulfinyl radicals with styrene.

Further support for the reversible addition of sulfinyl radicals into alkenes was offered by Iino and coworkers.[9] The thermal decomposition of benzhydryl *p*-tolyl and benzhydryl methyl sulfoxides in the presence of *cis*-β-deuteriostyrene led to the observation of both *cis*- and *trans*-β-deuterostyrene. This was explained by an addition-elimination reaction shown in Figure 3.

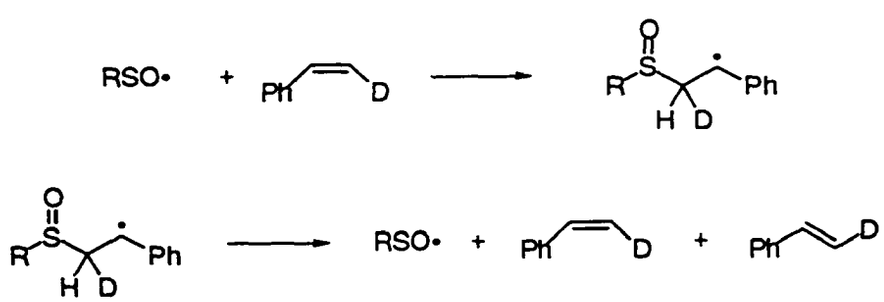

Figure 3. Proposed mechanism for the cis/trans isomerization of *cis*-ß-deuteriostyrene.

Boothe and coworkers added support for this reversible addition by investigating four diastereomeric 2-bromo-3-phenyl sulfinyl butanes.[10] Treatment of 2-bromo-3-phenyl sulfinylbutane **1** with tributyltin radicals generates β-phenyl sulfinyl *sec*-butyl radicals **2**. It was shown these radicals eliminate the PhSO• very quickly to form the corresponding alkene with complete retention of stereochemistry (Figure 4). This suggests the rate constant for elimination of the PhSO• radical is much faster than that of C-C bond rotation which contradicts the conclusions of Iino.

Because of their importance in atmospheric chemistry, the reactivity of simple sulfinyl radicals towards molecules prevalent in the atmosphere, such as O_3, and O_2 has been investigated. Howard and coworkers used discharge flow laser magnetic resonance (LMR)

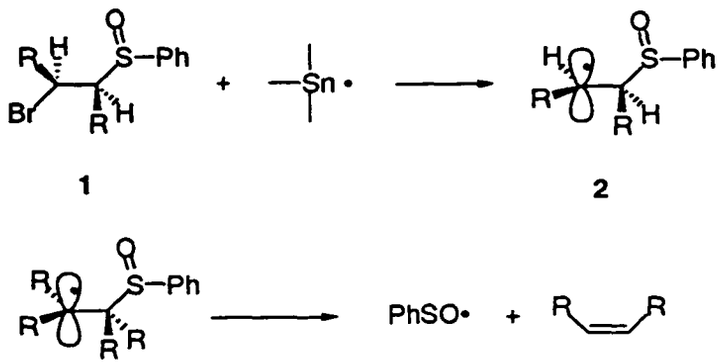

Figure 4. The proposed mechanism for the elimination of PhSO• radical catalyzed by tributyltin.

to investigate the kinetics of HSO• with O_3, and O_2.[4] The LMR technique is very similar to other magnetic resonance methods such as EPR and NMR. NMR uses radio frequency radiation to produce transitions between nuclear spin levels, and EPR uses microwave radiation to produce transitions between electron spin levels. LMR uses far infrared radiation to produce transitions between rotational levels in paramagnetic molecules.[11]

The hydrosulfinyl radical was produced prior to the experiment using the reaction of the HS• with O_3. The reaction of HSO• with O_3 is fairly complicated and several potential reactions must be considered. Figure 5 shows some of the possible reaction channels. The direct measurement of the reaction rate constant for the HSO• with O_3 was not possible due to the very fast formation of HSO• from the reaction of HS• with O_3. Thus, estimates were calculated using a computer model based on the GEAR differential equation algorithm.[12] Using this technique a reaction rate constant for the reaction of HSO• with O_3 was estimated at 2.1×10^7 M^{-1} s^{-1}. Evidence for the reaction of HSO• with O_2 was not found and thus a the reaction rate constant was estimated to be $\leq 1.2 \times 10^4$ M^{-1} s^{-1}. Even though this reaction was

$HSO\bullet + O_3$	→	$HS\bullet + 2O_2$	$\Delta H°_{298}$= 1 kcal/mol
	→	$\bullet OH + SO + O_2$	$\Delta H°_{298}$= -22 kcal/mol
	→	$HSO_2\bullet + O_2$	$\Delta H°_{298}$= -86 kcal/mol
	→	$HO_2\bullet + SO_2$	$\Delta H°_{298}$= -101 kcal/mol
	→	$H\bullet + O_2 + SO_2$	$\Delta H°_{298}$= -52 kcal/mol

Figure 5. Partial reaction scheme of HSO• with O_3. The enthalpies of reaction were estimated in previous work.[13,14]

determined to be slow, it is suggested that in the atmosphere it could still be important due to the high concentration of O_2.

Recently, Jenks and coworkers investigated the reactions of ArSO• radicals with several nitroxides using laser flash photolysis of substituted aryl benzyl sulfoxides in solution.[15] What was found was the rate of reactions were fast ($\sim 10^9$ M^{-1} s^{-1}) but below the diffusion controlled rate constant. They were about an order of magnitude higher than the reaction of $PhCH_2\bullet$ with the same nitroxides. The rate constants are shown below in Table 1.

Although products resulting from these reactions were not isolated it was assumed the reaction proceeded by coupling between the O atom of the nitroxide and the S and/or O of the sulfinyl radical. The unpaired electron is expected to reside in an N-O π^* orbital in the nitroxides.[16] However, unlike the sulfinyl radicals, the nitroxides can only react at the partially negative oxygen center. Because the rate constants for sulfinyl-nitroxide coupling were within less than an order of magnitude of the dimerization rate constants of the phenyl sulfinyl radicals, and the two systems have comparable dipoles of the N-O and S-O bond, these data were taken as support for the formation of a head-to-tail dimer in ArSO• coupling

Table 1. Rate constants for reaction of PhSO• with stable radicals

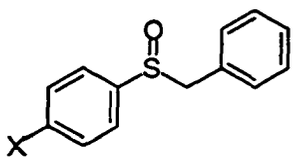

	k_{rxn} (10^8 M^{-1} s^{-1})		
Radical	TEMPO	DTBN	Solvent
X = Cl	15.6	14.4	acetonitrile
X = H	9.4	10.0	acetonitrile
X = CH_3	8.4	9.7	acetonitrile
X = OCH_3	7.8	8.1	acetonitrile
X = Cl		32	hexane
X = H		29	hexane
X = CH_3		23	hexane
X = OCH_3		23	hexane
X = CH_3		13	cyclohexane
X = Cl		16	cyclohexane
X = H		17	acetonitrile
X = H		13	cyclohexane
X = CH_3		7.5	cyclohexane
X = OCH_3		3.3	cyclohexane

[a] TEMPO = 2,2,6,6-tetramethyl-1-piperidinyloxy [b] DTBN = di-*tert*-butyl nitoxide

reaction. Thus one would assume the products from this coupling would resemble those formed in the self-quenching of ArSO• (Section 4.5).

4.2 Experimental structure of sulfinyl radicals

The majority of both the experimental and computational work done on sulfinyl radicals has focused on HSO•; however, several other systems such as methyl sulfinyl, *tert*-butyl sulfinyl, and substituted phenyl sulfinyl radicals have been explored to a lesser extent.

One of the first reported investigations of sulfinyl radicals was by Schurath and coworkers in 1975.[2] The HSO• radical was investigated by analyzing the chemiluminescence spectra produced in the reaction of HS• with ozone.

$$HS\bullet + O_3 \longrightarrow HSO\bullet + O_2$$

The authors showed the reaction of H_2S with ozone led to the formation of electronically excited SO_2 whose chemiluminescence spectra could be detected below 520 nm.[17] However, due to the complexity of the spectra at wavelengths above 520 nm, it was concluded that the excited state SO_2 molecule could not be used to explain this region of the chemiluminescence spectra. Because the spectra were consistent with a triatomic molecule and the reaction could be quenched by NO_2, it was suggested an excited state HSO• radical was also produced in the reaction. This is supported by the absence of a new spectrum in the CH_3SH/O_3 and $(CH_3)_2S$ systems that do not produce HS•.

In 1977, Schurath and coworkers were able to use these same techniques to gain insight into the electronic states and structure of the HSO• radical.[2] It was concluded the chemiluminescence spectrum in the range of 520 – 960 nm was a result of an $^2A' - {}^2A''$ transition of the HSO• radical. The assignment of the $^2A''$ electronic state for the ground state is consistent with calculations done on HSO• (see Section 4.3) and experimental work using other techniques.[18] Although the experimental estimate of the radiative lifetime of HSO• is not available, an estimate of ≈40 μs was given. This was based on a calculated oscillator strength of 1.8×10^{-4} for the $^2A' - {}^2A''$ transition.[19] The upper limit for the heat of formation of the ground state of HSO• was estimated as $\Delta H_f \leq 14.9$ kcal/mol. The S-O bond length for the A' and A" states of HSO• were estimated to be 1.71 Å and 1.54 Å respectively. The S-H bond lengths for the A' and A" state were estimated at 1.34 Å and 1.36 Å respectively. The HSO• bond angle was calculated to be ∠HSO = 102°.

The methyl sulfinyl radical was investigated by Williams and coworkers in the mid 1970's.[20] The CH_3SO• (produced by γ-irradiation of a single crystal of dimethyl sulfoxide) was investigated using epr techniques. From the ^{33}S hyperfine spin anisotropy, a spin density of 0.91 is calculated to reside in a sulfur 3p orbital. Thus the unpaired electron was suggested to occupy a π^* orbital largely concentrated on the sulfur atom which is consistent with the HSO•. Electronically, the methyl sulfinyl radical resembles the hydrosulfinyl radical. However, structurally there is an issue of a hindered internal rotation that is not found in HSO•. A detailed analysis of the temperature dependent epr spectra led to an estimate of 2.6 kcal/mol for the hindered internal rotation of the methyl group. At a temperature of –185° the epr spectra shows this hindered internal rotation is stopped and the

radical adopts a single conformation. The structure is consistent with one hydrogen atom lying in the nodal plane of the 3p orbital on sulfur. A similar result was reported by Kawamura.[21] One can imagine two possible structures for this; one where the hydrogen is eclipsed with the oxygen **3** and one where it is anti to the oxygen **4**. However, the authors could not distinguish experimentally or computationally which of the two structures is energetically favored.[22]

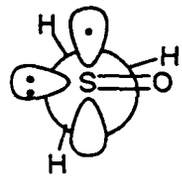

3

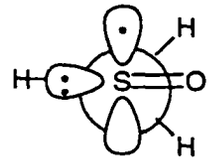

4

Gilbert and coworkers also studied a series of sulfinyl radicals using epr techniques at low temperatures.[23] The epr spectra of several alkyl sulfinyl radicals ($HOCH_2SO•$, $MeCH_2SO•$, $MeCH_2CH_2SO•$, $Me_2CHSO•$) all exhibited conformational interconversion as was the case for MeSO•. Again it was found that one of the C-H bonds is located in, or close to, the nodal plane of the 3p orbital on the sulfur in most of the cases. Estimates of the interconversion rates for several different temperatures were used to estimate the rotational barrier of $MeCH_2CH_2SO•$ at 4.3 kcal/mol. The epr spectrum for the $(CH_3)_2CHSO•$, however, was consistent with a 50° angle between the hydrogen and the z-axis of the singly occupied p orbital. This suggests molecules **5** and **6** are the most likely conformations out of the four

possibilities shown in Figure 6. Of compounds **5** and **6** the authors suggest compound **6** would be the most likely conformation on steric grounds.

Gilbert and coworkers have also characterized several aromatic sulfinyl radicals.[23,24] Several substituted aryl sulfinyl radicals were synthesized (chemically and photolytically) and characterized using epr. Due to the relatively large hyperfine splittings from the ring protons, it was concluded by that the aromatic sulfinyl radicals were π type radicals with extensive delocalization of the unpaired electron on to the aromatic ring.[23]

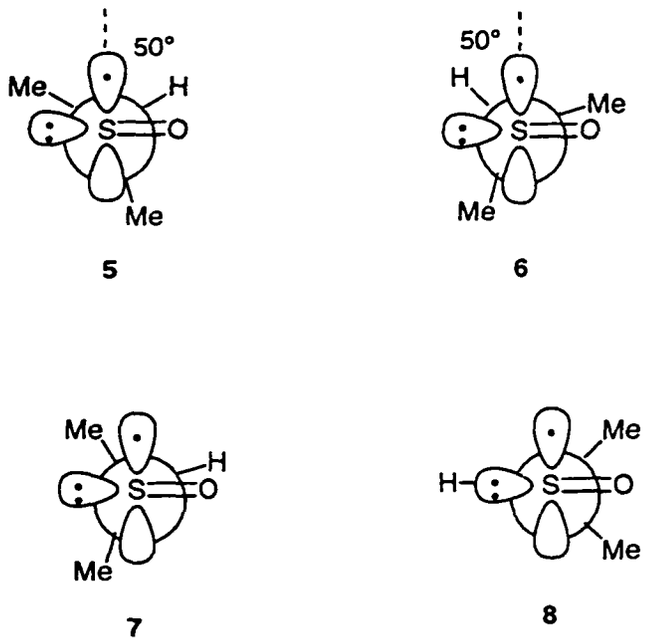

Figure 6. Four possible configurations of the $(Me)_2CHSO\bullet$.

4.3 Computational characterization of sulfinyl radicals

Due to their importance and the only qualitative picture of sulfinyl radicals from experiment, an extensive computational study was started. The primary goal of this research was to use computational techniques to gain a better understanding of both the electronic

structure and reactivity of the sulfinyl radicals. Although several authors have investigated the HSO• radical and the HOS• isomer,[22,25-30] computational work on larger alkyl sulfinyl radicals is lacking.[31,32]

The sulfinyl radicals investigated are shown in Figure 7. The HSO• radical **9** was chosen for its environmental importance. The energetic effects of adding a heavy atom into the system were investigated with the methyl sulfinyl radical **10**. Effects of a conjugated π system were investigated with the vinyl **11** and phenyl **12** sulfinyl radicals.

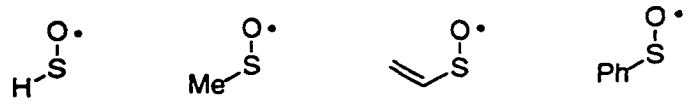

9 **10** **11** **12**

Figure 7. The sulfinyl radicals systems investigated

All of the geometries were calculated at the MP2(full)/6-31G(d) level with the exception of the phenyl sulfinyl radical. Due to computational expense the phenyl sulfinyl radical was optimized at the restricted open-shell Hartree-Fock ROHF/6-31+G(d) and B3LYP/6-311+G(3df,2p) and will be discussed separately. The geometries obtained for the HSO•, MeSO•, and C_2H_3SO• are shown in Table 2. The R-S bond increases in length while the S-O bond decreases with the substitution of heavy atoms in the sulfinyl radical. The ∠RSO bond angle also increases slightly. Nonetheless, the overall geometry of the three sulfinyl radicals remains fairly constant.

Table 2. Predicted bond lengths and angles of several sulfinyl radicals[a]

R	R-S (Å)	S-O (Å)	∠RSO
H	1.33	1.56	101.0°
	(1.36)	(1.54)	(102°)
Me	1.80	1.54	103.7°
C_2H_3	1.76	1.53	106.4°

[a] Numbers in parentheses are experimental values[2]

The geometry of the phenyl sulfinyl radical was more complex than the sulfinyl radicals in Table 2. Three general conformation of PhSO• were considered: a C_1 conformation, where the CSO plane is rotated to an arbitrary degree relative to the phenyl plane, and two limiting C_s conformations with the CSO plane parallel and perpendicular to the phenyl plane. No stationary points were found that were not essentially C_s in symmetry. (Shallow potentials allowed the structure to "optimize" without coming to the exact 0 or 90° dihedral angle.) The geometry with the CSO plane at a 90° dihedral angle was found to be a transition state with a single imaginary vibrational frequency whose vectors involved rotation of the C-S bond. The planar form was a true minimum at all computational levels.

Preliminary calculations on PhSO• were carried out at the UHF/3-21G(d) level. These served as useful starting geometries for other calculations. However, it was evident that the UHF model would not be appropriate for these systems given the significant spin contamination obvious from the S^2 value of 1.31. When the phenyl group was substituted with a non-conjugating group such as CH_3-, the spin contamination was much less.

Subsequent ab-initio calculations were done with the ROHF method, and the energies

were re-evaluated with single point calculations using Møller-Plesset perturbation theory, truncated at the second order (RMP2).[33] The Becke3LYP hybrid density functional was also used to optimize structures and single point energies were obtained with a larger basis set. The optimized geometry for the phenyl sulfinyl radical at the ROHF/6-31+G(d) and B3LYP/6-31G(d,p) are shown below.

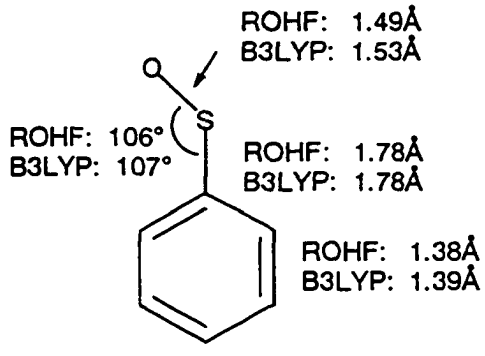

Because of the disagreement between the S-O bond lengths (1.49 Å *vs.* 1.53 Å) obtained at the ROHF/6-31+G(d) and Becke3LYP/6-311+G(d,p) levels of theory, the planar structure was also optimized at other levels. Several basis sets were examined with the ROHF model. Moving from double-ξ to triple-ξ had no significant effect; neither did adding p functions to the hydrogens or removing the diffuse functions. However, there was some variation with the number of d polarization functions. With one, two, or three d functions on the heavy atoms, the S-O bond length was found to be 1.49, 1.47 and 1.49 Å, respectively. Using the BLYP[34] functional in place of the Becke3LYP[35,36] with a basis set of 6-311+G(d,p), an S-O bond length of 1.55 Å was obtained.

Significant variation is observed between the ROHF, Becke3LYP, and BLYP S-O bond lengths for PhSO•. Comparison with the work of Cramer and co-workers may shed light on this issue. They carried out a series of computational studies on phosphorus-containing radicals, some of which have considerable structural analogy to the present sulfinyl radicals (e.g., Me_2PO•).[37,38] Using the 6-31G(d,p) basis set, they found that UHF geometries are more reliable than BLYP and other density functionals for predicting hyperfine coupling constants, with the latter producing P-X bonds longer than other methods by 0.02-0.06 Å. Even the hyperfine coupling constants calculated with Becke3LYP were more accurate when done at the UHF geometry, though the difference is not as large as with other density functional methods. Using this experience as a guide, one may suggest that the 1.53 Å value is an upper limit, and the true length may be closer to 1.49 Å, that is, about the same as or a little longer than, that of the sulfoxide.

It has been known for some time that polarization functions in the basis set is necessary for accurate calculations of the properties of hypervalent sulfur compounds such as sulfoxides.[39] Given the results at the various basis sets, the estimate of 1.49 Å is probably the best value of the S-O bond length. Experimental and computed bond lengths of typical sulfoxides are 1.48-1.49 Å.[40] Given this, the rather large S-O bond lengthening (0.06 Å) predicted by the ROHF calculations for the transition state (where the Ph-SO bond is rotated 90°) is somewhat surprising.

Including zero point energies, the barrier to rotation (i.e., the difference in energy between this conformation and the transition state with a 90° dihedral angle) is 2 kcal/mol (Table 4). With the RMP2 electron correlation correction, this barrier rises to 13 kcal/mol.

Using the Becke3LYP hybrid density functional method, the structures were optimized with the 6-31+G(d,p) basis set, and single point energies were done with the 6-311+G(3df,2p) basis set. This basis set was chosen because of results with other, smaller sulfinyl radicals that indicated it was necessary for good energies. (see Section 3.6) The calculated rotational barriers are effectively identical for the two basis sets with Becke3LYP at about 5 kcal/mol.

In a previous computational study on sulfoxides in which S-O bond dissociation energies were determined by isodesmic exchange of the oxygen between a test sulfoxide and dimethyl sulfide, it was found that certain structural features led to a significant difference in computed bond energies between Hartree-Fock and Møller-Plesset methods.[40] Moreover, Hartree-Fock methods are not generally reliable for predicting transition state energies. Therefore, it is not surprising to see a significant difference in the rotational barriers for PhSO• calculated by ROHF and RMP2 methods, though the magnitude of the difference (2 kcal/mol *vs.* 13 kcal/mol) is large in this case. The Becke3LYP data (*ca.* 5 kcal/mol) are intermediate. One may speculate that very likely the ROHF number is too low, and the true value may lie between the density functional and ROMP2 results. The Becke3LYP calculations show a S-O bond length which varies much less with C-S bond rotation than in the ROHF calculations but is much larger in the ground state structure than in the ROHF calculation.

A series of computations were carried out to determine the character of the singly-occupied molecular orbital (SOMO) of sulfinyl radicals. The SOMO for the small sulfinyl radicals was characterized using Complete Active Space SCF (CASSCF) calculations. Both HSO• and CH_3SO• are C_s symmetry. In principle, the ground state could be either $^2A'$ or $^2A''$,

corresponding to a σ-type or π-type singly occupied orbital. The CASSCF calculations on these species showed both ground states to be of $^2A''$ symmetry, consistent with previous theoretical[25,29,30] and experimental[27,28] determinations on HSO•. ROHF calculations also give an $^2A''$ ground state in all cases, and the singly occupied orbitals obtained from the CASSCF calculations were very similar to those from ROHF. The pictorial representation of these orbitals is consistent with the single electron residing in a π^* orbital.

Unlike the experimental results that suggest the majority of the spin being concentrated on the sulfur atom, ROHF calculations predict much of the spin is delocalized on the oxygen atom, Table 3.

Table 3. Mulliken population, atomic spin density, and atomic charges of sulfinyl radicals.[a]

Species	Spin Density Sulfur	Spin Density Oxygen	Atomic Charge Sulfur	Atomic Charge Oxygen	Bond Order S-O bond
HSO•	0.18	0.81	0.33	-0.40	1.2
CH_3SO•	0.27	0.71	0.48	-0.42	1.5
C_2H_3SO•	0.29	0.67	0.55	-0.46	1.5

[a] Results from a ROHF/6-31G(d)

Table 3 shows the Mulliken Spin Population for each of the sulfinyl radicals. For the HSO• radical, the Mulliken spin population analysis puts ~80% of the spin on the oxygen. Substitution of the hydrogen with a methyl or vinyl group increases the electron density on the sulfur atom to 0.29. The Mulliken analysis on HSO• puts a +0.33 charge on the sulfur atom and a –0.40 charge on the oxygen. The sulfur atom becomes more positively charged

upon substitution of a carbon atom and the oxygen becomes more negatively charged, as expected. Analysis of the bond order shows that the decrease in the S-O bond length when going from HSO• to CH_3SO•, is accompanied by an increase in the bond order.

It should be noted that Sevilla and coworkers have shown both the spin densities and the atomic charges predicted by the Hartree-Fock method for the MeSO• are somewhat dependent on the basis set when applying small basis sets.[41] However, analysis of Table 4 shows this effect is minimal for larger basis sets for the methyl sulfinyl radical and thus the values reported in Table 3 for the other sulfinyl radicals are taken as being reasonable.

Table 4. Basis set dependence of the spin density and atomic charges for MeSO•

ROHF Basis set	Spin Density Sulfur	Spin Density Oxygen	Atomic Charge Sulfur	Atomic Charge Oxygen
6-31G(d)	0.27	0.71	0.48	-0.42
6-31G(d,p)	0.25	0.74	0.50	-0.45
6-31+G(d,p)	0.28	0.71	0.35	-0.41
6-311G(d)	0.24	0.74	0.43	-0.40
6-311G(d,p)	0.24	0.75	0.41	-0.40
6-311+G(d,p)	0.26	0.73	0.34	-0.31

Because the singly occupied orbitals calculated with the CASSCF method in the smaller sulfinyl radicals resembled the ROHF orbitals very closely, the PhSO• radical was characterized using the less expensive ROHF method. Previous workers have described PhS• as having its spin essentially localized on the S atom on a p-type orbital, with a single

bond between the carbon and sulfur.[42] In a sense, the computational results for PhSO• are similar. Fundamentally, the computed singly occupied molecular orbital is essentially a π^* S-O orbital, with minor delocalization (ca. 1%) on the ortho and para carbon atoms. Mulliken analysis of the SOMO showed a 48% contribution from the S p-orbitals and a nearly identical 48% contribution from the O p-orbitals. Similarly, Mulliken analysis places a +0.55 charge on the sulfur and a –0.52 charge on the oxygen. Interestingly, although the delocalization of the SOMO into the phenyl ring is predicted to be minimal, conjugation apparently draws spin density onto the sulfur atom, at least at the ROHF level; the 90° transition state showed a 76% contribution from the O atom and 24% from the S atom. Mulliken charges on S and O and the bond order are all slightly lower at the transition state. The parameters computed for the PhSO• radical are shown in Table 5.

Table 5. Computed parameters for PhSO•

quantity	ROHF/ 6-31+G(d)	MP2/6-31+G(d)// ROHF/6-31+G(d)	B3LYP/ 6-31+G(d)	B3LYP/6-311+G(3df,2p) B3LYP/6-31+G(d,p)
S-O bond length (Å)	1.49		1.53	
spin density, S[a]	0.48		0.49	0.52
spin density, O[a]	0.48		0.41	0.39
rotational barrier (kcal/mol)	2.0	13.0	4.4	5.0
S-O bond length (Å) (transition state)	1.55		1.54	
spin density, S[a] (transition state)	0.23		0.49	0.54
spin density, O[a] (transition state)	0.76		0.48	0.46

[a] Mulliken approximation

Like the ROHF calculations, Becke3LYP places the unpaired electron of the phenyl sulfinyl radical in an orbital that is essentially S-O π^*. The planar structure has some delocalization ($\leq$ 10%) onto the ortho and para positions of the ring, but this delocalization is severely limited in the transition state, where the S-O π^* orbital has no overlap with the phenyl π systems.

4.4 Excited states of sulfinyl radicals

Along with developing the ground electronic state of sulfinyl radicals, development of their excited state was also of interest. Even though the excited state of the isoelectronic peroxyl radical has been explored both experimentally and computationally,[43-46] the investigation of the excited states of the sulfinyl radicals RSO• is limited to one study by Schurath and coworkers.[2] In the interest of consistency with literature, the energy gaps reported in this section will be reported in wavenumbers (cm^{-1}).

Recently, Jenks and coworkers investigated the excited state of PhSO• and several peroxyl radicals experimentally. The quenching of singlet oxygen luminescence at 1270 nm by PhS•, PhSO•, and peroxyl radicals PhOO•, *t*-BuOO•, $PhCH_2OO$•, Ph_2CHOO•, and Ph_3COO• in solution was investigated. The quantum yields of decomposition of different initiators, which lead to the formation of free radicals, were measured by using nanosecond transient absorption. This allowed the determination of singlet oxygen $O_2(^1\Delta_g)$ quenching rate constants by the radicals. They are < 2 x 10^8 M^{-1} s^{-1} for the sulfur-centered radicals and (2-7) x 10^9 $M^{-1}s^{-1}$ peroxyl radicals in acetonitrile. The rate of quenching for the peroxyl radicals are qualitatively similar and at least an order of magnitude greater than those for

PhS• and PhSO•. One plausible explanation for this result is that energy transfer from the $O_2(^1\Delta_g)$ to the peroxyl radicals is energetically possible, but a similar transfer to the sulfinyl radical is not.

The ground state of the hydroperoxyl radical is known to be $^2A''$, and the first excited state ($^2A'$) lies only 7041 cm^{-1} above the ground state.[44,45] This is ~840 cm^{-1} below the that of $O_2(^1\Delta_g)$ 7884 cm^{-1}. A similar trend was observed for several alkyl substituted peroxyl radicals ($CH_3OO•$, $C_2H_5OO•$, and $C_2H_5OO•$) all of which had excited state energies below that of $O_2(^1\Delta_g)$.[45,46] Schurath and coworkers were able to show the ground state of HSO• was $^2A''$ and the first excited state was $^2A'$.[2] An estimate of the energy gap can be made at ~17 000 cm^{-1} from the reported chemiluminescence spectrum (520 – 960 nm). Two absorption bands for the phenysulfinyl radical have been observed by solution phase flash photolysis, Figure 8 (see also Section 4.3).[15] The lower energy band is broad and structureless, with a low extinction coefficient and an onset at approximately 17 500 cm^{-1} (575 nm), far above the singlet oxygen excitation level. However, this does not answer the relevant question about the existence of a state lying below 7800 cm^{-1}, which was outside the experimental range of wavelengths investigated.

Because PhSO• and PhOO• are comparatively large molecules, a relatively modest computational approach was sought. A "test band" of several radicals was used to help evaluate methods: HOO• (C_s symmetry), HSO• (C_s), HSS• (C_s), $CH_3OO•$ (C_s), $CH_3COO_2•$ (C_s), $CH_3O•$ (C_{3v}), and $CH_3P•^+$ (C_{3v}). For each of the C_s radicals, the ground state is $^2A''$ and the first excited state is $^2A'$. For the C_{3v} radicals, the ground state is ^2E and the first excited state is $^2A_1$. None of the radicals investigated has a low-lying quartet state.

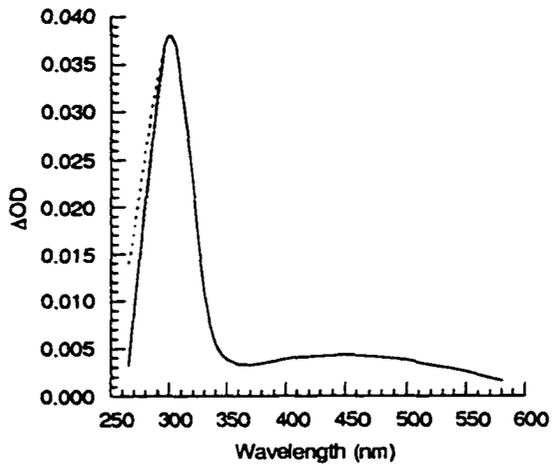

Figure 8. The absorption spectra of the PhSO• radical from solution phase flash photolysis.

Optimized geometries for each symmetry state were obtained at the ROHF/6-31G(d,p) level, and single point energies were found by using the RMP2 method.[33,47] The calculated energy of the excited states of each of the radicals is compared to the experimental values in Table 6. The accuracy of this method appeared to be sufficient for qualitative purposes for the smaller radicals, with a root-mean-square error of 12%. All of the C_s cases had energy gaps that were underestimated, relative to the experimental values. Even the worst case, HSO•, has an energy gap that is underestimated by only 20%; a significant improvement over that is not found until the CASSCF/cc-pVTZ level, at which point the calculated energy gap is about 7% too low.[29,30]

The C_{3v} energy gaps are underestimated less than those for the C_s cases or are slightly overestimated. This may be an artifact, as the ^2E states do not converge in true C_{3v} symmetry because of orbital degeneracy; therefore, they were allowed to optimize without symmetry.

As a result, the ^2E states have an additional stabilization not available to the rigorously symmetric C_{3v} $^2A_1$ states.

Analysis of Table 6 shows that overall the RMP2/6-31G(d,p)//ROHF/6-31G(d,p) method performed fairly well for the smaller radicals investigated, and thus it was applied to the PhSO• system and conjugated peroxyls. The data in Table 6 show the low-energy transition available to the alkylperoxyl radicals. For systems such as $PhCH_2OO$• where a phenyl group is insulated from the peroxyl center by a saturated carbon, little perturbation is expected. The phenyl group in PhOO•, however, is directly conjugated. Nonetheless, a quite similar excitation energy is calculated. The substituent effect of the acetyl group is correctly predicted, so there is no reason to believe the phenyl substituent effect is anything but very small.

As mentioned in section 4.3, the phenyl sulfinyl radical is, like the other C_s species in Table 6, found to have a ground state of $^2A''$ symmetry. Its ground state is fully planar and the unpaired spin resides in a π^* orbital localized on the S and O atoms.[15] A limited configuration interaction calculation (single excitation only) indicated that the lowest excited state was composed almost entirely of a single configuration that corresponded to the first $^2A'$ state, 19 500 cm^{-1} above the ground state. The RMP2 energy difference between the lowest $^2A''$ and $^2A'$ states for the relaxed planar conformations of PhSO• is about 16 900 cm^{-1} (592 nm), consistent with the CIS calculation and the absorption spectrum. This is consistent with the experimentally observed onset of absorption at $\sim$ 575 nm[15] and rules out the existence of any low lying electronic state in the IR region

Table 6. Calculated and experimental electronic energy gaps[a]

	E, hartrees		ΔE, cm^{-1}		
radical	ground state[b]	excited state[c]	calcd	exptl[d]	% error
CH_3O•	-114.70957	-114.55704	33559	31614	6
CH_3S•	-437.35513	-437.21945	29565	26397	12
$CH_3CN^{+\cdot}$	-131.90845	-131.88068	6956	7580	-8
$CH_3CP^{+\cdot}$	-418.18698	-418.10941	17582	18656	-6
HOO•	-150.50781	-150.47685	6683	7030	-5
HSS•	-795.81936	-795.78944	6501	7255	-10
HSO•	-473.17727	-173.1245	11548	14367	-20
CH_3OO•	-189.68129	-189.65034	6805	7375	-8
CH_3COO_2•	-302.72519	-302.70477	4451	5562	-20
PhOO•	-380.71867	-380.80040	6964		
PhSO•	-703.53534	-703.33882	16903	17500[e]	

[a] calculated energies are RMP2/6-31G(d,p)//ROHf/6-31G(d,p). ROHF/6-31G(d,p) zero point energies, scaled by 0.9, are included. [b] Ground state for all C_s species is $^2A''$; ground state for C_{3v} species is ^2E. Convergence was achieved on the C_{3v} species by removing symmetry constraints. [c] Excited state for all C_s species is $^2A'$; excited state for C_{3v} is $^2A_1$. [d] Ref.[46] [e] Estimated form the onset of absorption from solution phase transient absorption.

While the planar conformation of PhSO• is a minimum for the $^2A''$ state, a similar planar conformation is a transition state for the $^2A'$ state. Rotation of the C-S bond by 90° gives a new conformation of C_s symmetry as discussed previously. Conformations of this nature will be referred to as T-shaped. Along the $^2A''$ surface, a T-shaped conformation is the transition state for C-S bond rotation. In contrast, along the $^2A'$ surface, the minimum is a T-

shaped conformation, and the planar conformation represents the transition state for C-S bond rotation.

Because of this added complication in the excited state, a more sophisticated computational approach was taken for PhSO•. Using the geometries obtained at the ROHF level for the $^2A''$ and $^2A'$ states, CASSCF (15,11) calculations were performed for both the planar and T-shaped geometries. Multireference second-order Møller-Plesset (MRMP2) corrections were made to these energies. The results are presented in Figure 9. These calculations gave similar gaps to the RMP2 energies shown in Table 6 and again lend credence to the rest of the computational values it contains.

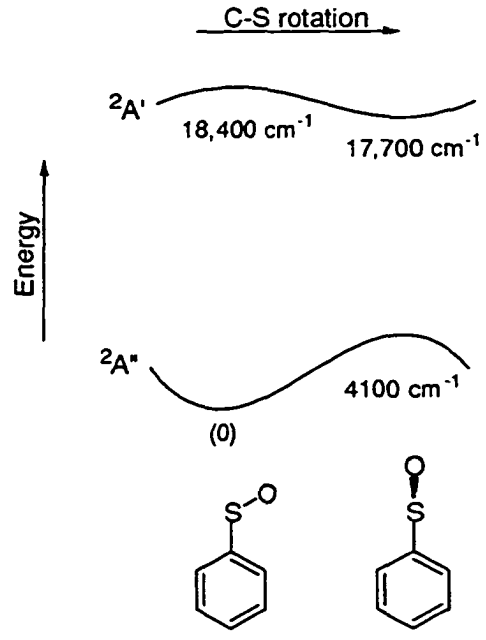

Figure 9. Potential energy surfaces for the S-O rotation of both the $^2A''$ and $^2A'$.

Finally, it is worth noting that the energy transfer interpretation for quenching of $^1O_2$ by peroxyl radicals and the data in Table 6 allows one to make a prediction not tested in is work. Like the peroxyl radicals, HSS• has a very low-lying n→π* transition, which was calculated at 7255 cm^{-1}. It is therefore quite likely that it and other perthiyl radicals would also be very rapid singlet oxygen quenchers, in contrast to sulfinyl radicals.

4.5 Self coupling reaction of sulfinyl radicals

Among the earliest work on the self-coupling reaction of sulfinyl radicals was that done by Howard and coworkers.[48] The *tert*-butyl sulfinyl radical was generated via the reaction of photochemically generated *tert*-butoxyl radicals with *tert*-butyl sulfenic acid.

$$CH_3COOC(CH_3)_3 \longrightarrow 2(CH_3)_3CO\bullet$$

$$(CH_3)_3CO\bullet + (CH_3)_3CSOH \longrightarrow (CH_3)_3CSO\bullet + (CH_3)_3COH$$

The decay kinetics observed for the *tert*-butyl sulfinyl radical by epr led to the conclusion that the sulfinyl radical undergoes a bimolecular reaction with itself as the major mode of decay. In a 2.5 x 10^{-7} M solution, the bimolecular rate constant for the *tert*-butyl sulfinyl radical was estimated at 6 x 10^7 M^{-1} s^{-1} which corresponds to a half life of 0.07 s at –100°. Interestingly, the *tert*-butylperoxyl radical has a half-life of 4.5 years in solution. This long lifetime is attributed to the fact that it exists in equilibrium with a rather unstable dimer, di-*tert*-butyl tetroxide **13**, and only the decomposition of this tetroxide can lead to disappearance of the peroxyl radical. The role of a similar oxygen-to-oxygen coupling in the sulfinyl

radicals could not be determined in this study, but recent computational work shows this molecule is not even a minimum on the potential energy surface (see Section 4.6).

$$2(CH_3)_3COO\bullet \rightleftharpoons (CH_3)_3COOOOC(CH_3)_3 \longrightarrow 2(CH_3)_3CO\bullet + O_2$$

13

Recently, Jenks and coworkers have investigated the self coupling reaction of several substituted phenyl sulfinyl radicals at room temperature using laser flash photolysis .[15] The sulfoxide systems used to produce the phenyl sulfinyl radicals are shown in Figure 10.

Photolysis of compound **17** (X=H) led to the formation of a transient species with absorption maximums at 300 and 450 nm (Figure 8). These maxima were not affected significantly by a change of the precursor sulfoxide or solvent. The decay of the 300 nm transient was very well fit to second order kinetics, and the initial intensity of the signal was

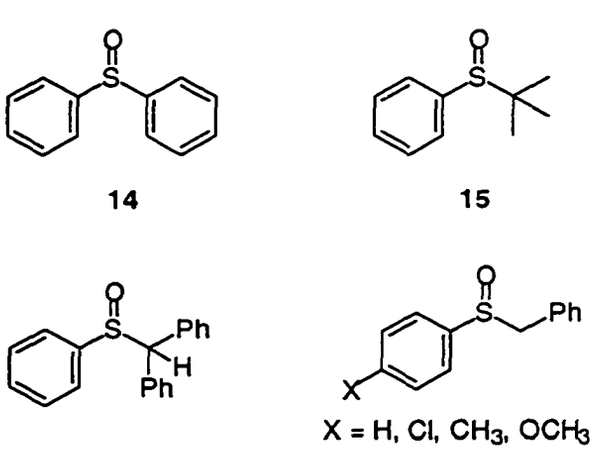

14 **15**

16 **17**

Figure 10. Sulfoxide systems used to generate the phenyl sulfinyl radical.

directly proportional to the energy of the incident laser pulse. As expected, it was shown the transients formed by the carbon centered radicals formed in the photolysis of **14** and **15** (phenyl and *tert*-butyl radicals) did not significantly distort the sulfinyl radical signals in deaerated or air saturated solutions. However, the benzyl type radicals do interfere with the transient in Figure 8. The Figure 8 transient, attributed to PhSO•, did not measurably react with O_2. Because $PhCH_2$• reacts with oxygen very rapidly, its absorption was eliminated from the spectra by quenching it with oxygen and collecting the signal 100 ns after the laser pulse. The rate of self coupling of the phenyl sulfinyl radical was estimated in several solvents and ranged from 1.8 – 7.7 x 10^9 M^{-1} s^{-1} depending on the viscosity. These experiments provide strong evidence for nearly diffusion controlled self coupling of sulfinyl radicals.[15,48]

Even though several authors have estimated the rate constants for the self-termination reaction under various conditions,[15,48,49] the mechanism for this reaction has not been resolved. It is generally accepted, however, that combination of two sulfinyl radicals leads to the formation of the thiosulfonate as the final isolated product, and that this product cannot be the primary adduct formed.[50] There are three paths the sulfinyl radicals might follow in the initial dimerization (Figure 11). Path **A** is a head-to-tail dimerization to form the OS-sulfenyl sulfinate **18**. Path **B** is a tail-to-tail coupling to form the α-disulfoxide **19**, and path **C** is head-to-head coupling to form the peroxide type intermediate **20**.

Although it has proven difficult, the α-disulfoxide **19** has been detected experimentally in certain systems,[50,51] but there remains no direct experimental evidence for the formation of the OS-sulfenyl sulfinate **18**. Despite this, support for the formation of the

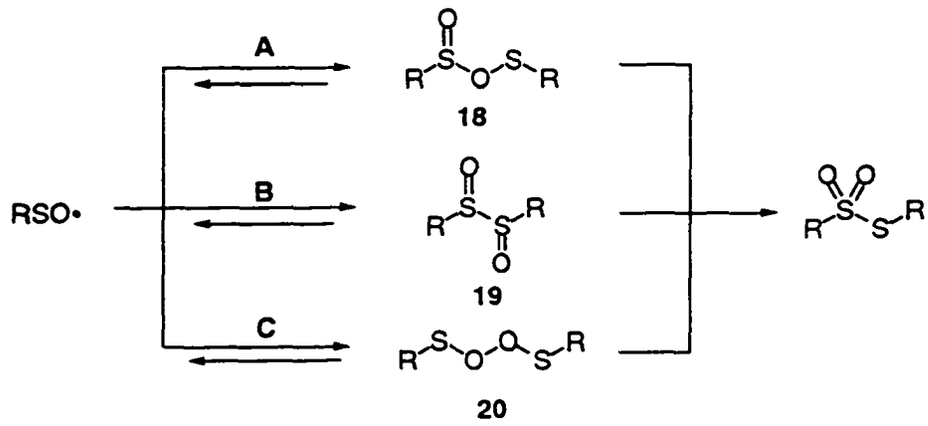

Figure 10. Three possible self-coupling pathways for sulfinyl radicals.

OS-sulfenyl sulfinate was given by Jenks and coworkers from the reaction of phenyl sulfinyl radicals with TEMPO (2,2,6,6-tetramethyl-1-piperidinyloxy) (see Section 4.1). Unlike the sulfinyl radical the TEMPO can only react at the oxygen atom. Because the rate constants for the reaction of the sulfinyl radical with the nitroxides were within less than an order of magnitude of the dimerization rate constants of phenyl sulfinyl radicals, and the two systems have comparable dipoles of the N-O and S-O bond, these data were taken as support for the formation of a head-to-tail dimer in the ArSO• system.

Related sets of compounds have also been investigated as intermediates of thiosulfinate oxidations by peracids. The final product of a single oxidation of a thiosulfinate **21** is the thiosulfonate **25**. However, the primary event could occur at either of the S-atoms. The mechanism for this oxidation has been the subject of discussion for some time.

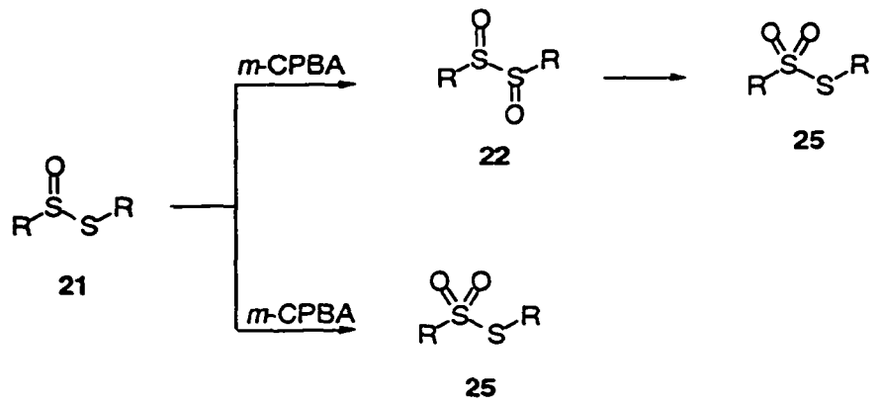

Early mechanistic work on this oxidation showed some unsymmetrical thiosulfonates, such as *p*-fluorophenyl benzene thiosulfinate and methyl benzenethiosulfinate led to the formation of large amounts of the corresponding cross-coupled thiosulfonates which was taken as evidence for S-S homolysis.[52]

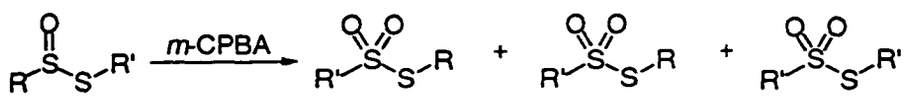

This led to the proposal of two possible mechanism for the peracid oxidation of thiosulfinates.[52] For thiosulfinates with strong electron withdrawing groups on the sulfinyl side, one would expect the peracid to oxidize the sulfinyl sulfur to form the thiosulfonate directly. However, if both groups attached to the thiosulfinate had similar electron drawing abilities, one would expect oxidation at the sulfenyl sulfur to form the α-disulfoxide **22**.[53] Kice and coworkers suggest the α-disulfoxide then undergoes very rapid S-S bond homolysis to form 2 sulfinyl radicals **23** that coupled to form the OS-sulfenyl sulfinate **24** (Figure 12).[52] Intermediate **24** then rearranges by either a concerted mechanism to form the thiosulfonate

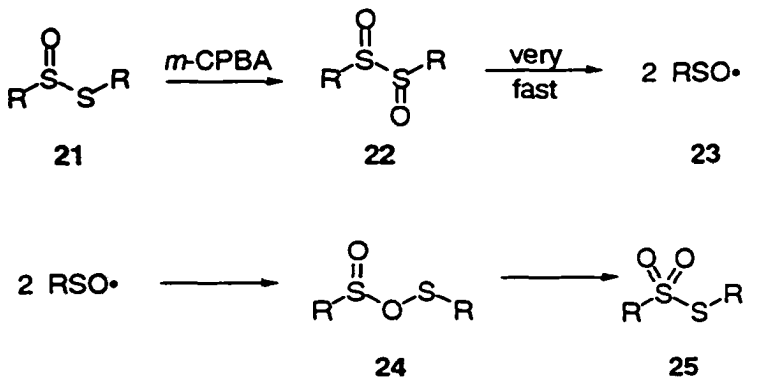

Figure 12. Proposed mechanism for the oxidation of thiosulfinates

25 directly or by homolysis of the O-S bond followed by recombination to form the thiosulfonate **25**.

Modena and coworkers suggested a different mechanism.[54,55] These authors suggested that the α-disulfoxides formed during the oxidation of S-aryl arenethiosulfinates in dioxane undergo rapid concerted isomerization to the thiosulfonates without cleavage of the S-S bond. Homolysis of the O-S bond in **24** would lead to the formation of RS(O)O• and RS• radicals. None of the RS• coupling product (RSSR) was detected, which led the authors to suggest the concerted mechanism.

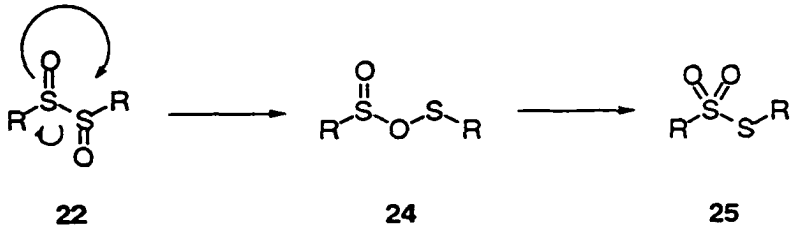

This conclusion is supported by the work of Freeman and coworkers who have investigated the oxidation of thiosulfinates using low temperature nmr techniques.[50,56,57] The low temperature oxidation of several alkanethiosulfinates led to the formation of α-disulfoxides, which decomposed to form the corresponding sulfines **28**, sulfinic acids **27**, and thiosulfinates **26**. Because the thiosulfonate was not observed as an initial product of the decomposition of the α-disulfoxide, it was suggested that sulfinyl radicals did not play a major role in the decomposition and/or rearrangement of alkyl α-disulfoxides.[56-58] Subsequent reactions of the initial products formed were proposed to lead to the formation of the thiosulfonate.

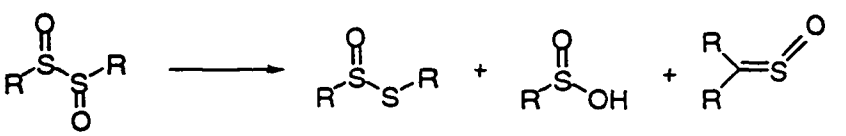

22 **26** **27** **28**

Even though NMR peaks corresponding to the OS-sulfenyl sulfinates **24** were not detected, it is suggested that they are still possible intermediates.[50] The low concentration of OS-sulfenyl sulfinates was attributed to an unfavorable equilibrium between the α-disulfoxide and the OS-sulfenyl sulfinates. The equilibrium lying far to the left is supported by comparison with similar sulfur compounds.[50] For example, although the free energy difference is small, a sulfoxide structure is generally thermodynamically more stable than a sulfenic ester.

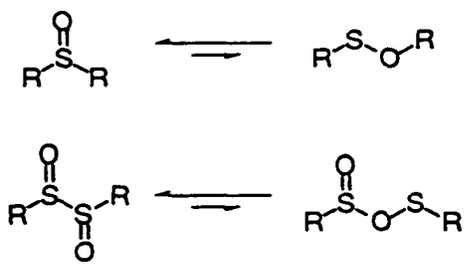

A concerted mechanism for the rearrangement of α-disulfoxides to the thiosulfonate was also proposed by Harpp and Folkins.[51] The bridged bicyclic α-disulfoxides used in is study were more stable than the α-disulfoxides reported by Freeman and were shown to be stable at temperatures up to 30 °C.

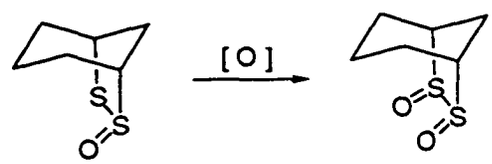

29

The oxidation of α-disulfoxides has also been investigated computationally.[59] The energy of several hydrogen-substituted α-disulfoxides were investigated using Hartree-Fock method and the basis sets 3-21G(d) and 6-31G(d). Because the calculated energy of the OS-thiosulfinate was lower than the α-disulfoxide and the S-S bond length increased upon oxidation of the thiosulfinate, the authors suggest these calculations support Kice's mechanism of S-S homolysis to form two sulfinyl radicals followed by the formation of the thiosulfonate. However, it has since been shown that the omission of alkyl substituents can lead to poor results and misleading mechanistic conclusions in systems similar to this.[60]

Recently, Benassi and coworkers investigated the mechanism for the oxidation of methyl methanethiosulfinates by performic acid.[61] Several transition states corresponding to the oxidation of dimethyl thiosulfinates with performic acid were located and characterized using Møller-Plesset perturbation theory truncated at the second order: MP2/3-21G(d) and MP2/6-31G(d). It was concluded from these calculations that the α-disulfoxide was an unstable intermediate and decomposed via homolytic cleavage of the S-S bond.

4.6 Computational study of the sulfinyl radical coupling reaction

Due to our interest in the coupling reaction of sulfinyl radicals, the inconsistency between the computational and observed chemistry of intermediates **22** and **24**, and the relatively low level of theory used to investigate this issue thus far, an ab-initio study was started. The focus of the study was to characterize the sulfinyl radical dimerization intermediates in order to understand the role of these species in both the dimerization of sulfinyl radicals and the oxidation of thiosulfinates.

Because of the relatively high number of heavy atoms for the molecules formed by the coupling of even simple sulfinyl radicals, a relatively inexpensive yet reliable computational method was sought. The G2(MP2) method was particularly attractive as it preformed well in a related study (see Chapter 3) and it is relatively inexpensive computationally for determining the enthalpies of formation. Nonetheless, the G2(MP2) method is still a somewhat demanding method and is limited to molecules of about six heavy atoms or less. Thus, the systems investigated were limited to methyl sulfinyl radical and the corresponding dimers. The molecules included in the investigation are shown below.

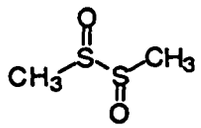

30

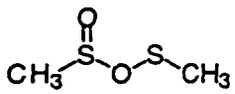

31

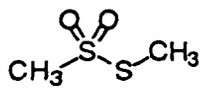

32

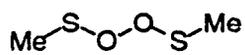

33

The three potential dimers produced by tail-to-tail **30**, head-to-tail **31**, and head-to-head **33** coupling of the methyl sulfinyl radical were investigated to get a better understanding of their structures and energetics. The thiosulfonate **32**, which is the only isolated product in the oxidation of thiosulfinates, was also investigated.

Tail-to-Tail Dimers 34, 35. Two possible stereoisomers for the α-disulfoxide **30** were considered; a meso (RS) structure (**34**), in the anti conformation, and a *dl* structure (RR) (**35**) in the eclipsed conformation. Each of the rotomers are calculated to be the respective global minimum with respect to S-S bond rotation for the isomer.

At first glance one would expect **34** to be lower in energy than **35** due to steric and electronic interactions. However, it was shown by Benassi coworkers that **35** is more stable than **34** by 5.3 kcal/mol at the MP2/6-31G(d) level.[62] Despite this, analysis of the natural

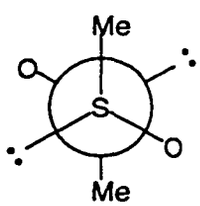

34

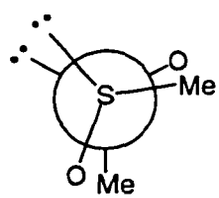

35

orbitals resulting from the single reference MP2/6-31G(d) calculation shows there is negative occupation numbers for some of the orbitals. This means the MP2 method fails for this molecule and the results reported above are invalid. Thus, **34** was taken as the minimum energy structure for the α-disulfoxide.

Head-To-Head Dimer 33. Molecule **33**, formed in the head-to-head coupling of methyl sulfinyl radicals has also proven to be problematic. Optimization of this molecule at the RHF/6-31G(d) level led to a stable molecule. However, the MP2 method also fails on this molecule as indicated by the negative occupancy numbers. Optimization with CASSCF (2,2) calculation shows the molecule has ~ 3 kcal/mol barrier to S-S homolysis, but when the MP2 corrections are made on the CASSCF calculation (MRMP2) this barrier disappears. The MRMP2 calculation predicts **33** is dissociative by ~ 25 kcal/mol which is what is expected based on additivity arguments from MeOOMe and MeSOMe. Work is currently underway which is aimed at characterizing molecule **33** more completely.

Head-To-Tail Dimer 31 and Thiosulfonate 32. Both the OS-sulfenyl sulfinate and the thiosulfonate were well behaved and optimized at MP2(full)/6-31G(d).

The complete optimized geometries are shown in Figure 13 below. A few selected bond lengths are also presented in Table 9. For the reasons discussed above structures **30-32** are MP2(full)/6-31G(d) geometries while **33** is the RHF/6-31G(d) predicted geometry.

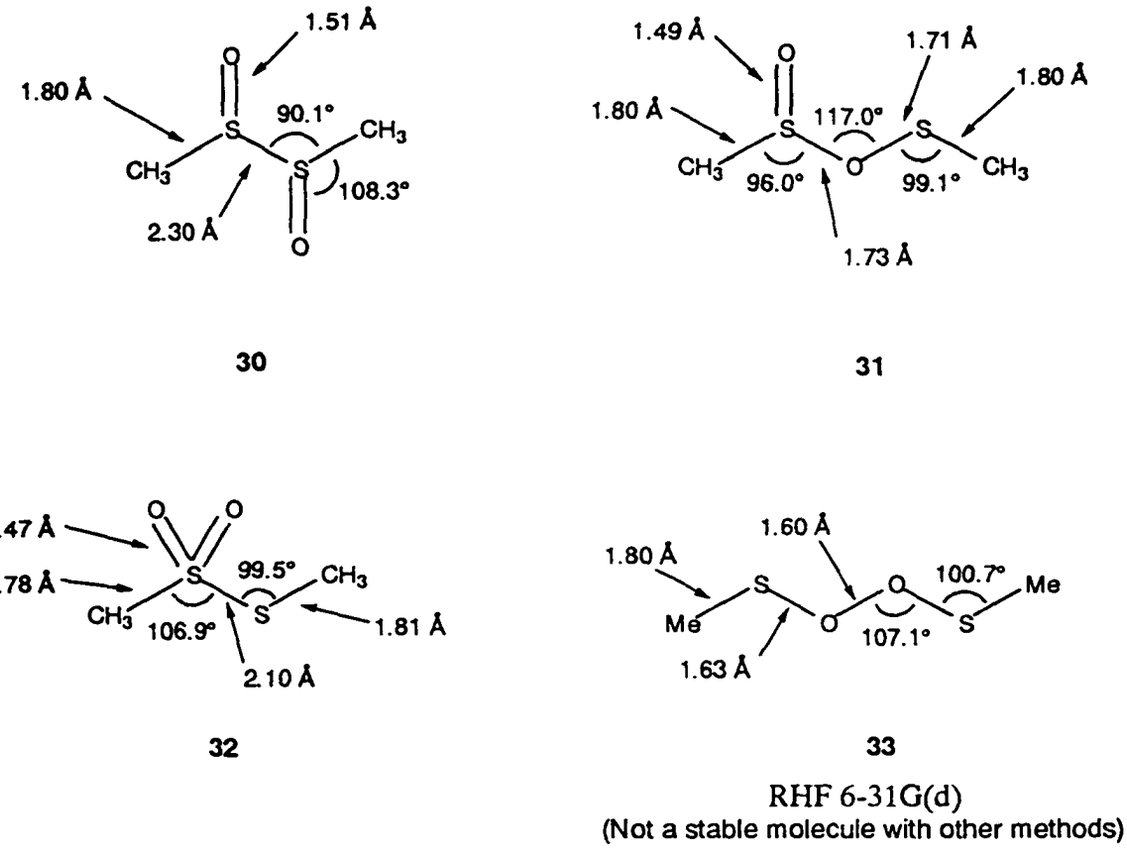

Figure 13. MP2(full)/6-31G(d) and RHF/6-31G(d) optimized geometries.

As shown in Table 9, the oxidation state of the sulfur has very little effect on the carbon-sulfur bond length. However, this oxidation state does have an effect on the S-S bond length. Oxidation of the disulfide to the thiosulfinate increases the S-S bond length from 2.04 to 2.15 Å. Oxidation of the thiosulfinate on the sulfinyl sulfur atom lowers the S-S bond distance slightly from 2.15 to 2.10Å. Oxidation of the sulfenyl sulfur atom of the thiosulfinate results in extraordinary bond lengthening from 2.15 to 2.30 Å possibly due to the repulsion of the positively charged sulfur atoms due to the polarization of the S-O bond.

Table 9. Selected bond lengths

compound	C-S (Å)	S-S (Å)	S=O (Å)	S(O)-O	S-O
MeSSMe	-	2.04[63]	-	-	-
MeSO•	1.80	-	1.54	-	-
MeS(O)OSMe	1.80	-	1.49	1.73	1.71
MeS(O)S(O)Me	1.80	2.30	1.51	-	-
MeSOOSMe*	1.80	-	-	-	1.63
$MeS(O)_2SMe$	1.78	2.10	1.47	-	-
MeS(O)SMe	1.81	2.15	1.50	-	-

* RHF/6-31G(d) optimized structure

The longest S=O bond is found in the methyl sulfinyl radical at 1.54 Å. The thiosulfonate has the shortest S=O bond at 1.47 Å. All of the dimer structures have S=O bond lengths that in within these values.

The calculated G2(MP2) energies along with the $\Delta H_f(298K)$ for the molecules of interest in this study are shown in Table 10.

As mentioned above, one can imagine three possible combinations in which the sulfinyl radical could dimerize (Figure 14). The dimer produced by head-to-head coupling **33** (path **C**) is considered first. As mentioned above optimization of structure **33** at the MRMP2 level showed this molecule is not a minimum on the potential energy surface and undergoes homolysis of the O-O bond to form 2 methyl sulfinyl radicals. It is clear that

Table 10. G2(MP2) calculated energies and ΔH_f(298K)

compound		E (G2(MP2) hartrees	ΔH_f (298 K) (kcal/mol) Calc.	ΔH_f (298 K) (kcal/mol) Expt.
MeS•		-437.5049392	+28.6	+29.8[a]
MeSO•		-512.6526079	-18.8	-14.8[b]
$MeSO_2$•		-587.7711332	-48.5	
MeS(O)S(O)Me	**34**	-1025.338890	-59.6	
MeS(O)OSMe	**31**	-1025.343406	-62.4	
$MeS(O)_2SMe$	**32**	-1025.374884	-82.3	

[a] Ref.[64] [b] Ref.[32]

further work is needed to completely characterize this pathway. However, estimates of the bond energy based on the additivity of the enthalpy of formations show that the O-O bond energy is ≈ -25 kcal/mol which makes this molecule nonexistent. Thus, this pathway is not expected to play a major role in the coupling of sulfinyl radicals.

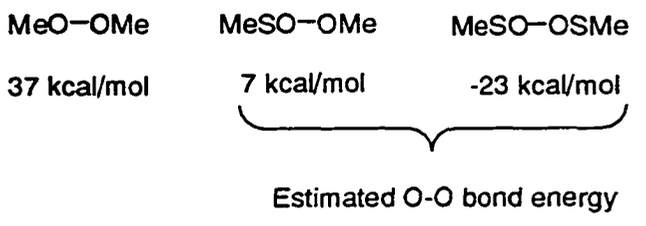

This conclusion is further supported by a comparison of the lifetimes between the peroxyl radicals and sulfinyl radicals. As mention in Section 4.5 the half life of the *tert*-butylperoxyl

radical in solution is 4.5 years, while the half life of the *tert*-butyl sulfinyl radial was estimated at 0.07 s at −100°. Because the O-O bond is not polarized, the only form of decomposition available to the peroxyl radical is the formation of the unstable head-to-head dimer similar to **33**. However, the polarization of the S-O bond in the sulfinyl radical allows for more favorable modes of coupling. Of the three possible modes of coupling two sulfinyl radicals, the head-to-head coupling which brings two negatively charged oxygen atoms together is expected to be the least favorable.

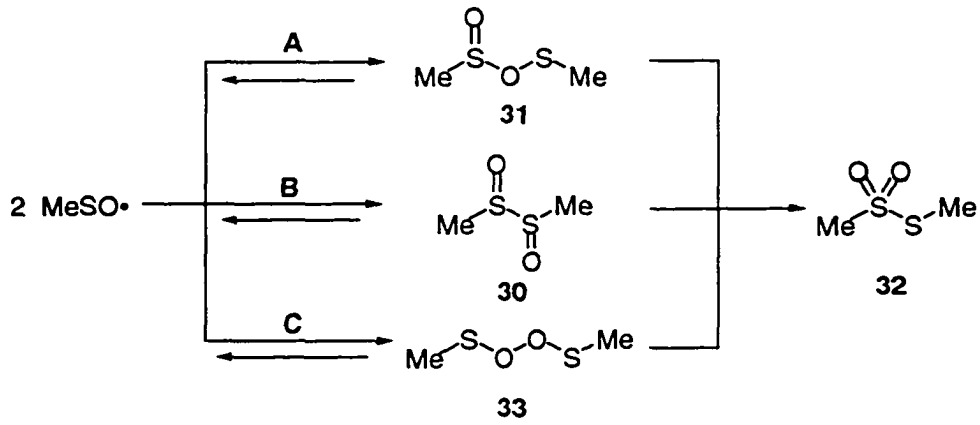

Figure 14. Three possible dimerization pathways of the methyl sulfinyl radical.

Paths **A** and **B** are considered next. Chemical intuition would suggest path **A** is the most reasonable mode of coupling of sulfinyl radicals, as it couples the more negative oxygen atom from one sulfinyl radical with a more positive sulfur atom of another. This is supported by the estimated rate constants for the self coupling reaction which are essentially diffusion controlled. The coupling of two negatively charged oxygen atoms (head-to-head) or two positively charged sulfur atoms (tail-to-tail) would not be expected to be this fast.

However, experimentally intermediates related to **31** have not been detected, while several α-disulfoxides have been experimentally characterized.[50] The energetics for the coupling of methyl sulfinyl radicals to form the dimethyl thiosulfonate are represented in Figure 15 below. The barriers for each of these pathways remain to be calculated.

The head-to-head coupling of two methyl sulfinyl radicals is exothermic by 22 kcal/mol while the head-to-tail coupling is exothermic by 25 kcal/mol. Thus, it is at least reasonable to conclude that both of the species could be formed as initial products in the reaction. Not surprisingly, rearrangement of both of these molecules to form the dimethyl thiosulfonate is exothermic.

However, the rearrangement to the thiosulfonate could be different for each of them.

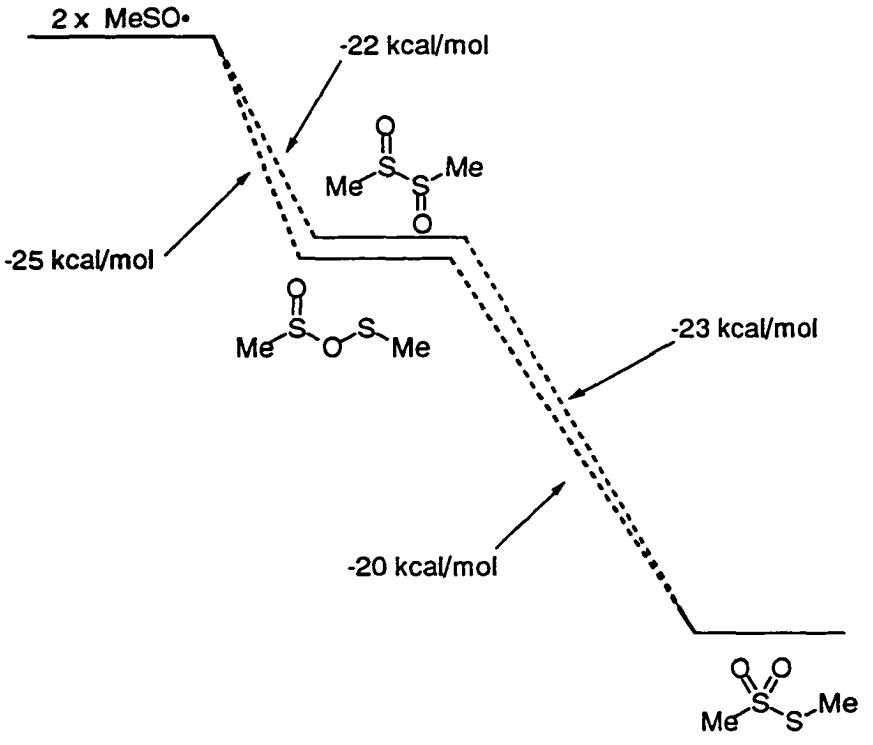

Figure 15. Energetics of methyl sulfinyl radical coupling reaction at G2(MP2).

For instance, the α-disulfoxide can either transfer an oxygen atom in a concerted fashion to form the thiosulfonate directly, or it could undergo homolysis of the S-S bond to form two sulfinyl radicals that recouple in a head-to-tail fashion to form the OS-sulfenyl sulfinate intermediate. The OS-sulfenyl sulfinate could then rearrange to form the corresponding thiosulfonate. The mechanism of the OS-sulfenyl sulfinate rearrangement is also of interest. This molecule could rearrange in a concerted fashion to form the thiosulfonate directly, or it could undergo O-S homolysis to form a sulfonyl and sulfenyl radical, which could recouple to form the thiosulfonate. Although further work needs to be done to locate the transition states for these concerted rearrangements, some preliminary results pertaining to bond homolysis are presented below.

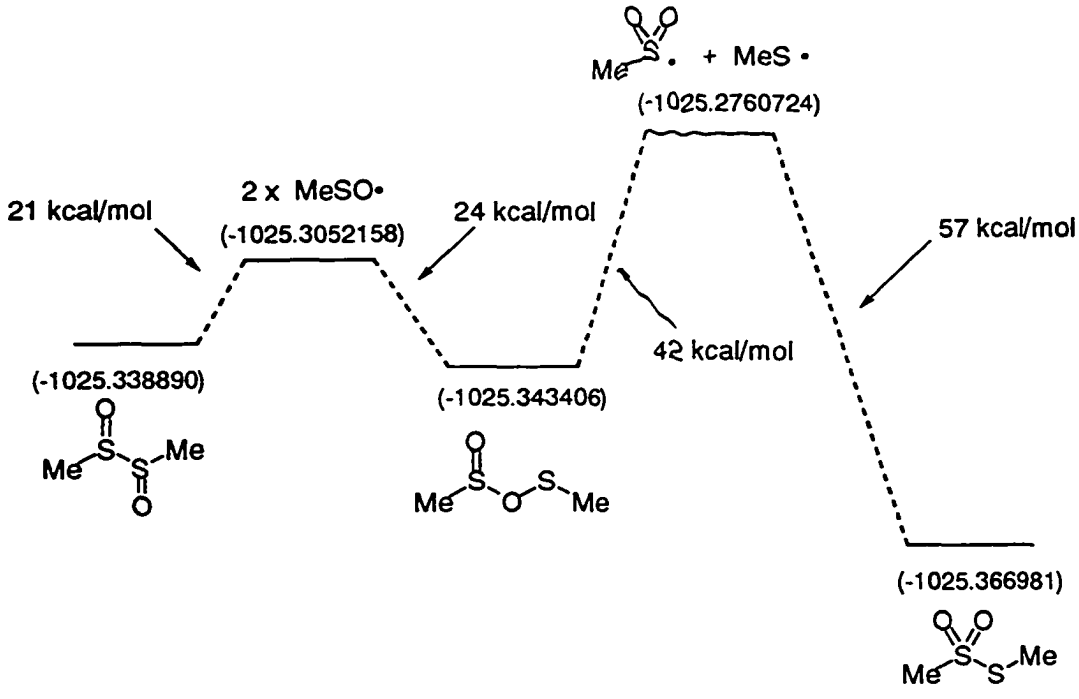

Figure 16. Reaction profile of the rearrangement to form thiosulfonate. The numbers in parentheses are absolute energies in hartrees.

The S-S homolysis in the dimethyl α-disulfoxide **30** to form the 2 methyl sulfinyl radicals is endothermic by 21 kcal/mol. The homolysis of the O-S bond in the OS-sulfenyl sulfinate to form the methyl sulfonyl and methyl sulfenyl radicals is endothermic by 42 kcal/mol. Thus, at 298 K the homolysis of the O-S bond is expected to be very slow. Although the transition state for the rearrangement of the OS-sulfenyl sulfinate to the thiosulfonate has not been characterized, a bond cleavage of 42 kcal/mol suggests this rearrangement may proceed in a concerted fashion.

It is clear that further work is needed before any real meaningful conclusions can be drawn pertaining to the overall energetics of the sulfinyl coupling reaction. However, several preliminary conclusions can be drawn about particular parts of the reaction. First, the previously reported MP2 energies calculated for the *dl* (RR) **35** were found to be invalid as indicated by negative occupancy numbers in the natural orbitals.[62,65] Of the three possible paths sulfinyl radicals can couple, chemical intuition and kinetics would suggest the head-to-tail coupling A seems to be the most reasonable. This is supported by the recent work by Jenks and coworkers which showed the rate of phenyl sulfinyl radicals coupling was similar to the rate of the phenyl sulfinyl radical with nitroxides.[15] However, the calculated energies for the two intermediates **30** and **31** show them as being very close in energy. No barriers for this reaction have been calculated and are expected to be key to the branching between the two systems. A barrier of 42 kcal/mol for the rearrangement of the methyl OS-sulfenyl sulfinate to the thiosulfonate via S-S homolysis was calculated, which may suggest a concerted rearrangement. Work aimed at establishing the energetics of this concerted

rearrangement along with establishing the rearrangement of the α-disulfoxides to the thiosulfonate is currently underway.

4.7 Reaction of sulfenyl radicals with Oxygen

Sulfenyl radicals have been proposed as important intermediates in both atmospheric chemistry and the chemistry of biological systems. They are produced in biological systems when the corresponding thiol donates a hydrogen atom to free-radical damaged biomolecule.[66] The donation of a hydrogen atom restores the biomolecule to its original structure at the expense of forming a less active sulfur radical.[67,68] In the presence of oxygen, however, a competitive reaction of the alkyl radical and oxygen is also of importance.

$$R\bullet + R'SH \longrightarrow R'S\bullet + RH \qquad (1)$$

$$R\bullet + O_2 \longrightarrow ROO\bullet \qquad (2)$$

Reaction 2 is typically estimated to be 1-3 orders of magnitude faster than reaction 1.[69,70] The overall reaction scheme is further complicated by the reaction of sulfenyl radicals with the oxygen to form a thiol peroxyl intermediate **37** shown in reaction 3. Even though the reaction of alkyl radicals with oxygen has been well developed, the reaction of sulfenyl and sulfinyl radicals with oxygen have received much less attention.

$$R'S\bullet + O_2 \longrightarrow \underset{\textbf{37}}{R'SOO\bullet} \longrightarrow R'SO\bullet + \text{other products} \qquad (3)$$

As mention in Section 4.1, the gas phase reactions of simple sulfur centered radicals with molecules found in the earth's atmosphere have been a point of interest for some time. Among these reactions, the reaction of small sulfenyl radicals that are prevalent in the earth's atmosphere are of particular importance. Though the kinetics of these reaction have been established, less is known about the mechanism of the reaction.

There are several different proposed mechanisms for the reaction of sulfenyl radicals with molecular oxygen. One of the earliest proposed mechanisms was suggested by Alla and Heicklen.[71] It was based on a study of the gas phase photolysis of MeSSMe in the presence of O_2, which led to the formation of SO_2 along with other products. Shown below is the proposed mechanism, which consisted of coupling of the methanethioperoxyl radical to form a $MeSO_4$• radical **38**. Although there are several potential isomers for $MeSO_4$• the authors suggested a structure were both oxygen molecules attack the sulfur atom.

$$CH_3S\bullet + O_2 \longrightarrow CH_3SOO\bullet$$

$$CH_3SOO\bullet\ O_2 \longrightarrow CH_3SO_4\bullet$$

$$CH_3SO_4\bullet \longrightarrow HO\bullet + HCHO + SO_2$$

$CH_3SO_4\bullet$ = 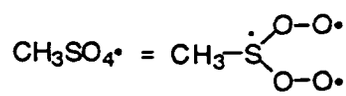

38

It was suggested subsequent decomposition of **38** led to the formation of the observed products. However, this mechanism is generally dismissed on the grounds of the energetics

of the $MeSO_4$• molecule.[72] It is argued that the triradical structure shown above would be highly unstable. It was suggested that another more plausible structure for the intermediate would be MeSOO-OO•, which is also expected to be very unstable and thermodynamically unfavorable. Finally, work done by Tyndall showed that •OH radicals are not formed in the reaction of MeS• with O_2 this implies that SO_2 is not produced from the $MeSO_4$• intermediate,[73] thus eliminating the relevance of $MeSO_4$•.

Two other mechanisms have received support. The major difference in the mechanisms has to do with the lifetime of the first intermediate (methanthioperoxyl radical) **39** formed in the reaction. Seinfeld and coworkers proposed the mechanistic scheme shown in Figure 17.[72] The reaction of methansulfenyl radical with oxygen forms the methanethioperoxyl radical **39** intermediate. Intermediate **39** then undergoes several reactions including decomposition back to starting material, isomerization to the sulfonyl radical **40**, and reaction with another methansulfenyl radical to produce two sulfinyl radicals.

$$CH_3S\bullet + O_2 \longrightarrow \underset{\mathbf{39}}{CH_3SOO\bullet}$$

$$CH_3SOO\bullet \longrightarrow CH_3S\bullet + O_2$$

$$CH_3SOO\bullet \longrightarrow \underset{\mathbf{40}}{CH_3SO_2\bullet}$$

$$CH_3SOO\bullet + CH_3S\bullet \longrightarrow CH_3SO\bullet + CH_3SO\bullet$$

Figure 17. Reaction scheme for the methansulfenyl radical with oxygen

Upper limits for the reaction of the methansulfenyl radical with oxygen were estimated as 2×10^{-17} to 2×10^{-18} cm^3 $molecule^{-1}$ s^{-1}.[73,74] The authors suggest these values are surprisingly slow considering the rate constant of a methyl radical with oxygen is estimated at 1.0×10^{-12} cm^3 $molecule^{-1}$ s^{-1}, and the oxygen molecule is expected to have strong electrophilic character. It is suggested this may be due to the very fast decomposition of the methanethioperoxyl radical back to starting material, due to a very weak MeS-OO bond. The reversible nature of the reaction would distort the observed kinetics and only a small amount of MeSO• would be observed.

Electron withdrawing groups attached to the sulfur substitution is thought to increase the stability and lifetime of the methanethioperoxyl radical, based on an increase in the sulfinyl radical production.[1] The sulfinyl radical then undergoes further chemistry.

It is suggested the isomerization of the methanethioperoxyl radical **39** to the sulfonyl radical **40** is likely unimportant.[74] This was based on the fact that the intramolecular rearrangement, proceeding by a three-member ring, should be hindered by ring strain and by the large lone-pair repulsion involving six lone-pairs of electrons. Further support for this proposal can be gained by analysis of a similar compound MeS(O)OO•. Isomerization of MeS(O)OO• to $MeS(O)_2O$• is expected to be faster than in the MeSOO• case due to the electron withdrawing oxygen on the sulfur, and the $MeSO_3H$ is expected to be the final product. However, the $MeSO_3H$ was not detected experimentally.[75]

Attempts to detect the methanesulfenylperoxyl radical **39** using epr techniques were made by Sevilla and coworkers.[76] However, only the corresponding sulfinyl radical could be detected, even at low temperatures. By employing ^{17}O enriched oxygen, it was shown the

oxygen in the sulfinyl radical originated from the molecular oxygen. Because its detection was not afforded, it was suggested the methanesulfenylperoxyl radical was formed as a transition state or metastable intermediate that was highly unstable toward cleavage of the peroxyl bond. As expected the oxygen atom was not detected in the epr experiments. Thus, a distinction between the production of an oxygen atom or a concerted reaction could not be made.

$$CH_3S\bullet + O_2 \longrightarrow \underset{\mathbf{39}}{CH_3SOO\bullet}$$

$$\underset{\mathbf{39}}{CH_3SOO\bullet} \longrightarrow CH_3SO\bullet + O(^3P)$$

Although the specifics were not given, results of an *ab initio* investigation that showed the RSOO• radical was energetically unstable toward dissociation to form RSO• and "O" were reported by Sevilla and coworkers.[76] Computationally, the RSOO• was shown to have epr parameters that were very close to those of peroxyl radicals, and thus the authors suggest it may be difficult to distinguish between the two radicals with epr.[41] Nonetheless, the methanethioperoxyl radical remains elusive.

Computational work on the formation and decomposition of methanethioperoxyl radicals is limited to one study.[77] Using MP2/3-21G(d) and MP2/6-31G(d) calculations Chatgilialoglu and Guerra investigated the reaction of the methyl sulfenyl radical with molecular oxygen and the energetics of the resulting molecules. There are several possible unsymmetrical approaches the oxygen can follow in the reaction with methanesulfenyl

radical and two symmetrical approaches. Two of these approaches (one symmetrical and one unsymmetrical) have been investigated. In the asymmetric approach, the bond between the sulfur and the oxygen atom is formed by interaction of the 3p singly occupied molecular orbital on sulfur with the π^* molecular orbital on molecular oxygen. This approach led to a relatively small transition state energy of 25 kcal/mol. The singly occupied orbital is localized mainly on the terminal oxygen.

The symmetric approach is consistent with the oxygen keeping the C-S bond approximately perpendicular to the SOO plane.

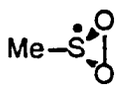

Although no geometrical information was given by Chatgilialoglu pertaining to the transition state, an energy barrier for this symmetrical path is reported to be 66 kcal/mol. The resulting dioxathiirane sulfuranyl type radical was found to be 20 kcal/mol less stable than the methanethioperoxyl radical. The unpaired electron occupies a σ_{SO}^* orbital and the highest energy doubly occupied orbital is consistent with a pseudo-π_{OO}^* orbital, making the molecule unstable. This led the authors to suggest the mechanism shown in Figure 18 in which the oxygen attacked in an unsymmetrical fashion.

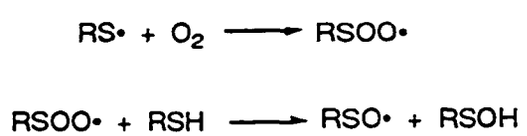

Figure 18. Proposed mechanism of a thiyl radical with oxygen

4.8 Computational Study of the reaction of sulfinyl radicals with oxygen

Due to the conflicting experimental conclusions, and the lack of computational study, the reaction of methanesulfenyl radical with oxygen was investigated using the G2 method. The intention of this study was to use more advanced computational methods than what has been used before to gain a better understanding of the mechanism of this reaction. The species of interest are shown below in Figure 19.

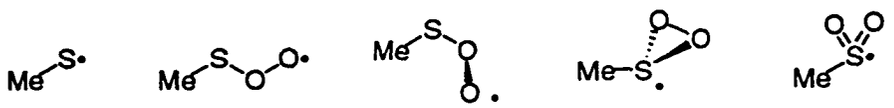

41 **39 a** **39 b** **42** **40**

Figure 19. Various sulfur containing molecules investigated using the G2 method

Two possible configurations for the methanethioperoxyl radical (compounds **39a** and **39b**) were investigated due to some discrepancies pertaining to which conformation is the global minimum. Sevilla and coworkers reported conformer **39a**, where the ∠CSOO dihedral angle was 180°, was the minimum energy structure at the UHF/6-31G(d) level of theory.[41] However, according to our earlier work with sulfenic esters (Chapter 3) the C_1 structure, with a dihedral angle of ~90°, should be the minimum energy conformation, due to minimization of the lone pair repulsion on the sulfur and oxygen. The calculated energies for each of the conformations at various computational levels are shown in Table 11. At the MP2(full)/6-31G(d) level compound **39b** is in fact more stable than **39a** by 2.4 kcal/mol. However, at the G2 level this energy difference is lowered to 0.73 kcal/mol, still in favor **39b**. Although this energy difference is very small, structure **39b** was taken as the minimum

Table 11. Calculated energies of the C_1 and C_s structures

method	C_1 structure	C_s structure	ΔE ($C_1 - C_s$) (kcal/mol)
MP2(full)/6-31G(d)	-587.29288	-587.28962	-2.1
MP4/6-311G(d,p)	-587.47396	-587.47041	-2.2
MP4/6-311+G(d,p)	-587.48670	-587.48347	-2.0
MP4/6-311G(2df,p)	-587.62797	-587.62513	-1.8
QCISD(T)/6-311G(d,p)	-587.47808	-587.47566	-1.5
MP2/6-311+G(3df,2p)	-587.57804	-587.57593	-1.3
G2	-587.67778	-587.67661	-0.7

energy conformation based on the facts that it was lower in energy with all of the methods investigated and the related sulfenic esters are consistent with this structure.

Compound **43** was investigated to get a good estimate at the energy barrier for the isomerization of compound **39b** to compound **40**. Calculated frequencies at the ROHF/6-31G(d) level showed one imaginary frequency consistent with the O-O cleavage to form the sulfonyl radical. The original starting structure **39** was C_1 symmetry, however, upon optimization the structure collapsed to the C_s structure **43**.

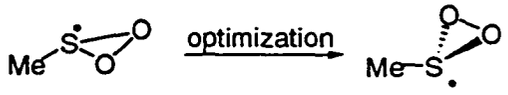

43 **42**

T.S.

The MP2(full)/6-31G(d) optimized geometries for all of the molecules of interest are shown in Table 12.

The C-S bond remains essentially unchanged in all of the molecules investigated. The S-O bond distance, however, shows a stronger dependence on the molecular structure. In compounds **39a** and **39b**, the change from 1.74 to 1.78 Å respectively could be due to the optimizations converging on different sides of a shallow potential. The shortening of the S-O bond in structure **38** is reasonable considering the fact that it is a transition state linking compound **39b** and **40**. These same trends are also observed in the O-O bond lengths. The CSO bond angle also increases when going from **39b** to **40.**

The calculated G2 energies along with the calculated heats of formation for all of the molecules involved in the reaction are shown in Table 13. These heats of formation were used in calculating the energetics of the reaction of MeS• with O_2.

Table 12. MP2(full)/6-31G(d) geometries

compound	C-S (Å)	S-O (Å)	O-O (Å)	∠CSOO	∠CSO
39a	1.79	1.78	1.30	0°	93.2°
39b	1.79	1.75	1.31	73.5°	97.1°
40	1.81	1.48	2.61	-	106.5°
37	1.80				
38	1.79	1.73	1.58	-	99.7°

Table 13. Calculated G2 energies and heats of formation

molecule	G2 (hartrees)	ΔH_{f} (0 K) (kcal/mol)	ΔH_{f} (298 K) (kcal/mol)
$CH_3S\bullet$	-437.51317	31.8	30.0
$CH_3SOO\bullet$ (C_s)	-587.67661	28.5	26.0
$CH_3SOO\bullet$ (C_1)	-587.67778	27.6	24.9
$CH_3SO_2\bullet$ (T. S.)	-587.647459	48.6	47.9
$CH_3SO_2\bullet$	-587.78689	-31.3	-34.3

The possible reactions of MeS• with O_2 are shown in Figure 20. The first issue of concern is the initial interaction of oxygen and methyl sulfenyl radicals. Both the symmetrical and unsymmetrical approaches of the oxygen are potential candidates. A local minimum for the symmetrical approach of the oxygen molecule has not yet been found at the any computational level. However, Chatgilialoglu and Guerra calculated the transition state was 66 kcal/mol higher in energy than the methanethioperoxyl radical formed by the unsymmetrical attack, but no structural information was given.[77] Thus, the unsymmetrical attack is assumed to be the only important mode of oxygen addition. Upon formation of the methanethioperoxyl radical **39b**, several reactions can occur. Early computational work by Sevilla and coworkers showed radical **39a** was energetically unstable toward dissociation to form the MeSO• and a triplet oxygen atom.[76] Another more common proposal is the isomerization of the methanethioperoxyl radical to form the sulfonyl radical. Finally, radical **39b** could undergo a reaction with MeS• to form two methyl sulfinyl radicals.

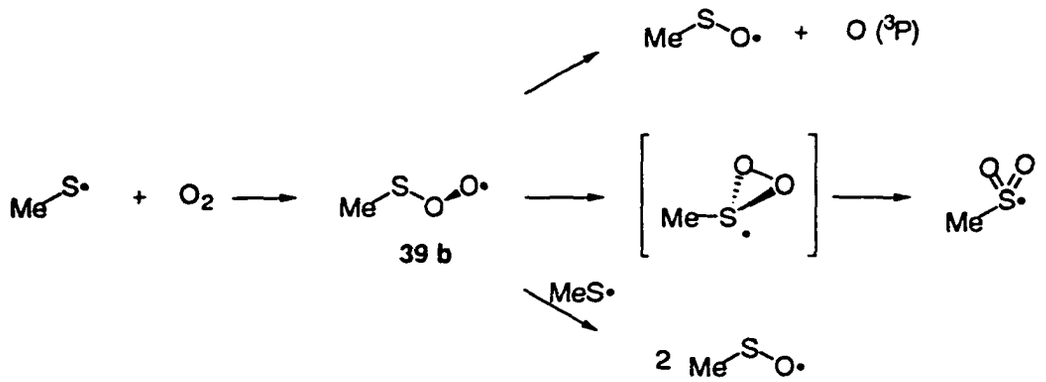

Figure 20. Proposed decomposition pathways of methanethioperoxide

The estimated reaction enthalpies are shown in Figure 21. The unsymmetrical attack of the oxygen atom on the methanesulfenyl radical is exothermic by 5 kcal/mol. This supports the notion that the methanethioperoxyl radical is fairly unstable molecule. Also, with an energy difference of only 5.1 kcal/mol, one would expect a significant amount of the methanethioperoxyl radical to decompose to form starting material as was suggested by Seinfeld and coworkers.[72] Due to this instability, one would also expect the lifetime of radical **39b** would be relatively short, making its detection experimentally difficult. The decomposition of this radical to form the methyl sulfinyl radical and triplet oxygen was calculated to be endothermic by 19 kcal/mol. The isomerization of the methanethioperoxyl radical to form the sulfonyl radical is exothermic by 44 kcal/mol. The energy barrier calculated from the transition state is 23 kcal/mol. The reaction of the radical **39b** with MeS• is also calculated to be exothermic by 45 kcal/mol. The transition state for this reaction (presumably MeSOOSMe) has been problematic to locate (see section 4.6.2) and is currently under investigation. Thus no estimate for the barrier of this reaction could be calculated at this time.

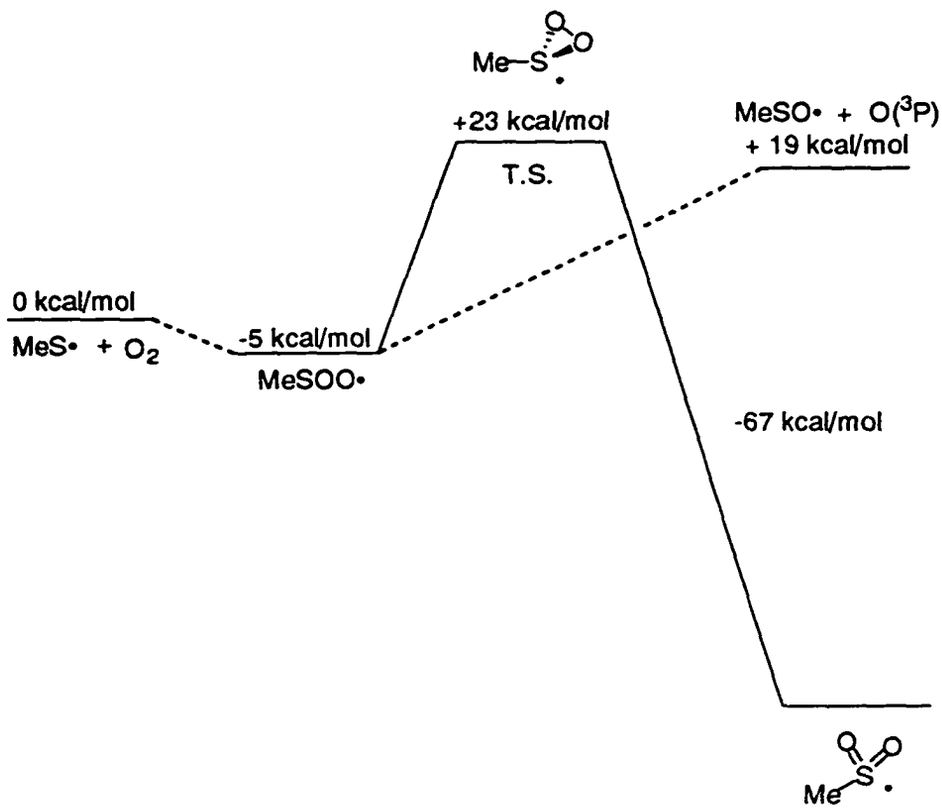

Figure 21. Calculated reaction enthalpies. The $\Delta H_f(298K)$ for $O(^3P)$ was taken from Ref. [64] and was 59.5 kcal/mol.

As was the case for the coupling reaction of sulfinyl radicals, further work needs to be completed before any definitive conclusions can be drawn about the reaction mechanism of the methanesulfenyl radical with oxygen. Nonetheless, several results can be commented on now. Despite earlier computational results, analysis with more advanced methods show the low energy conformation of the methanethioperoxyl radical to be where the CSOO dihedral is ~90°. The rearrangement of the methanethioperoxyl radical to form the methyl sulfonyl radical has an energy barrier of 23 kcal/mol. The decomposition of radical **39b** to form a methyl sulfinyl radical and a triplet oxygen atom is endothermic by 19 kcal/mol. This suggests that if Seinfeld's proposal that the rearrangement to sulfonyl radical is unimportant,

then the direct cleavage of the O-O bond is not expected to be the major mode of sulfinyl radical formation either. Work designed to characterize the reaction of the methyl sulfinyl radical with the thiyl radical is currently underway.

References

(1) Tyndall, G. S.; Ravishankara, A. R. *Int. J. Chem. Kin.* **1991**, *23*, 483-527.

(2) Schurath, U.; Weber, M.; Becker, K. H. *J. Chem. Phys.* **1977**, *67*, 110-119.

(3) Balucani, N.; Beneventi, L.; Casavecchia, P.; Stranges, D.; Volpi, G. G. *J. Chem. Phys.* **1991**, *94*, 8611-86-14.

(4) Wang, N. S.; Howard, C. J. *J. Phys. Chem.* **1990**, *94*, 8787-8794.

(5) Logan, J. A. *J. Geophys. Res.* **1983**, *88*, 10785-10796.

(6) Fehsenfeld, F. C.; Boolinger, M. J.; Liu, S. C.; Parrish, D. D.; McFarland, M.; Trainer, M.; Kley, D.; Murphy, P. C.; Albritton, D. L. *J. Atmos. Chem.* **1983**, *1*, 87-96.

(7) Friedl, R. R.; Brune, W. H.; Anderson, J. G. *J. Phys. Chem.* **1985**, *89*, 5505-5510.

(8) Koch, P.; Ciuffarin, E.; Fava, A. *J. Am. Chem. Soc.* **1970**, *92*, 5971-5977.

(9) Iino, M.; Matsuda, M. *J. Org. Chem.* **1983**, *48*, 3108-3109.

(10) Boothe, T., E.; Greene, J. L.; Shevlin, P. B.; Willcott III, R. M.; Inners, R. R.; Cornelis, A. *J. Am. Chem. Soc.* **1978**, *100*, 3874-3879.

(11) Stimpfle, R. M.; Perry, R. A.; Howard, C. J. *J. Chem. Phys.* **1979**, *71*, 5183-5190.

(12) Hills, A. J.; Howard, C. J. *J. Chem. Phys.* **1984**, *81*, 4458-4463.

(13) Baulch, D. L.; Cox, R. A.; Hampson, R. F.; Kerr, J. A.; Troe, J.; Watson, R. T. *J. Phys. Chem. Ref. Data* **1984**, *13*, 1259.

(14) Lovejoy, E. R.; Wang, N. S.; Howard, C. J. *J. Phys. Chem.* **1987**, *91*, 5749-5757.

(15) Darmanyan, A. P.; Gregory, D. D.; Guo, Y.; Jenks, W. S. *J. Phys. Chem. A* **1997**, *101*, 6855-6863.

(16) Aurich, H. G. In *Nitrones, Nitronates, and Nitroxides*; S. Patai and Z. Rappoport, Ed.; Wiley & Sons, Ltd.: New York, 1989.

(17) Becker, K. H.; Inocencio, M. A.; Schurath, U. *Int. J. Chem. Kinet. Symp.* **1975**, *1*, 205-220.

(18) Endo, Y.; Saito, S.; Hirota, E. *J. Chem. Phys.* **1981**, *79*, 4379-4384.

(19) Herzberg, G. *Molecular Spectra and Molecular Structure III. Electronic Spectra and Electronic Structure of Polyatomic Molecules.*; Van Nostrand Reinhold: New York, 1966.

(20) Nishidida, K.; Williams, F. *J. Am. Chem. Soc.* **1974**, *96*, 4781-4784.

(21) Kawamura, T.; Krusic, P. J.; Kochi, J. K. *Tetrahedron Lett.* **1972**, 4075-4078.

(22) Hinchliffe, A. *J. Mol. Struct.* **1982**, *88*, 213-216.

(23) Gilbert, B. C.; Kirk, C. M.; Norman, O. C.; Laue, H. A. H. *J. Chem. Soc. Perkins 2* **1977**, 497-501.

(24) Chatgilialoglu, C.; Gilbert, B. C.; Gill, B.; Sexton, M. D. *J. Chem. Soc. Perkin Trans. 2* **1980**, 1141-1150.

(25) Luke, B. T.; McLean, A. D. *J. Phys. Chem.* **1985**, *89*, 4592-4596.

(26) Xantheas, S. S.; Dunning Jr., T. H. *J. Phys. Chem.* **1993**, *97*, 6616-6627.

(27) White, J. N.; Gradiner Jr., W. C. *Chem. Phys. Lett.* **1978**, *58*, 470-472.

(28) O'Hair, R. A. J.; DePuy, C. H.; Bierbaum, B. M. *J. Phys. Chem.* **1993**, *97*, 7955-7961.

(29) Xantheas, S. S.; Dunning Jr., T. H. *J. Phys. Chem.* **1993**, *97*, 18-19.

(30) Plummer, P. L. M. *J. Chem. Phys.* **1990**, *92*, 6627-6634.

(31) Turecek, F. *J. Phys. Chem.* **1994**, *98*, 3701-3706.

(32) Zhao, H. Q.; Cheung, Y. S.; Heck, D. P.; Ng, C. Y.; Tetzlaff, T.; Jenks, W. S. *J. Chem. Phys.* **1996**, *106*, 86-93.

(33) Knowles, P. J.; Andrews, J. S.; AMos, R. D.; Handy, N. C.; Pople, J. A. *Chem. Phys. Lett.* **1991**, *186*, 130-136.

(34) Becke, A. D. *Phys. Rev. A* **1988**, *38*, 3098-3100.

(35) Kohn, W.; Becke, A. D.; Parr, R. G. *J. Phys. Chem.* **1996**, *100*, 12974-12980.

(36) Lee, C.; Yang, W.; Parr, T. G. *Phys. Rev. B* **1988**, *37*, 785-789.

(37) Lim, M. H.; Worthington, S. E.; Dulles, F. J.; Cramer, C. J. In *ACS Symposium Series 629*; Washington D. C., 1996; pp 402-422.

(38) Cramer, C. J.; Lim, M. H. *J. Phys. Chem.* **1994**, *98*, 5024-5033.

(39) Amato, J. S.; Karady, S.; Reamer, R. A.; Schlegel, H. B.; Springer, J. P.; Weinstock, L. M. *J. Am. Chem. Soc.* **1982**, *104*, 1375-1380.

(40) Jenks, W. S.; Matsunaga, N.; Gordon, M. G. *J. Org. Chem.* **1996**, *61*, 1275-1283.

(41) Swarts, S. G.; Becker, D.; De Bolt, S.; Sevilla, M. D. *J. Phys. Chem.* **1989**, *93*, 155-161.

(42) Tripathi, G. N. R.; Sun, Q.; Armstrong, D. A.; Chipman, D. M.; Schuler, R. H. *J. Phys. Chem.* **1992**, *96*, 5344-5350.

(43) Becker, K. H.; Fink, E. H.; Langen, P.; Scurath, U. *J. Chem. Phys.* **1974**, *60*, 4623-4625.

(44) Hunziker, H. E.; Wendt, H. R. *J. Chem. Phys.* **1974**, *60*, 4622-4623.

(45) Hunziker, H. E.; Wendt, H. R. *J. Chem. Phys.* **1976**, *64*, 3488-3490.

(46) Jacox, M. E. *J. Phys. Chem. Ref. Data* **1994**, *Monograph 3*, 1-461.

(47) Lauderdale, W. J.; Stanton, J. F.; Gauss, J.; Watts, J. D.; Bartlett, R. J. *Chem. Phys. Lett.* **1991**, *187*, 21-28.

(48) Howard, J. A.; Furimsky, E. *Can. J. Chem.* **1974**, *52*, 555-556.

(49) Baban, J. A.; Roberts, B. P. *J. Chem. Soc., Perkin Trans. 2* **1978**, 678-682.

(50) Freeman, F. *Chem. Rev.* **1984**, *84*, 117-135.

(51) Folkins, P. L.; Harpp, D. N. *J. Am. Chem. Soc.* **1993**, *115*, 3066-3070.

(52) Chau, M. M.; Kice, J. L. *J. Amer. Chem. Soc.* **1976**, *98*, 7711-7717.

(53) Battacharaya, A. K.; Hortmann, A. G. *J. Org. Chem.* **1978**, *43*,

(54) Modena, G.; Todesco, P. E. *Ric. Sci.* **1960**, *30*, 1788.

(55) Marangelli, U.; Modena, G.; Todesco, P. E. *Gazz. Chim. Ital.* **1960**, *90*, 681.

(56) Freeman, F.; Angeletakis, C. N. *J. Am. Chem. Soc.* **1982**, *104*, 5766-5774.

(57) Freeman, F.; Angeletakis, C. N. *J. Am. Chem. Soc.* **1983**, *105*, 4039-4049.

(58) Freeman, F.; Angeletakis, C. N. *J. Am. Chem. Soc.* **1981**, *103*, 6232-6240.

(59) Freeman, F.; Angeletakis, C. N.; Pietro, W. J.; Hehre, W. J. *J. Am. Chem. Soc.* **1982**, *104*, 1161-1165.

(60) Bach, R. D.; Winter, J. E.; McDougall, J. J. *J. Am. Chem. Soc.* **1995**, *117*, 8586-8593.

(61) Benassi, R.; Fiandri, L. G.; Taddei, F. *J. Org. Chem.* **1997**, *62*, 8018-8023.

(62) Benassi, R.; Fiandri, G. L.; Taddei, F. *Tetrahedron* **1994**, *50*, 12469-12476.

(63) Sutter, D.; Dreizler, H.; Rudolph, H. D. *Z. Naturforsch., Teil A* **1976**, *20*, 1676-1681.

(64) Stein, S. E.; Lias, S. G.; Liebman, J. F.; Levin, R. D.; Kafafi, S. A. In U.S. Department of Commerce, NIST: Gaithersburg, MD, 1994; pp .

(65) Lacombe, S.; Loudet, M.; Dargelos, A.; Robert-Banchereau, E. *J. Org. Chem.* **1998**, *63*, 2281-2291.

(66) Howard-Flanders, P. *Nature* **1960**, *186*, 485-494.

(67) Adams, G. E.; Armstrong, R. C.; Charlesby, A.; Micael, B. D.; Willson, R. L. *Trans. Faraday Soc.* **1969**, 732-740.

(68) Bonifacic, M.; Asmus, K. D. *J. Phys. Chem.* **1984**, *88*, 6286-6290.

(69) Adams, G. E.; Willson, R. L. *Trans. Faraday Soc.* **1969**, *65*, 2981-2993.

(70) Adams, G. E.; McNaughton, G. S.; Michael, B. D. *Trans. Faraday Soc.* **1968**, *64*, 902-907.

(71) Balla, R. J.; Heicklen, J. *J. Photochem.* **1985**, *29*, 297-310.

(72) Yin, F.; Grosjean, D.; Seinfeld, J. H. *J. Atm. Chem.* **1994**, *18*, 309-364.

(73) Tyndall, G. S.; Ravinshankara, A. R. *J. Phys. Chem.* **1989**, *93*, 4707-4710.

(74) Balla, R. J.; Nelson, H. H.; McDonald, J. R. *Chem. Phys.* **1986**, *109*, 101-107.

(75) Hatakeyama, S.; Izumi, K.; Akimoto, H. *J. Phys. Chem.* **1983**, *87*, 2387-2395.

(76) Sevilla, M. D.; Becker, D.; Swarts, S.; Herrington, J. *Biochem. Biophys. Res. commun.* **1987**, *144*, 1037-1042.

(77) Chatgilialoglu, C.; Guerra, M. In *Sulfur-Centered Reative Intermediates in Chemistry and Biology*; C. Chatgilialoglu and K. D. Asmus, Ed.; Plenum Press: New York, 1990.

CHAPTER V

GENERAL CONCLUSION

Photolysis of dibenzothiophene sulfoxide (DBTO) produces dibenzothiophene (DBT) in very high chemical yield and low quantum yield. The quantum yield is independent of sulfoxide concentration. This and other experiments rule out the formation of any sort of sulfoxide dimer as part of the mechanism for formation of DBT. A proposed mechanism for deoxygenation based on O-atom transfer by sulfinyl radicals is ruled out on an energetic basis. Mechanisms based on direct interaction between solvent and the excited state of DBTO in a reaction analogous to carbonyl photochemistry cannot be ruled out, but seems unlikely due to the pattern of quantum yields in different solvents.

In addition to DBT, photolysis of DBTO produces a species that is capable of oxidizing benzene to phenol and hydroxylating alkanes. The yield of such oxidized products ranges from modest to nearly quantitative. The pattern of reactivity is consistent with intuitive expectations for $O(^3P)$ or a similar substance, and it is suggested that this is the mechanism for the formation of DBT. Dehydrogenation of alkanes has also been demonstrated. The stepwise nature of the hydroxylation reaction has been demonstrated by formation of both alcohols derivable from a 1-phenylallyl radical. The stepwise nature of epoxidations is demonstrated by the partial loss of stereochemistry in acyclic substrates. Product competition studies are consistent with kinetic comparisons to rate constants for removal of $O(^3P)$, as determined by Scaiano.

It should be emphasized that our data are merely *consistent with* the formation of $O(^3P)$. We have made no observation that directly implies the existence of this or any other short-lived intermediate. Nonetheless, it is exceedingly clear that photolysis of DBTO produces a transient of some sort that is a very powerful oxidizing agent. Circumstantial evidence described herein suggests that the oxidizing agent may be $O(^3P)$ or a solvated complex with similar reactivity.

The photolysis of 2,5-diphenyl thiophene sulfoxide leads to the formation of the sulfide along with other products. However, the quantum yield for deoxygenation is not significantly increased over that of DBTO. The photolysis of 2,5-di-*tert*-butylthiophene sulfoxide leads to very fast desulfurization. It may be possible the difference in the observed photochemistry between these molecules is due to electronic effects of the phenyl rings, but further work is needed before any definitive conclusions can be drawn.

The thermochemistry of the peroxide, disulfide and sulfenic ester functional groups has been compared. G2 calculations were shown to reproduce the experimental $\Delta H_f°$ (298 K) data for the sulfur containing species when available, and were used to generate data for sulfenic esters and several radicals whose heats of formation are unknown.

When compared to RY'-R' bonds, RYY'-R' are weaker for the peroxide, disulfide, and sulfenic ester. This is due to the reorganization of the electronic structure of the remaining RYY'• radical by placement of three electrons into a new set of π and π^* orbitals. The sulfinyl radical (RSO•) is the most stabilized of the four types of radicals and its O-C bond is the most destabilized among the set. For any simple alkyl sulfenate, the weakest bond is expected to be the O-C bond. For vinyl or aryl sulfenates, a strong stabilization of

the O-centered radical resulting from S-O homolysis is expected to make the S-O bond the most labile. The S-O and O-H bonds of sulfenic acids are expected to have comparable BDEs, depending somewhat on substitution.

The extraordinarily low BDE for O-O bonds in peroxides (~37 kcal/mol) is not reproduced in the sulfenic esters. The S-O bond is much closer to the S-S bond strength (*ca.* 64 kcal/mol for CH_3SOCH_3). This is attributed to less effective lone pair repulsion and the difference in electronegativity between S and O, both of which increase bond enthalpy relative to O-O.

In short, while sulfenic esters are isoelectronic to peroxides, the thermochemistry of the two species stands in distinct contrast. Without allyl-type stabilization of the putative alkoxy radical provided by vinyl or aryl substitution on the O terminus, the O-C bond of a sulfenic ester will be markedly weaker than the central S-O bond. This makes the photochemistry of sulfenic esters seem all the more interesting.

The ground state for several sulfinyl radicals was characterized computationally. The SOMO was consistent with a π^* orbital sharing electron density between both the sulfur and oxygen atoms. The excited state of the methylsulfinyl and phenylsulfinyl radicals supported the experimental results that there was not an excited state below 17 000 cm^{-1}.

It is clear that further work is needed before any real meaningful conclusions can be drawn pertaining to the overall energetics of the sulfinyl coupling reaction. However, several preliminary conclusions can be drawn about particular parts of the reaction. First, the meso (RS) isomer was found to be more stable than the eclipsed dl (RR) isomer by 4.2 kcal/mol at the G2(MP2) level of theory. This is inconsistent with what is found at lower levels of

theory.[62,63] Of the three possible paths sulfinyl radicals can couple, chemical intuition and kinetics would suggest the head-to-tail coupling seems to be the most reasonable. This is supported by the recent work by Jenks and coworkers which showed the rate of phenyl sulfinyl radicals coupling was similar to the rate of the phenyl sulfinyl radical with N-oxides.[15] However, the calculated energies for the two intermediates (the α-disulfoxide and OS-sulfenyl sulfinate) show them as being very close in energy. However, no barriers for this reaction have been calculated and are expected to be key to the branching between the two systems. A barrier of 44 kcal/mol for the rearrangement of the methyl OS-sulfenyl sulfinate to the thiosulfonate via S-S homolysis was calculated which may suggest a concerted rearrangement. Work aimed at establishing the energetics of this concerted rearrangement along with establishing the rearrangement of the α-disulfoxides to the thiosulfonate is currently underway.

As was the case for the coupling reaction of sulfinyl radicals, further work needs to be completed before any definitive conclusions can be drawn about the reaction mechanism of the methanesulfenyl radical with oxygen. Nonetheless, several results can be commented on now. Despite earlier computational results, analysis with more advanced methods show the low energy conformation of the methanethioperoxyl radical to be where the CSOO dihedral is ≈90°. The rearrangement of the methanethioperoxyl radical to form the methyl sulfonyl radical has an energy barrier of 23 kcal/mol. The decomposition of the methylthiyl peroxyl radical to form a methyl sulfinyl radical and a triplet oxygen atom is endothermic by 23 kcal/mol. This suggests that if Seinfeld's proposal that the rearrangement to sulfonyl radical is unimportant, then the direct cleavage of the O-O bond is not expected to be the major

mode of sulfinyl radical formation either. Work designed to characterize the reaction of the methyl sulfinyl radical with the thiyl radical is currently underway.

APPENDIX A:

COMPUTATIONAL METHODS AND COMPUTERS

Programs

All of the computations were carried out with the Gaussian 92/DFT[1], Gaussian 94[2], or GAMESS[3] suites of programs. Orbitals were visualized with Mac-MolPlot, which is available as a utility with GAMESS. The default 6-311G basis sets in Gaussian were modified to conform with those in GAMESS, as developed by McLean and Chandler.[4] This change effects only the sulfur containing molecules investigated in this dissertation. The G2 energies were calculated using the G2ing program.[5] The temperature correction for the calculated heats of formation were calculated using the delhf program.

The G2ing program was written to take the single point energies from the various methods involved in the G2 calculation and calculate the corresponding G2 energy.[5] The input file is as follows:

-All lines must start with a blank space and line numbers are not included in the input.

1) G1 or G2 (Chooses which method will be calculated)
2) #, # (The first number is the number of electron pairs and the second is the number of unpaired electrons in the molecule.)
3) MP2 or HF Chooses the scale factor for frequencies. (0.933 for MP2, 0.893 for HF)
4) Energy of MP4/6-311G(d,p)

5) Energy of MP4/6-311+G(d,p)

6) Energy of MP4/6-311G(2df,p)

7) Energy of QCISD(T)/6-311G(d,p)

8) Zero point energy

9) MP2/6-311G(d,p)

10) MP2/6-311+G(d,p)

11) MP2/6-311G(2df,p)

The program is initiated by the following command at the % prompt: g2ing filename >& filename.log&. This puts the results of the calculation into a filename.log file. The output consists of a display of the input followed by the calculated G1 and G2 energies. The energy correction between the G1 and G2 are also given.

The Delhf program was written to calculate the heat of formation temperature correction for molecules. Although a detailed discussion of the calculation of heats of formation will be discussed later in this appendix, a short discussion of the estimation of the temperature calculation is needed here. The heat of formation of a molecule at a temperature above 0 K is calculated with the following equation.

$$\Delta H_{f\,298K}(X) = \Delta H_{f\,0K}(X) + \Delta H_{\Delta TK} - \sum \Delta H_{298K}(\text{elements})$$

The program approximates the $\Delta H_{\Delta TK}$ by separating the partition functions into a product of translational, rotational, and vibrational components and a PV term. The contribution of the

translational component is 3/2RT and the rotational component is as 3/2 RT for nonlinear molecules and RT for linear molecules. The vibrational component is approximated by using the harmonic oscillator approximation.

$$N\hbar\nu(e^{h\nu/kT} - 1)$$

The heats of formation for the elements at 298 K are taken from the JANAF tables.[6] Because the program applies the harmonic oscillator approximation to the vibrational frequencies, the calculated frequencies must be entered into the input file. The format of the input file is shown below.

-Line numbers are not included in the input file

1)	P or D	(P=polyatomic and D=diatomic)
2)	6 or 5, # of atoms	(6=nonlinear and 5=linear)
3)	298.15	(Temperature you want to calculate the correction for)
4)	Scale factor	(0.89 for HF and 0.93 for MP2)
5)	frequencies	(Copy and paste from Hessian run)

The program is started with the command (delhf <filename> x.log&) at the % prompt. This puts the output in the X.log file.

Computational Methods Used

With the exception of the density functional theory, all of the methods used in the computational work were *ab initio* methods. In *ab initio* methods, properties of the molecule are calculated in a rigorous, nonparametrized manner starting with first principles. Actually, this is not completely true as there are several simplifying assumptions in *ab initio* theory. Nonetheless, they are more complete than semi-empirical methods.

Th first item of concern when talking about an *ab initio* method is that of a basis set. A basis set is a series of probability functions used to describe each atomic orbital. Most methods employ Gaussian type oribtals which means the atomic orbitals are described with a series of Gaussian probability functions. Gaussian type orbitals are much faster computationally than other probability functions such as Slater orbitals. The simplest basis set is known as the minimal basis set and is represented by STO-3G. This simply means each Slater type orbital is described by 3 Gaussians. While, the STO-3G basis set is the only minimal basis set that has received much attention but STO-2G and STO-6G have both been used. The minimal basis set means it has only as many orbitals as are necessary to accommodate the electrons of the neutral atom. This means for hydrogen it has only one basis function (1s), for Li-Ne it has 5 basis functions per atom (1s, 2s, $2p_x$, $2p_y$, $2p_z$), and for the second row elements Na-Ar there are 9 basis functions per atom (1s, 2s, $2p_x$, $2p_y$, $2p_z$, 3s, $3p_x$, $3p_y$, $3p_z$). Because of the relatively small number of basis functions per atom, the minimal basis set is very efficient.

The biggest problem with the minimal basis set is its inability to expand or contract its orbitals. A good example of this was given by Clark.[7]. Take for example water molecule and a hydronium molecule. In the water molecule, the p-orbital is perpendicular to the

molecular plane and is doubly occupied. Each of the two electrons is being attracted by a total of 10 nuclear charges and repelled by eight electrons. In the hydronium molecule however, these two electrons are being attracted by 11 nuclear charges and repelled by only eight other electrons.

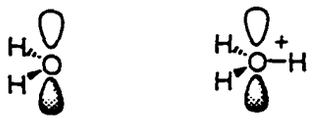

Thus, the molecule could be stabilized by contracting the electrons closer to the nucleus. Because the minimal basis set can not contract or expand its orbitals, it misses this stabilization. Another problem with the minimal basis set in the above example is the descriptions of the molecular orbitals of water. The lone pair orbitals are expected to be more diffuse than the orbitals involved in the O-H bond. However, because the minimal basis set uses the same atomic orbitals for both types of bonding, its description of the molecular orbitals in water is not accurate.

To get around the problem of not being able to contract or expand the orbitals with the minimal basis sets, split valence basis sets were developed. In the split valence basis set each atomic orbital is broken up into two parts, an inner more compact one and an outer more diffuse one. The coefficients of each of the parts can be varied independently but the total ratio remains constant. Within the split valence basis sets are the double (6-31G) and triple zeta (6-311G) basis sets. In the double zeta basis sets, the orbitals are simply split into two parts as above. In the triple zeta basis set, each atomic orbital is broken into three parts.

A further improvement in the basis set is the addition of diffuse functions. The diffuse functions are most useful for anions or molecules that require very good descriptions of nonbonding electron pairs. These basis sets are formed by adding a set of very diffuse s- and p-orbitals to the heavy atoms in a standard basis, 6-31G for example. The new basis set is then represented as 6-31+G. If additional s- diffuse functions are added to the hydrogens the basis set is represented as 6-31++G. The addition of the diffuse functions allows for an improvement of the basis set at large distances from the nucleus.

In certain molecular environments, it is not sufficient to simply increase or decrease the size of the orbital, but rather the direction of the orbital may have to be distorted. Thus, d-orbitals are added to the basis set on all heavy atoms in the system. The d orbitals do not function in the normal sense of being involved in bond formation as in transition-metal compounds, but rather they are mixed with p orbitals and allow for a certain amount of distortion. This is illustrated below in Figure 1. Mixing of the d-orbital with the p-orbital results in a deformation of the resulting orbital to one side of the atom.

Figure 1. Mixing of a p orbital and a d orbital

The new basis set is represented by 6-31G(d) or sometimes 6-31G*. Further modifications along the same lines are done by adding a set of p functions to the hydrogens (6-31G(d,p)) and a set of f-functions to the heavy atoms (6-31G(df,p)). It is important to keep in mind the

number of basis functions increase rapidly with an increase in the basis set, and the increase in cost of the calculation also increases accordingly. Thus, accuracy of calculations is often times, out of necessity, sacrificed in order to use smaller basis sets.

There were several different methods used in the computational work reported in this dissertation. The simplest theory used is know as the Hartree-Fock theory. It is also referred to as the single determinant theory. At this level of theory, the electron-electron repulsion is taken into account by considering the interaction between an electron in a given orbital an the mean field of the other electrons. This is known as the self-consistent field (SCF) method. In general, this method overestimates the electron-electron repulsion due to the fact that it assumes that their instantaneous positions are independent of one another. Another problem with this method is it forces each of the oribtals constructed to be either completely filled or unfilled and thus it is referred to as Restricted Hartree-Fock (RHF). For open shell molecules with one unpaired electron, this method cannot be used.

One solution to this problem is using the Unrestricted Hartree-Fock (UHF) method. This method deals with unpaired electrons by constructing two sets of orbitals (α and ß) each of which are coupled but not identical. The difference between the RHF and UHF is represented pictorially in Figure 2.

The UHF method is considered to be more flexible than the RHF in terms of electron interactions. This is because the paired alpha and beta orbitals, do not need to be identical. This is considered both the strength and the weakness of the UHF method. It allows for spin polarization, where the spin of the unpaired electron can perturb those formally spin paired orbital, but it also gives more negative electronic energy than the RHF method. A further

disadvantage is, because the UHF wave function is not limited to one pure electronic state, contamination of unwanted spin states is possible. For example, when examining a doublet spin state (radical) it is possible for higher spin states such as the quadruplet state to interfere. This contamination can lead to unrealistic spin densities and a too negative energy. Fortunately, several programs have incorporated methods to eliminate this spin contamination and give spin projected energies along with the unprojected energies.[1,2]

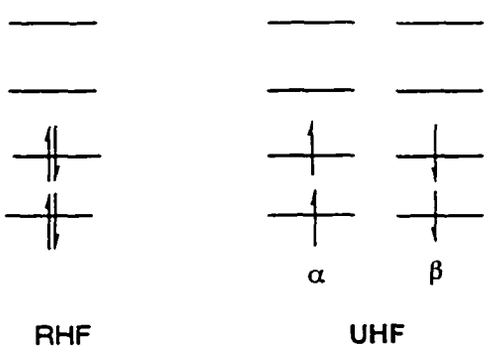

Figure 2. Pictorial representation of the RHF and UHF methods

The problem of spin contamination can be eliminated by using the Restricted Open-shell Hartree-Fock (ROHF). In this method, the doubly occupied orbitals are restricted to be identical for the α and ß spins with the exception of the unpaired electron. Thus, no interaction between the unpaired and paired electrons is allowed and spin contamination is not an issue.

As mentioned above, a major disadvantage to the SCF method is the interactions between electrons are not taken into account. Thus, several methods which attempt to correct for these interactions are used. The least expensive and most common way to deal with this

problem is to apply the Rayleigh-Schrödinger many-body perturbation theory which was applied to molecular systems by Møller and Plesset.[8] This method can be truncated at the second (MP2), third (MP3) and fourth (MP4) order. However, of these the MP2 and MP4 are by far the most common. It is important to keep in mind the Møller-Plesset method relies on a good description of the virtual orbitals in the original SCF wave function. Thus, the calculated correlation energy is dependent on the quality of the basis set used and smaller basis sets will result in less accurate correlation energies.

A major weakness of the single determinant theory is it is restricted to only one electronic configuration. It turns out that for most systems this is ok because one configuration usually makes up 99% of the ground electronic state. However, when investigating reactions mechanism, homolytic cleavage for example, it is often times important to include higher electronic states into the calculation. It can also often times be important when estimating the correlation energy. Consider for example the set of σ and σ^* orbitals. If the σ orbital is doubly occupied in the ground state, the SCF method will over estimate the electron repulsion energy as discussed above. If, however, one electron is promoted to the first excited state this electron repulsion is reduced with one electron being centered on the first atom and one electron on centered on the second. If these two states are allowed to mix the overall state will reflect the reduced electron-electron repulsion gained by the partially unpairing of the electrons. The configuration interaction (CI) method allows for this mixing.

In the CI method, a single determinant calculation is performed. The orbitals generated from this part of the calculation are used as the base orbitals for the rest of the

calculation. The excited states are then calculated by simply promoting electrons from the occupied orbitals to the unoccupied orbitals. The contributions of these excited states are then calculated and applied to the overall configuration. It is not hard to realize there will be millions of possible configurations for even simple molecules and it is not possible to calculated them all in a molecule of any size. Thus, there are methods designed to systematically limit the number of configurations included in the calculation. One of these methods is discussed in detail below.

Another method which allows for mixing of electronic states is the Multi-Configurational SCF (MCSCF). This method is similar to the CI method, however, in a MCSCF calculation a new set of orbitals is generated for every electronic configuration. This allows for a more accurate description of both the ground state and excited state orbitals. It can be particularly useful is situations that bond cleavage or formation reactions are of interest. Because a new set of orbitals are calculated for every electronic configuration, the MCSCF method is very computationally expensive. Thus, as is the case for a CI calculation, the number of orbitals and electrons involved in the calculation has to be limited, and one must chose an active space. Only the orbitals and electrons of interest in a particular molecular system are included in the active space. Picking these orbitals can often times prove to be a difficult task and a wrong choice in the active space can lead to an incorrect result. Most often, all of the possible electronic configurations in a given active space are calculated, and this type of calculation is often referred to as a Complete Active Space-SCF (CASSCF).

The method used to chosse the active space was developed by Gordon and coworkers and is an illustrative method based on GVB diagrams.[9] A very thorough review of this method has been recently published.[10] This method uses figures based on Lewis dot structures to represent all of the orbitals and valence electrons important to a particular problem. Because it is of relevance to some of the computational work reported in this dissertation, the method of designing an active space will be described for an excited state CASSCF calculation of thiophene sulfoxide.

Consider the thiophene-S-oxide molecule. Figure 3 illustrates all of the electrons and orbitals that are thought to be important to describe the excited states of thiophene sulfoxide. The three lone pairs on oxygen along with the lone pair on the sulfur atom are included in the active space. The S-O sigma bond along with four π electrons are also included. This gives a total of 14 electrons in 10 orbitals and so the calculation is represented as CASSCF(14,10).

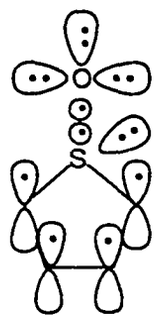

14 electrons, 10 orbitals

Figure 3. Orbitals and electrons included in MCSCF calculation

The next step in constructing the active space is picking the correct starting orbitals. The first issue to consider is one of symmetry. In this case, the molecule is C_s symmetry which makes the orbitals either A' (symmetrical) or A'' (unsymmetrical) with respect of the

mirror plane. There are 2A' and 2A'' orbitals from the π system, 3A' and 1A'' from the oxygen, and 2A' orbitals from the sulfur atom. This gives a total of 7A' orbitals and 3A'' orbitals needed in the active space. Good starting orbitals for the CASSCF were generated from a Hartree-Fock calculation with the Boys localization method. The orbitals from the localized run corresponding to the orbitals of interest in Figure 3 were chosen and used as the occupied orbitals in the CASSCF calculation. The 3 unoccupied orbitals in the CASSCF run were chosen from the non-localized orbitals form a RHF calculation.

Another method which takes into account electron correlation is based on the density functional theory. It should be stated at the onset that density functional theory is a non-Hartree-Fock method as it does not solve the exchange operator found in the Hartree-Fock theory. Rather, it replaces the exchange operator with a less computationally demanding exchange-correlation potential. The electronic density distribution is calculated for the ground state molecule. The Hohenberg-Kohn theorem shows that in principle all of the ground state molecular properties can then be calculated from this distribution. The challenge comes in when designing ways to solve for these properties in as efficient as possible method. One popular method is the Becke3LYP. This is a 3 parameter exchange correlation function method developed by Becke and coworkers[11] and uses the Lee, Yang, Parr exchange functional.[12]

Calculating heats of formation

Different methods have been advocated for arriving at computed heats of formation generally using either atomization[13,14] or bond separation[14,15] approaches. The bond

separation method, which uses isodesmic reactions and molecular rather than atomic reference compounds, has some advantages, but it requires that there be appropriate reference compounds with experimentally known ΔH_f° values. Among the sulfenic acids and esters which were investigated in Chapter 3, there is only one experimental estimate of ΔH_f (for HSOH), thus the atomization method was used to calculated the heat of formation of all the molecules in this dissertation.

With the atomization method the enthalpies of formation at 0 K are calculated by subtracting calculated nonrelativistic atomization energies $\sum D_e$ from the known enthalpies of formation of the isolated atoms.[16] For example, the G2 calculated enthalpy of formation (0 K) for the methyl sulfinyl radical ($CH_3SO\bullet$) is calculated by the equation shown below.

$$\Delta H_{f0}(MeSO\bullet) = G2_0(MeSO\bullet) + G2_0(S_g) + G2_0(O_g) + 2xG2_0(C_g) + 3xG2_0(H_g) - \sum D_e$$

The $G2_0$ values for the atoms are obtained from tabulated values calculated by Pople and coworkers.[17] The experimental enthalpies of formation for the atoms, which make up $\sum D_e$ term, are taken from the JANAF[18] tables.

The enthalpy of formation at an elevated temperature is calculated by adding in the temperature correction discussed earlier. Thus the enthalpy of formation at 298 K for the methyl sulfinyl radical is given by the equation

$$\Delta H_{f298}(MeSO\bullet) = \Delta H_{f0}(MeSO\bullet) + \Delta H_{f\Delta T}(MeSO\bullet) - \Delta H_{f\Delta T}(C_g) - \Delta H_{f\Delta T}(O_g) - 3x\Delta H_{f\Delta T}(H_g)$$

where $\Delta H_{f\ T}(X)$ is the temperature correction of X. The $\Delta H_{f\Delta T}(X)$ for the atoms are again obtained from the JANAF tables.[18]

References

(1) Frisch, M. J.; Trucks, G. W.; Schlegel, H. B.; Gill, P. M. W.; Johnson, B. G.; Wong, M. W.; Foresman, J. B.; Robb, M. A.; Head-Gordon, M.; Replogle, E. S.; Gomperts, R.; Andres, J. L.; Raghavachari, K.; Binkley, J. S.; Gonzalez, C.; Martin, R. L.; Fox, D. J.; Defrees, D. J.; Baker, J.; Stewart, J. J. P.; Pople, J. A. In Gaussian, Inc.: Pittsburgh PA, 1993; pp .

(2) Frisch, M. J.; Trucks, G. W.; Schlegel, H. B.; Gill, P. M. W.; Johnson, B. G.; Robb, M. A.; Cheeseman, J. R.; Keith, T.; Petersson, G. A.; Montgomery, J. A.; Raghavachari, K.; Al-Laham, M. A.; Zakrzewski, V. G.; Ortiz, J. V.; Foresman, J. B.; Cioslowski, J.; Stefanov, B. B.; Nanayakkara, A.; Challacombe, M.; Peng, C. Y.; Ayala, P. Y.; Chen, W.; Wong, M. W.; Andres, J. L.; Replogle, E. S.; Gamperts, R.; Martin, R. L.; Fox, D. J.; Binkley, J. S.; Degrees, D. J.; Baker, J.; Stewart, J. P.; Head-Gordon, M.; Gonzalez, C.; Pople, J. A. In Gaussian Inc.: Pittsburgh, 1995; pp .

(3) Schmidt, M. W.; Baldridge, K. K.; Boatz, J. A.; Elbert, S. T.; Gordon, M. S.; Jensen, J. H.; Koseki, S.; Matsunaga, N.; Nguyen, N.; Su, S. J.; Windus, T. L.; Dupuis, M.; Montgomery, J. A. *J. Comput. Chem.* **1993**, *14*, 1347-1363.

(4) McLean, A. D.; Chandler, G. S. *J. Chem. Phys.* **1980**, *72*, 5639-5648.

(5) Glezakou, V. In Ames, 1996; pp .

(6) Baulch, D. L.; Cox, R. A.; Hampson, R. F.; Kerr, J. A.; Troe, J.; Watson, R. T. *J. Phys. Chem. Ref. Data* **1984**, *13*, 1259.

(7) Clark *A Handbook of Computational Chemistry: A Practical Guide to Chemical Structure and Energy Calculations*; John Wiley and Sons: New York, 1985, pp 327.

(8) Møller, C.; Plesset, M. S. *Phys. Rev* **1934**, *46*, 618.

(9) Goddard, W.; Dunning, T.; Hunt, W.; Hay, P. *Acc. Chem. Res.* **1973**, *6*, 368-376.

(10) Schmidt, M. W.; Gordon, M. S. *Annul. Rev. Phys. Chem.* **1998**, *49*, 233-266.

(11) Becke, A. D. *J. Chem. Phys.* **1993**, *98*, 5648-5652.

(12) Lee, C.; Yang, W.; Parr, T. G. *Phys. Rev. B* **1988**, *37*, 785-789.

(13) Curtiss, L. A.; Raghavachari, K.; Redfern, P. C.; Pople, J. A. *J. Chem. Phys.* **1997**, *106*, 1063-1079.

(14) Nicolaides, A.; Rauk, A.; Glukhovtsev, M.; Radom, L. *J. Phys. Chem.* **1996**, *100*, 17460-17464.

(15) Raghavachari, K.; Stefanov, B. B.; Curtiss, L. A. *J. Chem. Phys.* **1997**, *106*, 6764-6767.

(16) Curtiss, L. A.; Raghavachari, K.; Deutsch, P. W.; Pople, J. A. *J. Chem. Phys.* **1991**, *95*, 2433-2441.

(17) Curtiss, L. A.; Raghavachari, K.; Redfern, P. C.; Pople, J. A. *J. Chem. Phys.* **1996**, *106*, 1063-1079.

(18) Chase, M. W.; Davies, C. A.; Downey, J. R.; Frurip, D. J.; McDanald, R. A.; Syverud, A. N. *J. Phys. Chem. Ref. Data 14, Suppl. No. 1* **1985**,

APPENDIX B

CARTESIAN CORRDINATES OF MOLECULES

Geometries coordinates (Ångstroms)

HO•		X	Y	Z
Oxygen	8	0.000000	0.000000	-0.108773
Hydrogen	1	0.000000	0.000000	0.870183
HS•				
Sulfur	16	0.000000	0.000000	-0.079128
Hydrogen	1	0.000000	0.000000	1.266042
HSO•				
Hydrogen	1	-1.101856	1.047392	0.000000
Sulfur	16	-0.439334	-0.150094	0.000000
Oxygen	8	1.016400	0.169264	0.000000
HOS•				
Oxygen	8	0.127145	0.000000	-1.040027
Hydrogen	1	-0.775294	0.000000	-1.414675
Sulfur	16	-0.015117	0.000000	0.608431
HSOH				
Sulfur	16	0.008189	-0.013850	-0.590898
Hydrogen	1	-1.297270	0.290793	-0.706056

Oxygen	8	0.145446	0.092450	1.090928
Hydrogen	1	0.002679	-0.808787	1.432997

CH_3•

Hydrogen	1	0.539359	0.934197	-0.000091
Carbon	6	0.000000	0.000000	0.000046
Hydrogen	1	0.539359	-0.934197	-0.000091
Hdyrogne	1	-1.078718	0.000000	-0.000091

CH_3O•

Oxygen	8	0.766189	-0.229269	0.000000
Carbon	6	-0.557791	0.182351	0.000000
Hydrogen	1	-1.143148	-0.749684	0.000000
Hydrogen	1	-0.819807	0.744865	0.903281
Hydrogen	1	-0.819807	0.744865	-0.903281

CH_3S•

Sulfur	16	-0.573751	0.387977	0.000000
Carbon	6	0.910775	-0.628010	0.000000
Hydrogen	1	1.766681	0.055260	0.000000
Hydrogen	1	0.974346	-1.247415	0.895237
Hydrogen	1	0.974346	-1.247415	-0.895237

CH_3SO•

Sulfur	16	-0.196839	0.505869	0.000000
Oxygen	8	-1.269827	-0.524541	0.000000

Carbon	6	1.375504	-0.373105	0.000000
Hydrogen	1	2.195457	0.348730	0.000000
Hydrogen	1	1.429782	-1.003835	0.889680
Hydrogen	1	1.429782	-1.003835	-0.889680

$CH_3OS\bullet$

Oxygen	8	0.605031	0.000000	0.398851
Carbon	6	-0.333312	0.000000	1.499565
Hydrogen	1	-0.957567	-0.894379	1.462588
Hydrogen	1	-0.957567	0.894379	1.462588
Hydrogen	1	0.280216	0.000000	2.399809
Sulfur	16	-0.075341	0.000000	-1.094574

CH_3SOCH_3

Sulfur	16	-0.523738	0.576453	-0.456738
Carbon	6	-0.985691	0.656041	1.277085
Hydrogen	1	-0.113890	0.689919	1.933125
Hydrogen	1	-1.618798	-0.191543	1.542561
Hydrogen	1	-1.555370	1.580612	1.408840
Oxygen	8	0.229522	-0.932765	-0.479307
Carbon	6	1.631239	-0.862487	-0.180627
Hydrogen	1	1.992099	-1.890191	-0.241884
Hydrogen	1	1.807393	-0.473258	0.827563
Hydrogen	1	2.158913	-0.237994	-0.906693

C_2H_3•

Hydrogen	1	0.512956	0.000000	-1.568004
Carbon	6	-0.130871	0.000000	-0.700402
Carbon	6	0.016624	0.000000	0.578082
Hydrogen	1	-0.830459	0.000000	1.257989
Hydrogen	1	1.002985	0.000000	1.043934

C_2H_3O•

Hydrogen	1	1.518585	0.000000	-0.077062
Carbon	6	0.409548	0.000000	-0.127760
Carbon	6	-0.261480	0.000000	1.164737
Oxygen	8	-0.170497	0.000000	-1.178091
Hydrogen	1	0.300065	0.000000	2.090148
Hydrogen	1	-1.343084	0.000000	1.189780

C_2H_3S•

Hydrogen	1	1.569411	0.000000	0.683304
Carbon	6	0.493928	0.000000	0.519762
Carbon	6	-0.329780	0.000000	1.583223
Sulfur	16	-0.075330	0.000000	-1.084555
Hydrogen	1	0.056875	0.000000	2.597005
Hydrogen	1	-1.405902	0.000000	1.454665

C_2H_3SO•

Sulfur	16	0.657471	-0.358182	-0.099807
Oxygen	8	1.616626	0.774052	-0.287450

Carbon	6	-0.933296	0.336734	0.146903
Carbon	6	-1.997117	-0.407800	0.340405
Hydrogen	1	-2.975007	0.033913	0.491530
Hydrogen	1	-0.947092	1.423901	0.123135
Hydrogen	1	-1.947970	-1.492913	0.357998

$C_2H_3OS\bullet$

Hydrogen	1	-1.260215	0.000000	-1.877138
Carbon	6	-0.401902	0.000000	-1.214144
Carbon	6	0.845655	0.000000	-1.625265
Oxygen	8	-0.889390	0.000000	0.098687
Hydrogen	1	1.034906	0.000000	-2.690499
Hydrogen	1	1.692301	0.000000	-0.952512
Sulfur	16	0.186601	0.000000	1.360444

CH_3SOH

Sulfur	16	-0.182542	0.365177	-0.468554
Carbon	6	-0.337152	0.463605	1.316618
Hydrogen	1	0.635617	0.532722	1.807050
Hydrogen	1	-0.885714	-0.398319	1.698433
Hydrogen	1	-0.906530	1.371729	1.535498
Oxygen	8	0.571130	-1.144728	-0.603953
Hydrogen	1	1.531173	-0.972774	-0.612207

$HSOCH_3$

Oxygen	8	-0.364483	0.673263	-0.175825

Carbon	6	-0.544376	0.765176	1.244191
Hydrogen	1	0.420221	0.834080	1.758941
Hydrogen	1	-1.100645	-0.093293	1.630139
Hydrogen	1	-1.112014	1.682776	1.403487
Sulfur	16	0.393817	-0.751472	-0.650276
Hydrogen	1	1.673484	-0.377169	-0.446689

CH_3SSH

Sulfur	16	-0.375515	0.700592	-0.316790
Carbon	6	-0.595836	0.770042	1.478671
Hydrogen	1	0.361640	0.856411	1.993866
Hydrogen	1	-1.132667	-0.107876	1.838630
Hydrogen	1	-1.191614	1.663403	1.682673
Sulfur	16	0.604416	-1.097483	-0.557049
Hydrogen	1	1.875246	-0.681926	-0.405764

C_2H_3SOH

Hydrogen	1	0.967178	0.660498	-1.311559
Carbon	6	0.942998	0.277338	-0.294193
Carbon	6	2.060536	0.001167	0.390449
Sulfur	16	-0.647289	0.190254	0.435037
Hydrogen	1	3.037906	0.184207	-0.042819
Hydrogen	1	2.028490	-0.389952	1.402292
Oxygen	8	-1.532728	-0.466771	-0.850427
Hydrogen	1	-1.436326	-1.435679	-0.782622

$HSOC_2H_3$

Hydrogen	1	0.181359	-0.168339	-2.291789
Carbon	6	0.425105	-0.110993	-1.235474
Carbon	6	1.674185	-0.152488	-0.770330
Oxygen	8	-0.759011	0.037009	-0.536329
Hydrogen	1	2.482596	-0.264236	-1.480768
Hydrogen	1	1.921791	-0.105546	0.281146
Sulfur	16	-0.682671	0.034148	1.156271
Hydrogen	1	-0.186662	1.276561	1.316530

H_2SO

Hydrogen	1	0.734727	-0.946263	-0.964658
Sulfur	16	-0.100686	0.000000	-0.419268
Oxygen	8	0.017690	0.000000	1.079701
Hydrogen	1	0.734727	0.946263	-0.964658

$(CH_3)_2SO$

Carbon	6	-0.804980	-1.339936	-0.197673
Sulfur	16	0.222534	0.000000	0.443338
Oxygen	8	1.508233	0.000000	-0.348102
Carbon	6	-0.804980	1.339936	-0.197673
Hydrogen	1	-0.314657	-2.279484	0.061988
Hydrogen	1	-0.869787	-1.256329	-1.285335
Hydrogen	1	-1.798878	-1.305403	0.255095
Hydrogen	1	-0.314657	2.279484	0.061988
Hydrogen	1	-1.798878	1.305403	0.255095

Hydrogen	1	-0.869787	1.256329	-1.285335

$CH_3OO\bullet$

Oxygen	8	0.557108	0.000000	-0.134469
Carbon	6	-0.237407	0.000000	1.079118
Hydrogen	1	-0.854143	-0.897709	1.098488
Hydrogen	1	-0.854143	0.897709	1.098488
Hydrogen	1	0.487110	0.000000	1.892017
Oxygen	8	-0.226405	0.000000	-1.185994

CH_3SOCH_3 Isomerization transition state

Sulfur	16	-0.556258	0.185295	-0.439692
Carbon	6	-0.643283	0.833936	1.234541
Hydrogen	1	0.341287	0.902021	1.705166
Hydrogen	1	-1.278320	0.168658	1.823966
Hydrogen	1	-1.097405	1.827353	1.193733
Oxygen	8	-0.098531	-1.401276	-0.254708
Carbon	6	1.459759	-0.293967	-0.417139
Hydrogen	1	1.704687	-0.621896	-1.421985
Hydrogen	1	1.873620	-0.942807	0.349978
Hydrogen	1	1.817312	0.733663	-0.252114

$CH_3S(O)_2SCH_3$

Sulfur	16	-0.382976	0.000000	1.033168
Carbon	6	1.159030	0.000000	1.917405
Hydrogen	1	1.710718	0.901352	1.647103

Hydrogen	1	1.710718	-0.901352	1.647103
Hydrogen	1	0.914254	0.000000	2.981740
Sulfur	16	0.382976	0.000000	-1.033168
Oxygen	8	-1.064991	1.285362	1.222577
Oxygen	8	-1.064991	-1.285362	1.222577
Oxygen	8	1.064991	-1.285362	-1.222577
Oxygen	8	1.064991	1.285362	-1.222577
Carbon	6	-1.159030	0.000000	-1.917405
Hydrogen	1	-0.914254	0.000000	-2.981740
Hydrogen	1	-1.710718	0.901352	-1.647103
Hydrogen	1	-1.710718	-0.901352	-1.647103

$CH_3S(O)OSCH_3$

Sulfur	16	-0.312782	-1.318519	-0.182356
Carbon	6	-0.766769	-1.365980	1.553859
Hydrogen	1	-0.204740	-0.589362	2.076709
Hydrogen	1	-0.487493	-2.346839	1.944070
Hydrogen	1	-1.841837	-1.207283	1.651028
Oxygen	8	1.175493	-1.332996	-0.200602
Oxygen	8	-0.917455	0.268542	-0.484419
Hydrogen	1	1.839796	1.016084	-1.138003
Sulfur	16	-0.062484	1.563898	0.231222
Carbon	6	1.148855	1.854143	-1.061581
Hydrogen	1	1.695415	2.758148	-0.775708
Hydrogen	1	0.646282	2.029832	-2.013459

$CH_3S(O)S(O)CH_3$

Sulfur	16	-0.226410	0.397287	-1.057160
Sulfur	16	0.226394	-0.397319	1.057159
Hydrogen	1	-1.639402	1.004277	1.566840
Oxygen	8	-0.681154	-1.584389	1.264003
Carbon	6	-0.568114	1.053233	1.775999
Oxygen	8	0.681078	1.584407	-1.263980
Hydrogen	1	-0.125831	1.948708	1.329548
Carbon	6	0.568203	-1.053199	-1.776015
Hydrogen	1	1.639483	-1.004178	-1.566832
Hydrogen	1	0.400337	-1.046537	-2.854265
Hydrogen	1	0.125971	-1.948714	-1.329612
Hydrogen	1	-0.400223	1.046601	2.854257

$CH_3SOOSCH_3$

Oxygen	8	-0.613307	-1.103861	0.83804
Oxygen	8	0.613307	1.103861	-0.83804
Sulfur	16	-1.385962	0.141679	3.56026
Sulfur	16	1.385962	-0.141679	-3.56026
Carbon	6	1.581232	-0.055057	5.20714
Carbon	6	1.581232	-0.055057	5.20714
Hydorgen	1	-2.981057	-1.137044	-4.31762
Hydorgen	1	2.981057	1.137044	4.31762
Hydorgen	1	-2.240284	1.987253	-5.28093
Hydorgen	1	-1.237405	-0.615488	-7.11267
Hydorgen	1	1.237405	0.615488	7.11267

$CH_3S(O)_2$ Transition State

Sulfur	16	-0.652107	1.318663	-0.886528
Carbon	6	0.072991	0.401812	-2.259988
Hydrogen	1	-0.719868	0.094274	-2.957155
Hydrogen	1	0.489075	-0.486787	-1.763828
Hydrogen	1	0.889949	0.877595	-2.821021
Hydrogen	1	0.050295	3.858671	1.405817
Hydrogen	1	1.250714	2.965984	2.374317
Sulfur	16	0.923768	2.056860	0.146701
Oxygen	8	2.046676	1.197101	0.360908
Carbon	6	0.422302	2.855391	1.659797
Oxygen	8	0.108992	3.194294	-1.410894
Hydrogen	1	-0.398649	2.291443	2.126249

CH_3SOO(symmetrical)

Hydrogen	1	-1.067203	-0.895993	1.769007
Carbon	6	-0.446006	0.000000	1.766074
Hydrogen	1	0.178449	0.000000	2.663608
Hydrogen	1	-1.067203	0.895993	1.769007
Sulfur	1	0.684389	0.000000	0.375839
Oxygen	8	-0.627494	0.000000	-0.820009
Oxygen	8	-0.162285	0.000000	-2.031428

CH_3SOO(unsymmetrical)

Hydrogen	1	-1.787533	-0.961544	0.901633
Hydrogen	1	-1.787533	-0.961544	-0.901633

Carbon	6	-1.180879	-1.030176	0.000000
Hydrogen	1	-0.595260	-1.951531	0.000000
Sulfur	16	0.001849	0.338793	0.000000
Oxygen	8	0.701626	0.289687	1.304420
Oxygen	8	0.701626	0.289687	-1.304420

ACKNOWLEDGEMENTS

First and foremost I would like to thank Professor William Jenks for his patience and guidance throughout my years at Iowa State. His constant drive for excellence both in chemistry and in life is admirable and has been a source of inspiration.

I would also like to thank Dr. Edward Carberry for his instrumental roll in helping me realize my passion for chemistry, and giving me the opportunities to pursue this passion.

Thanks to all of the members of the Jenks group Troy Tetzlaff, Jerry Cubbage, Woojae Lee, and Brian Vos for putting up with me in the lab. A special thanks goes to Dr. Yushen Guo for guidance early in my career. Thanks to Dr. Xiaoging Li and Dr. Alex Darmanyan for smiling when I was "hackin on ya".

Thanks to Kevin (Kroy) Roesch, Dr. Mitch (Tattoo) Refvik, Nate (Big Daddy) Classen and Steve (Lance) Gagnier for their very enlightening and fruitful lunchroom discussions. I hope this tradition is passed on and continues. A special thanks goes to Kevin (Kroy) Roesch for allowing me to remove his screen and introducing me to David Allen Coe and Kern (Coon) River.

I would also like to thank my family and friends for their love and support. Finally, I would like to thank my wife Mary for making sacrifices above and beyond all that can be expected. Without her, none of this would have been possible.

IMAGE EVALUATION
TEST TARGET (QA-3)

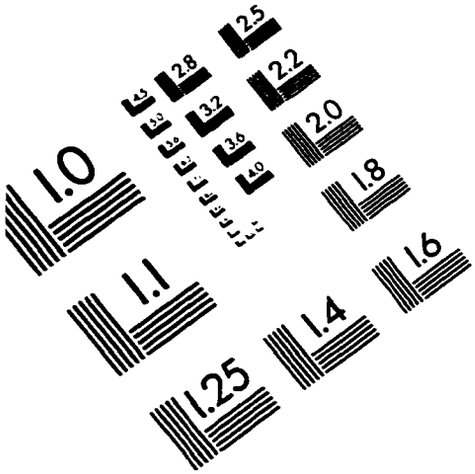

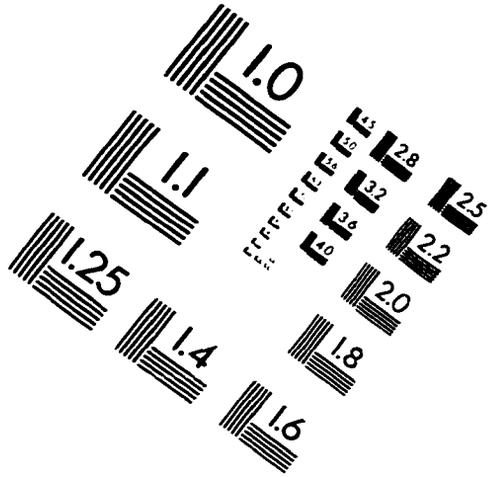

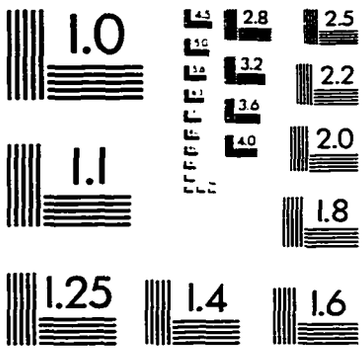

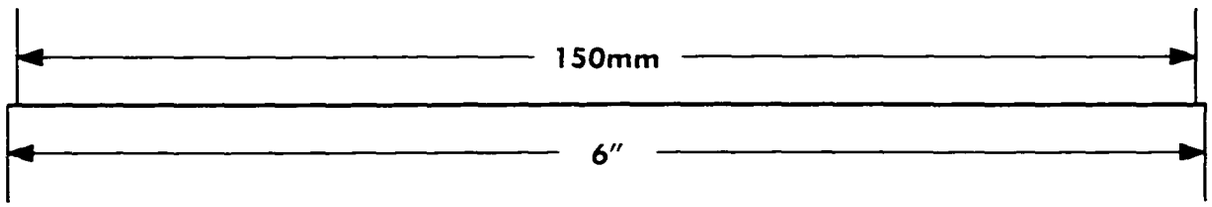

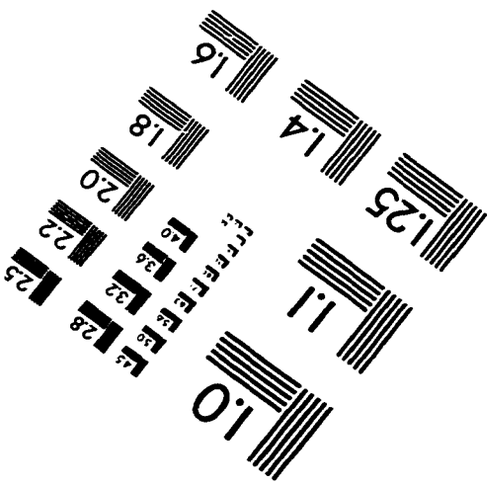

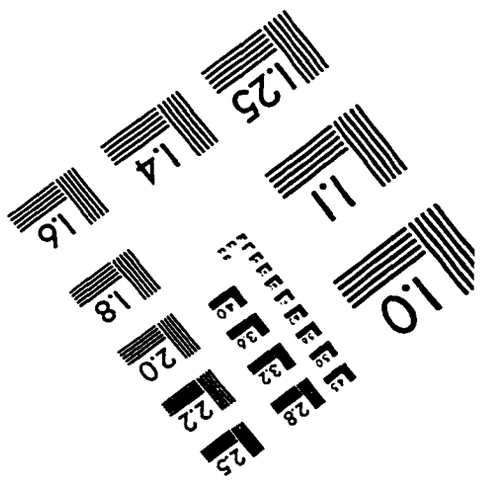

APPLIED IMAGE, Inc
1653 East Main Street
Rochester, NY 14609 USA
Phone: 716/482-0300
Fax: 716/288-5989